DEVELOPMENT OF REUSABLE ELECTROCHEMICAL IMMUNOSENSOR FOR DIRECT DETECTION OF BIOTIN MOLECULE

KHOO MAI MAI

FACULTY OF SCIENCE
UNIVERSITY OF MALAYA
KUALA LUMPUR

2017

DEVELOPMENT OF REUSABLE ELECTROCHEMICAL IMMUNOSENSOR FOR DIRECT DETECTION OF BIOTIN MOLECULE

KHOO MAI MAI

DISSERTATION SUBMITTED IN FULFILMENT OF THE REQUIREMENTS FOR THE DEGREE OF MASTER OF SCIENCE

DEPARTMENT OF CHEMISTRY
FACULTY OF SCIENCE
UNIVERSITY OF MALAYA
KUALA LUMPUR

2017

UNIVERSITY OF MALAYA

ORIGINAL LITERARY WORK DECLARATION

Name of Candidate: **KHOO MAI MAI**

Matric No: **SGR150020**

Name of Degree: **MASTER OF SCIENCE**

Title of Project Paper/Research Report/Dissertation/Thesis ("this Work"):

DEVELOPMENT OF REUSABLE ELECTROCHEMICAL IMMUNOSENSOR FOR DIRECT DETECTION OF BIOTIN MOLECULE

Field of Study: **ANALYTICAL CHEMISTRY**

I do solemnly and sincerely declare that:

(1) I am the sole author/writer of this Work;
(2) This Work is original;
(3) Any use of any work in which copyright exists was done by way of fair dealing and for permitted purposes and any excerpt or extract from, or reference to or reproduction of any copyright work has been disclosed expressly and sufficiently and the title of the Work and its authorship have been acknowledged in this Work;
(4) I do not have any actual knowledge nor do I ought reasonably to know that the making of this work constitutes an infringement of any copyright work;
(5) I hereby assign all and every rights in the copyright to this Work to the University of Malaya ("UM"), who henceforth shall be owner of the copyright in this Work and that any reproduction or use in any form or by any means whatsoever is prohibited without the written consent of UM having been first had and obtained;
(6) I am fully aware that if in the course of making this Work I have infringed any copyright whether intentionally or otherwise, I may be subject to legal action or any other action as may be determined by UM.

Candidate's Signature Date:

Subscribed and solemnly declared before,

Witness's Signature Date:

Name:

Designation:

ABSTRACT

Quantifying of small molecules such as biotin in complex matrices is very challenging in measurement sciences, despite the availability of several high technology instruments (e.g., chromatography and spectroscopy techniques) for small molecule detection. However, the use of such advanced instruments is limited by high costs, instrument portability, the necessity to pre-treat samples, and the need for skilled operators. Therefore, the focus of this study is on developing a reusable electrochemical immunosensor for the sensitive and specific detection of biotin, as the proposed immunosensor is capable of operating in turbid solutions, has potential for miniaturization or automation, and is easy to handle. Two electrochemical immunosensor versions were developed for biotin detection. The first version was fabricated with oligo(ethylene glycol), whereas the second version was fabricated with sulfanilic acid (Ph-SO_3^-) and (4-aminophenyl) trimethylammonium (Ph-NMe_3^+). The stepwise immunosensor fabrication of both immunosensor types was justified by cyclic voltammetry (CV), electrochemical impedance spectroscopy (EIS), Fourier transform infrared spectroscopy (FTIR) and scanning electron microscopy (FE–SEM). Biotin detection using immunosensors is based on the concept of a displacement assay. For repeated immunosensor use, electrode polarization at -800 mV was applied for 10 minutes to enhance the dissociation of the surface-bound antibody from the surface-bound biotin so the immunosensor surface could regenerate. After five regeneration cycles, the immunosensor surface exhibited little variation in electrochemical signal, with relative standard deviation (RSD) of 9.14%. The second immunosensor version was selected for further investigation, because it produced a significant signal in a low biotin concentration range. The 1,4-phenylenediamine (Ph-NH_2)/Ph-SO_3^-/Ph-NMe_3^+ immunosensor fabricated at a molar ratio of 2:1.5:1.5 (Mix 3) was selected for further investigation, as it possessed a good anti-fouling property and good sensor sensitivity

according to the decrement in charge transfer resistivity (R_{CT}) following a displacement assay. The second immunosensor version indicated high reproducibility upon testing 10 immunosensors with RSD of 8.44%, high specificity towards biotin, and stability for 28 days at 4°C. The developed immunosensor displayed high precision with RSD of 5–13% in intra-day (each concentration used 4 immunosensors) and inter-day (five consecutive days) precision studies based on the biotin detected at concentrations of 50, 75, and 100 µg mL^{-1}. According to the biotin concentrations stated on the packaging, the detection of biotin in infant formulas and supplements using immunosensors without sample preparation exhibited high recovery (>90%). The results obtained with the immunosensors from a real sample analysis were validated by high pressure liquid chromatography (HPLC). For the biotin concentration in serum, the linear relationship between detection signals obtained using the immunosensors and HPLC confirmed the correlation between the results obtained with both techniques. In conclusion, the Ph-NH_2/Ph-SO_3^-/Ph-NMe_3^+-fabricated immunosensor developed for biotin detection was found to be reproducible, selective, resistive to non-specific protein adsorption, stable, accurate and precise for the direct detection of biotin in food, and clinical samples. Besides, cathodic polarization was considered a suitable approach for constructing a reusable immunosensor that is able to perform multiple measurements without detection ability loss.

ABSTRAK

Kuantifikasi molekul kecil, seperti biotin, dalam matriks yang kompleks adalah sangat mencabar dalam sains pengukuran, walaupun terdapat beberapa peralatan berteknologi tinggi (contohnya, teknik-teknik kromatografi dan spektroskopi) untuk pengesanan molekul kecil. Walau bagaimanapun, penggunaan peralatan termaju adalah terhad oleh kos yang tinggi, mudah alih instrumen, keperluan untuk pra-merawat sampel, dan keperluan untuk operator yang mahir. Oleh itu, fokus kajian ini adalah untuk membangunkan satu imunosensor elektrokimia yang boleh diguna semula bagi mengesan biotin dengan sensitif dan spesifik, kerana imunosensor yang dicadangkan berupaya untuk beroperasi dalam larutan yang keruh, berpotensi untuk pengecilan saiz atau automasi, dan mudah untuk dikendalikan. Dua versi imunosensor elektrokimia telah dibangunkan untuk mengesan biotin. Versi pertama telah difabrikasi dengan oligo(etilena glikol), manakala versi kedua telah difabrikasi dengan asid sulfanilik (Ph-SO_3^-) dan (4 aminofenil) trimetilammonium (Ph-NMe_3^+). Langkah demi langkah fabrikasi imunosensor bagi kedua-dua versi imunosensor telah dikenalpasti oleh voltametri berkitar (CV), spektroskopi impedans elektrokimia (EIS), Fourier Transform spektroskopi inframerah (FTIR) dan mikroskopi elektron pengimbas (FE-SEM). Pengesanan biotin menggunakan imunosensor adalah berdasarkan konsep anjakan assai. Bagi penggunaan imunosensor yang berulang kali, elektrod polarisasi pada -800 mV telah digunakan selama 10 min untuk meningkatkan pelekangan permukaan-ikatan antibodi dari permukaan-ikatan biotin, supaya permukaan imunosensor boleh dijana semula. Selepas lima kitaran pembentukan semula, permukaan imunosensor menunjukkan sedikit variasi dalam isyarat elektrokimia, dengan relatif sisihan piawai (RSD) sebanyak 9.14%. Imunosensor versi kedua telah dipilih untuk siasatan lanjut, kerana ia boleh memberikan isyarat yang ketara dalam julat kepekatan biotin yang rendah. Permukaan imunosensor yang dibentukan oleh 1,4-fenildiamina (Ph-NH_2)/Ph-

SO_3^-/Ph-NMe_3^+ pada nisbah molar 2:1.5:1.5 (Mix 3) telah dipilih untuk siasatan lanjut, kerana ia mempunyai sifat anti-fouling yang baik dan sensitiviti sensor yang baik berdasarkan pengurangan resistivity pemindahan caj (R_{CT}) selepas anjakan assai. Imunosensor versi kedua mempunyai kebolehulangan yang tinggi diuji dengan sepuluh imunosensor dengan RSD sebanyak 8.44%, spesifikasi yang tinggi terhadap biotin, dan kestabilan selama 28 hari pada 4ºC. Imunosensor yang dibangunkan menunjukkan ketepatan yang tinggi, dengan RSD sebanyak 5-13% dari kajian ketepatan dalam sehari (setiap kepekatan menggunakan empat immunosensor) dan antara hari (lima hari berturut-turut) berdasarkan biotin yang dikesan pada kepekatan 50, 75, dan 100 μg mL^{-1}. Berdasarkan kepekatan biotin yang dinyatakan pada bungkusan, pengesanan biotin dalam formula bayi dan makanan tambahan dengan menggunakan imunosensor tanpa pra-rawatan sampel mendapat pemulihan yang tinggi (>90%). Keputusan yang diperolehi dengan imunosensor dalam analisis sampel sebenar telah disahkan oleh kromatografi cecair bertekanan tinggi (HPLC). Bagi kepekatan biotin dalam serum, hubungan linear antara isyarat pengesanan yang diperolehi menggunakan imunosensor dan HPLC mengesahkan korelasi antara keputusan yang diperolehi dengan menggunakan kedua-dua teknik. Kesimpulannya, imunosensor yang difabrikasi oleh Ph-NH_2/Ph-SO_3^-/Ph-NMe_3^+ dibentuk untuk pengesanan biotin didapati boleh dihasilkan semula, terpilih, resistif kepada penyerapan protein yang tidak spesifik, stabil, tepat dan jitu untuk mengesan secara terus biotin dalam sampel makanan dan sampel klinikal. Selain itu, polarisasi katod dianggap sebagai pendekatan yang sesuai untuk membina sebuah imunosensor yang boleh diguna semula, dimana ia boleh melaksanakan ukuran berganda tanpa kehilangan keupayaan pengesanan.

ACKNOWLEDGEMENTS

I would like to express my heartfelt thanks to those who have helped and supported me throughout my M.Sc. study. I would like to express my gratitude to my lovely supervisor, Dr. Khor Sook Mei, who has given her time and full dedication to guiding me along the study. Without her guidance in the research and dissertation writing, I believe I could not have completed my M.Sc. study on time. For all her guidance, kind words, and undivided support, I will always be thankful. Besides, I would like to thank my other supervisor, Prof. Dr. Yatimah binti Alias, who has supported me as well as given me useful advice and trusted me throughout my study. In addition, I would like to thank the chemistry teammates for their willingness to help with the arrangements and the reservation of equipment and facilities necessary to complete the research.

Finally, I would like to thank my family, friends, and lab mates for the continuous support and the encouragement all along the way, especially when I met difficulties in my research and through low tides.

TABLE OF CONTENTS

LIST OF FIGURES

LIST OF TABLES

LIST OF SYMBOLS AND ABBREVIATIONS

ΔR_{CT}	:	Difference in charge transfer resistivity
µg	:	Microgram
µg mL^{-1}	:	Microgram per milliliter
µg/100 g	:	Microgram per 100 gram
µg/capsule	:	Microgram per capsule
µg/tablet	:	Microgram per tablet
µL	:	Microliter
µm	:	Micrometer
A_{front}	:	Area from front
A_{side}	:	Area from side
A_{top}	:	Area from top
C_{dl}	:	Capacitance
cm^{-1}	:	Reciprocal centimeter
cm^{-2}	:	Per centimeter square
Da	:	Dalton
F	:	Farad
g	:	Gram
g mL^{-1}	:	Gram per milliliter
h	:	Hour
Hz	:	Hertz
kΩ	:	Kiloohm
M	:	Molar
mg mL^{-1}	:	Milligram per milliliter
Mho	:	Unit for constant phase element

min	:	Minute
mL	:	Milliliter
mL min^{-1}	:	Milliliter per minute
mm	:	Millimeter
mM	:	Millimolar
mV	:	Millivolt
mV s^{-1}	:	Millivolt per second
MΩ•cm	:	Megaohm•centimeter
n	:	Exponent of phase constant element
nm	:	Nanometer
nm^2	:	Nanometer square
ºC	:	Degree Celsius
ppb	:	Parts per billion
ppm	:	Parts per million
Q	:	Pre-factor of phase constant element
R^2	:	Square of correlation coefficient (refer to linearity)
R_{CT}	:	Charge transfer resistivity
$R_{CT(a)}$	:	Charge transfer resistivity after a displacement assay
$R_{CT(b)}$	:	Charge transfer resistivity before a displacement assay
rpm	:	Revolutions per minute
R_S	:	Resistivity of electrolyte solution
s	:	Second
V	:	Volt
Ω	:	Ohm
2,4-DNP	:	2,4-dinitrophenol
3D	:	Three dimensional

Ab	:	Antibody
AuNPs	:	Gold nanoparticles
BOD	:	Biochemical oxygen demand
BSA	:	Bovine serum albumin
C-CAD	:	Corona-charged aerosol detection
CNTs	:	Carbon nanotubes
Cty-C	:	Cytochrome-C
CV	:	Cyclic voltammetry
DC	:	Direct current
DCC	:	N,N'-dicyclohexylcarbodiimide
DNA	:	Deoxyribonucleic acid
EDC	:	1-ethyl-3-[3-dimethylaminopropyl]-carbodiimide
EIS	:	Electrochemical impedance spectroscopy
EtOH	:	Ethanol
FDMA	:	1-1'-di(aminomethyl)ferrocene
FE-SEM	:	Field-emission scanning electron microscopy
FTIR	:	Fourier transfer infrared
GC	:	Glassy carbon
GC-MS	:	Gas chromatography-mass spectroscopy
GO	:	Graphene oxide
GOX	:	Glucose oxidase
GPP	:	N-glycosylated pentapeptide
Hb	:	Haemoglobin
hCG	:	Human chorionic gonadotrophin
HIV	:	Human immunodeficiency virus
HPLC	:	High pressure liquid chromatography

HRP	:	Horseradish peroxidase
IgG	:	Immunoglobulin G
ITO	:	Indium tin oxide
MS/MS	:	Tandem mass spectroscopy
MW	:	Molecular wire
MWCNT	:	Multi-walled carbon nanotubes
NHS	:	N-hydroxysulfosuccinimide
OEG	:	Oligo(ethylene glycol)
OEG-COOH	:	2-[2-(2-methoxyethoxy)ethoxy]acetic acid
PBS	:	Phosphate buffered saline
PC	:	Phosphorylcholine
PEG	:	Poly(ethylene glycol)
PGs	:	Polyglycerols
Ph-NH_2	:	1,4-phenylenediamine
Ph-NMe_3^+	:	(4-aminophenyl)trimethylammonium
Ph-NO_2	:	4-nitroaniline
Ph-SO_3^-	:	Sulfanilic acid
PVA	:	Poly(vinylalcohol)
RC	:	Regenerated cellulose
RSD	:	Relative standard deviation
SAMs	:	Self-assembled monolayers
SWV	:	Squarewave voltammetry

LIST OF APPENDICES

CHAPTER 1: INTRODUCTION

Organic molecules <1000 Da in size are considered small molecules. They are normally nutrients, drugs and pesticides found in clinical, food and environmental samples (Khor et al., 2011). Small organic molecule quantification is very challenging in measurement science, especially in term of complex sample analysis by untrained personnel. Currently, several technology instruments including chromatography and spectroscopy techniques have been reported for small organic molecule detection (Höller et al., 2006; Staggs et al., 2004). In previous research works, gas chromatography-mass spectroscopy (GC–MS) has been reported for use in the detection of herbicide components (atrazine and metolachlor) in soil (Williams et al., 2014) and toxic components (3-monochloro-1,2-propanediol and 1,3-dichloropropanol) in soy sauce (Lee et al., 2016). The detection of fructose, sorbitol, glucose and sucrose in fruits using high pressure liquid chromatography (HPLC) with evaporative light scattering detection has also been reported by Ma et al. (2014). However, such hi-tech instruments are not always useful due to inaccessibility to the instrument, the requirement for complicated sample pre-treatment and professional operating skills. Therefore, the detection of small organic molecules using biosensors has become prominent. The simplicity, portability and fast response of biosensors allow patient bedside monitoring in clinical diagnostics as well as continuous monitoring of contaminants in food and environmental samples (Khor et al., 2011; Ricci et al., 2007; Wang, 2006).

In other words, a biosensor can be defined as an analytical device used to detect a specific target analyte in a sample. It typically consists of a bioreceptor, transducer and electronic system that includes an amplifier, processor and display. Electrochemical immunosensors among the biosensors in which antigens or antibodies serve as biorecognition molecules and the electrochemical transducer is employed to detect the

target analyte (Wang, 2006). Immunosensor detection is mainly based on the strong bioaffinity between antibodies and antigens to form a stable complex (Luppa et al., 2001). The high specific and extreme affinity of antigen-antibody interactions results in highly sensitive and selective immunosensors (Ghindilis et al., 1998). Electrochemical transducers are used to detect the electrochemical changes that occur when target analytes interact with the immobilized antibody on the immunosensor interface. The change in current and resistivity will be detected when an antigen-antibody interaction occurs at the immunosensor interface.

Small molecule biotin is the target analyte in this study due to its importance to human health. Biotin is known as vitamin H or vitamin B_7, which is a primary water-soluble coenzyme in certain carboxylase-mediated metabolisms (Gholivand et al., 2015). It is found in human serum, plasma and urine (Mock & Malik, 1992; Zempleni & Mock, 1999). Human biotin is essential for cell growth (Zhang et al., 2014), body metabolism (Höller et al., 2006), healthy skin, hair and nail strength (Höller et al., 2006) as well as for blood sugar level balancing (Albarracin et al., 2008; Maebashi et al., 1993). Besides, adequate biotin consumption is very important for normal fetal development as marginal biotin deficiency during pregnancy may lead to teratogenesis in humans (Gholivand et al., 2015; Staggs et al., 2004; Zempleni & Mock, 1999). According to the Food and Nutrition Board of the National Research Council, the adequate intake of biotin for a pregnant woman is 30 μg per day (Zempleni & Mock, 1999). Therefore, the biotin content in foods and the human body, especially pregnant women and patients receiving biotin treatment, has to be monitored periodically.

Many analytical techniques have been developed to determine biotin in biological fluids, foods and supplements. The techniques that have been reported generally include the microbiological assay using *Lactobacillus plantarum*, bioassays, instrumental

methods and binding assays based on the specific interaction between antigens and antibodies (Kergaravat et al., 2012). Owing to the advantages of immunosensors over other approaches, many researchers have focused on developing simple and low-cost immunosensors for biotin determination. For instance, a silicon nanowires nanostructured electrode functionalized with avidin was reported by Polese et al. (2014), an electrochemical magneto biosensor with streptavidin-modified magnetic microbeads as solid support was reported by Kergaravat et al. (2012) and 11-mercaptoundeconoic acid-modified gold electrode for biotin detection based on biotin-avidin reaction was developed by Ding et al. (2005).

The main challenge in immunosensor development regards the non-specific protein adsorption at the immunosensor interface, especially in real sample analysis. In order to achieve the goal of simple and direct immunosensor detection, the sample pre-treatment steps will be avoided for real sample analysis. Therefore, various interferences present in the real samples including human serum and food samples, can be adsorbed on the sensor interface and block target analyte access to the bioreceptor immobilized on the sensor interface. As a consequence, such undesired fouling phenomena will affect the accuracy, sensitivity and selectivity of the immunosensor, leading to the generation of unreliable results for target analyte detection in real samples. To overcome the non-specific protein adsorption problem, it is recommended to use long-chain molecules, such as oligo(ethylene glycol) (OEG) and poly(ethylene glycol) (PEG) as anti-fouling molecules (He et al., 2008). This is because the terminal groups of OEG chains have strong repulsive forces acting on the protein as it approaches the OEG-SAMs (self-assembled monolayers) (Zheng et al., 2004). Besides, the zwitterionic phosphorylcholine (PC) and aryl diazonium salts bearing single-charged or zwitterionic groups can be used to avoid the problem of non-specific protein adsorption (Gui, 2011). Sensor surface grafting with negatively-charged aryl diazonium salts can repel

negatively-charged proteins like bovine serum albumin (BSA), while positively-charged sensor surfaces can repel positively-charged proteins like cytochrome C (Cyt–C) (Gui et al., 2013).

Multiple-layer fabricated biosensor surfaces and long chain molecules such as OEG or PEG applied in biosensor surface fabrication lead to the formation of high-impedance biosensors. A high-impedance biosensor exhibits low sensitivity in target analyte detection because the electrode surface is surrounded by a thick layer of anti-fouling molecules and biorecognition molecules, which thus blocks the electron transfer between electrodes and bioreceptors. With the absence of electron transfer mediators, electrochemical biosensors exhibit poor analytical performance (Li et al., 2010). Due to the conductivity property of gold nanoparticles (AuNPs), they display a strong ability to transfer electrons between biomolecules and electrodes (Li et al., 2010; Liu et al., 2011). Besides, the attachment of AuNPs on biosensor surfaces increases sensor surface area, allowing larger amounts of bioreceptors to immobilize on the sensor surface. Therefore, sensor sensitivity can be significantly improved by attaching AuNPs onto the electrochemical sensor surface (Ahuja et al., 2011).

In attempts to develop a reusable immunosensor, several immunosensor surface regeneration approaches for repeated sensor use have been reported (Choi & Chae, 2009; Chung et al., 2006). The principle behind immunosensor surface regeneration is based on the high affinity interactions between antigens and antibodies; however, the antigen-antibody interaction is typically too strong for rapid reversibility (Khoo et al., 2016). Hence, the dissociation of bound antibodies from the immunosensor interface could be enhanced by treatments, such as extreme pH (Choi, 2011), temperature adjustments (Liu et al., 2008), chaotropic reagents (Choi, 2011) or additive assays (Chung et al., 2006). However, such treatments significantly affect the detection ability

of immunosensors, because the immobilized biomolecules on the sensor surface are denatured by extreme pH or temperatures. Apart from that, applying an electric field reportedly enhances the dissociation of bound antibodies from immobilized biotinylated molecules (Asanov et al., 1998). Morever, a successful attempt to produce a highly regenerative biosensor surface using electrode polarization at -900 mV for 30 min to entirely remove short-chain alkanethiols from gold electrodes was reported by Choi et al. (2009).

The main objective of the present study is to develop a reusable electrochemical immunosensor for direct detection of biotin molecule. The immunosensor surface was developed as follows: a clean glassy carbon (GC) plate was passivated with a mixed layer of aryl diazonium salts, attached with AuNPs, followed by sulfo-NHS-biotin, to which the monoclonal anti-biotin IgG antibody was complexed. The bottom-up stepwise immunosensor surface fabrication was investigated by cyclic voltammetry (CV), electrochemical impedance spectroscopy (EIS), field-emission scanning electron microscopy (FE–SEM) and Fourier transform infrared spectroscopy (FTIR). The detection of biotin molecules is based on the dissociation of surface-bound antibodies in the presence of free biotin. However, the dissociation of monoclonal anti-biotin IgG antibodies from the surface-bound biotin is difficult due to their high binding affinity. Therefore, an electrical field was applied to enhance the dissociation of surface-bound anti-biotin antibodies in the presence of free biotin (Asanov et al., 1998). Subsequently, a stable biotin/antibody complex was formed, because free biotin has a higher binding affinity to anti-biotin antibodies than surface-bound biotin. The high binding affinity between monoclonal anti-biotin IgG antibodies and free biotin can considerably improve the immunosensor's specificity, selectivity, and sensitivity to biotin (Khoo et al., 2016). The dissociation of surface-bound antibodies from the immunosensor surface in the presence of free biotin was detected using EIS measurements in a redox-active

species solution, potassium ferricyanide ($K_3Fe(CN)_6$). For immunosensor surface regeneration, electrode polarization was used to enhance the dissociation of surface-bound antibodies in the presence of free biotin. Figure 1.1 illustrates the development of an electrochemical immunosensor for the direct detection of biotin in real samples (e.g., serum, biotin-containing supplements, and infant formula).

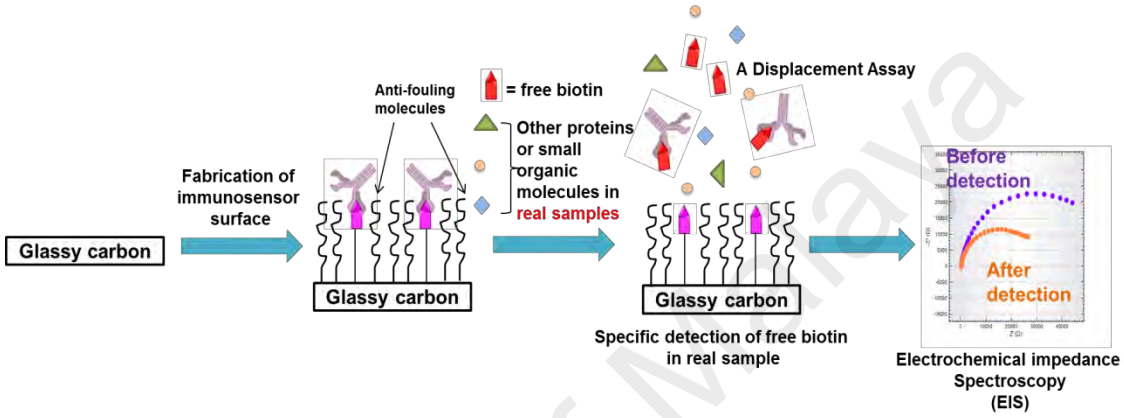

Figure 1.1: Development of an electrochemical immunosensor for the direct detection of biotin in real samples.

OBJECTIVES OF STUDY

1. To develop an electrochemical immunosensor for sensitive and specific detection of biotin molecules.
2. To regenerate the immunosensor interface via electrode polarization technique.
3. To investigate the reproducibility, selectivity, stability, anti-fouling property, accuracy and intra-day/inter-day precision of the electrochemical immunosensor developed.
4. To quantitatively detect target analytes in real samples (e.g., clinical samples and food samples) without sample pre-treatment.

CHAPTER 2: LITERATURE REVIEW

2.1 Small molecule biotin

Small molecule biotin, known as vitamin H or vitamin B_7, is a primary water-soluble coenzyme in certain carboxylase-mediated metabolisms (Gholivand et al., 2015). Figure 2.1 shows the chemical structure of small molecule biotin with molar mass of 244.31 Da, which is found in human serum, plasma and urine (Mock & Malik, 1992; Zempleni & Mock, 1999). Human biotin is essential for cell growth (Zhang et al., 2014), body metabolism (Höller et al., 2006), healthy skin, hair and nails (Höller et al., 2006) as well as for blood sugar level regulation (Albarracin et al., 2008; Maebashi et al., 1993). Besides, adequate biotin consumption is very important for normal fetal development, as marginal biotin deficiency during pregnancy may lead to teratogenesis in humans (Gholivand et al., 2015; Staggs et al., 2004; Zempleni & Mock, 1999). Therefore, the biotin content in foods and in the human body, especially pregnant women and patients receiving biotin treatment, has to be monitored from time to time.

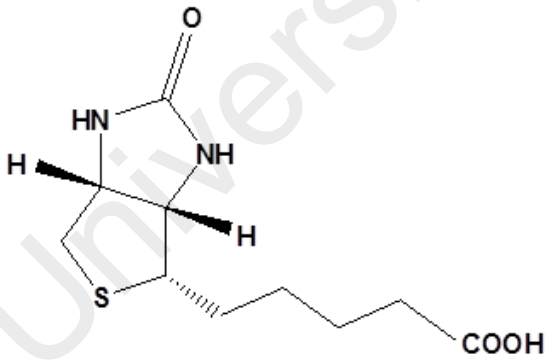

Figure 2.1: Chemical structure of biotin with molar mass of 244.31 Da.

Symptoms of biotin deficiency include scaly dermatitis, conjunctivitis, hair loss, appetite loss, hallucinations, depression and developmental delay (Staggs et al., 2004; Zhang et al., 2014). The daily biotin intake recommended for infants (0–5 months),

children, adults (>18 years) and pregnant women is 5 µg, ~20 µg, 30 µg and 30 µg, respectively (Zempleni & Mock, 1999). Biotin is present in many foods and is available as a supplement. Natural sources of biotin include raw egg yolk, nuts, liver, cauliflower and cereal (Zempleni et al., 2009). Therefore, most people can obtain sufficient biotin from a healthy diet.

Monitoring the biotin levels in patients receiving biotin treatment and quantifying biotin in foods and supplements are both important. Therefore, numerous analytical techniques have been developed to determine biotin in biological fluids, foods and supplements. The analytical techniques that have been reported include microbiological methods, bioassays, instrumental methods and binding assay (Kergaravat et al., 2012). Microbiological assay using *Lactobacillus plantarum* is based on the microorganism growth in the presence of biotin (Höller et al., 2006). This assay is very sensitive but lacks specificity because the biological activity determined does not reflect a single defined chemical compound (Höller et al., 2006; Kergaravat et al., 2012). Apart from traditional microbiological assay, a new microbiological assay known as the VitaFast test kit is also available. This test kit has several advantages over the traditional microbiological assay in terms of sample preparation time, reliability, productivity, and accuracy. However, it is still more time-consuming than other methods due to the long incubation periods (44 – 48 hours) (Zhang et al., 2014). Bioassays involve feeding animals with known amounts of biotin, then relating the weight gain to the logarithm of biotin amount (Kergaravat et al., 2012). Several high technology instruments such as liquid chromatography with fluorescence detection and HPLC with various detection methods [tandem mass spectrometer (MS/MS), corona-charged aerosol detection (C-CAD), fluorescence detection, or horseradish peroxidase (HRP)-avidin assay] have been reported for the small molecule biotin detection (Höller et al., 2006; Márquez-Sillero et al., 2013; Staggs et al., 2004; Uzuriaga-Sánchez et al., 2016). Although they exhibit

high sensitivity and specificity (discrimination between biotin and its metabolites), these methods are not so useful due to inaccessibility to instruments, the requirement for complicated sample pre-treatment and professional operating skills (Kergaravat et al., 2012; Márquez-Sillero et al., 2013). A binding assay based on the high affinity interactions between biotin and glycoprotein avidin and a binding assay based on the specific interactions between biotin and anti-biotin antibody have been reported (Ding et al., 2005; Kergaravat et al., 2012; Reyes et al., 2001). Bioaffinity reactions can be coupled to physiochemical methods such as optical detection (colorimetry, fluorescence or reflective index), piezoelectric detection, or electrochemical detection (amperometric, potentiometric, conductometric or impedimetric) to produce an immunosensor (Lu et al., 1997; Polese et al., 2014; Reyes et al., 2001). Detection of small molecule biotin using these specific immunoassays has become prominent on account of the simplicity, low cost, portability and short analysis time (Khor et al., 2011).

2.2 Introduction to biosensors

According to S.P.J. Higson, a biosensor is "a chemical sensing device in which a biologically derived recognition is coupled to a transducer, to allow the quantitative development of some complex biochemical parameter" (Mohanty & Kougianos, 2006). In other words, a biosensor is an analytical device used for the detection of a specific analyte in a sample. A typical biosensor is made up of a bio-recognition component (bioreceptor), a biotransducer component, and an electronic system including a signal amplifier, processor and display. Figure 2.2 shows a common biosensor model. The bioreceptor interacts with the target analyte to produce a signal, which is proportional to the concentration of the target analyte in the sample. The transducer measures the output signal.

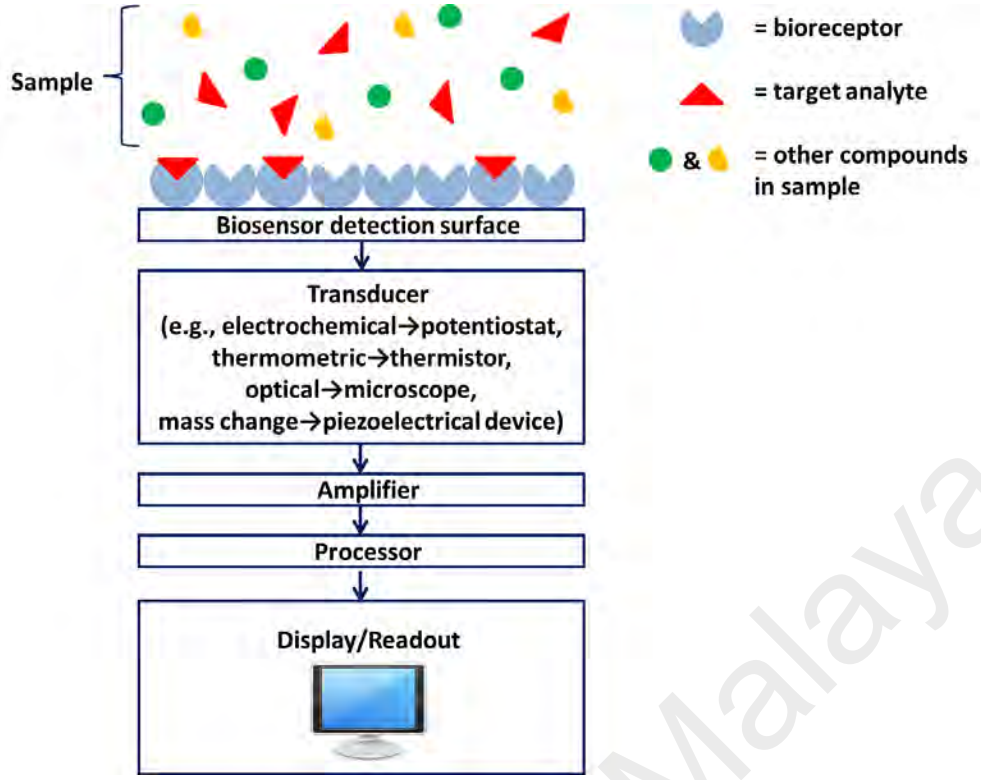

Figure 2.2: Common biosensor model.

Basically, biosensors are classified according to the types of bioreceptor and transducer. Examples of bioreceptors used in biosensors are enzymes, antibodies/antigens, nucleic acids, lectins, hormones, cell structures and tissues (Vo-Dinh & Cullum, 2000). Besides, biosensors can also be categorized according to transducer types, such as electrochemical, electrical, optical, piezoelectric and thermometric/calorimetric (Satvekar et al., 2014). Table 2.1 presents the examples of biotin-biosensors with different bioreceptors and transducers.

Table 2.1: Biotin-biosensors with different types of bioreceptors and transducers.

Biosensor	Type of bioreceptor	Type of transducer	Real sample matrices	References
Bimetallic gold-silver nanoplate array as surface-enhanced Raman scattering for biotin detection	Streptavidin	Optical (Raman scattering spectroscopy)	-	(Bi et al., 2013)
Fluorimetric detection of biotin	Streptavidin	Optical (spectrofluorimeter)	Medicines and fruit juices	(Reyes et al., 2001)
Electrochemical magneto biosensor for biotin determination	Streptavidin	Electrochemical (squarewave voltammetry, SWV)	Supplements and infant formulas	(Kergaravat et al., 2012)
Biotin detection based on the avidin-biotin interaction on self-assembled gold electrodes	Avidin	Electrochemical (EIS)	-	(Ding et al., 2005)
Reusable biotin-immunosensor	Monoclonal anti-biotin IgG antibody	Electrochemical (EIS)	-	(Khoo et al., 2016)
Biacore Qflex® biotin kit	Monoclonal mouse anti-biotin antibody	Optical (surface plasmon resonance)	Unfortified milk powder and infant formulas	(Indyk et al., 2000)

Electrochemical detection normally involves a three-electrode system, which consists of counter/auxiliary, reference and working electrodes. An electrochemical technique can be applied to transduce the recognition event into an amperometric, conductometric or potentiometric signal (Luppa et al., 2001). For optical biosensors, photodiodes, photomultipliers or microscopes can serve as detectors. Optical biosensors can detect changes in adsorption, fluorescence, luminescence and refractive index (Luppa et al., 2001; Satvekar et al., 2014). Piezoelectric biosensors, also known as microgravimetric biosensors, are mass-sensitive, and they can detect a mass change due to antigen-antibody complex formation (Ghindilis et al., 1998). Thermometric/calorimetric biosensors are utilized to detect the exothermic heat generated by chemical or biochemical processes. A thermistor or thermopile is normally employed as a temperature transducer to determine heat changes (Satvekar et al., 2014).

Although several high technology instruments (e.g., HPLC, GC–MS) are available for quantitative biomolecule detection, they have limitations of high cost, instrument portability, sample pre-treatment requirement and the need for skilled operators (Höller et al., 2006; Márquez-Sillero et al., 2013; Staggs et al., 2004). Therefore, biomolecule detection using biosensors has become prominent, because in addition to low cost and portability, biosensors can perform rapid, easy, specific and sensitive detection (Khor et al., 2011). Hence, biosensors are widely used in clinical diagnostics, food quality control, biothreat detection and environmental screening. Table 2.2 presents commercially-available biosensors.

Table 2.2: Commercially-available biosensors.

(Bahadır & Sezgintürk, 2015; Indyk et al., 2000; Tothill, 2001; Wang & Lee, 2015).

Fields	Target analyte	Brand/Company
Clinical diagnostics	Glucose	• GlucoDay (Menarini Diagnostics, Italy) • GlucoWatch (Cygnus Inc., USA)
	Insulin	• FreeStyle InsuLinx (Abbott, USA)
	Hemoglobin	• AmStrip hemoglobin meter (Germaine Laboratories Inc. USA) • HemoSmart (ApexBio, Taiwan)
	Uric acid	• UASure (ApexBio, Taiwan) • MultiSure (ApexBio, Taiwan)
	Cholesterol	• Total cholesterol test (Syntron Bioresearch Inc., USA) • Cardiocheck (Pts Diagnostics, China)
	Human chorionic gonadotropin (hCG)	• Clearblue Digital (Clearblue, USA) • Accu-Clear pregnancy test (Medic8, Scotland)
	Human immunodeficiency virus (HIV)	• HIV test strip (Ajosha Bio Teknik Pvt. Ltd., India) • Oral Fluid HIV Rapid test (ALUXBIO Co. Ltd., China)
	E. coli 0157	• 0157 Coli-Strip (Coris BioConcept, Belgium)
	Influenza A and B	• Sofia Influenza A+B (Quidel, USA)
Food quality control	Microorganisms	• Biomerieux, France • Biosensor Systems Design, USA
	Peanut allergens	• Texas Instruments Inc., USA
	Heavy metals	• IVA Co. Ltd., Russia
	Water soluble vitamins	• Biacore Qflex® (Sweden)
Biothreat detection	Ricin	• BADD (ADVNT, USA) • Ricin BioThreat Alert kit (Tetracore, USA)
	Anthrax	• Anthrox BioThreat Alert kit (Tetracore, USA)
Environmental screening	Metabolism of living cell	• Bactometer (Bactomatic Inc., USA) • Malthus 2000 (Malthus Inc., UK)
	Atrazine (herbicide component)	• Pharmacia Biacore™ (Sweden)
	Biochemical oxygen demand (BOD)	• Ra-BOD (AppliTek) • Biox-1010 (Endress+Hauser) • MB-DBO (Biosensores)

2.3 Electrochemical immunosensors

An immunosensor is an analytical device, in which antibodies or antigens serve as target analyte recognition elements (Ricci et al., 2007). Immunosensor detection is mainly based on the strong bioaffinity between antibodies and antigens to form a stable complex (Luppa et al., 2001). The high specific and extreme affinity of the antigen-antibody interactions results in high immunosensor sensitivity and selectivity (Ghindilis et al., 1998). Compared to traditional immunoassays, immunosensors, which are simple devices, require shorter analysis time and smaller sample size, and are portable, highly-specific to target analytes, and have potential for automation (Ghindilis et al., 1998). Therefore, trace analysis in clinical diagnosis, food quality control and environmental screening requires such simple, rapid and accurate device like an immunosensor for continuous monitoring purposes.

The simplicity, portability and miniaturization of electrochemical devices have attracted great attention for immunosensor applications. Electrochemical immunosensor refers to an analytical device in which the biological recognition element is coupled to an electrochemical transducer (Wang, 2006). Electrochemical signal generation is based on the changes in electron transfer caused by antigen-antibody interactions (Ghindilis et al., 1998). The signal can be detected via several electrochemical techniques: potentiometric, amperometric, conductimetric or impedimetric (Bahadır & Sezgintürk, 2016; Ricci et al., 2007). By applying a fixed potential (potentiostatic technique) or a range of potential (voltammetry technique), the amperometric transducer monitors the current associated with the reduction or oxidation of the redox-active species involved in the recognition event (Ghindilis et al., 1998; Ricci et al., 2007). A potentiometric transducer measures electrode surface potential alterations caused by the specific interactions between target analytes and bioreceptors at near-zero current flow, while a conductimetric transducer measures the alterations in electric conductivity caused by the

biochemical reactions in the ion solution at a constant potential (Choi, 2011; Ghindilis et al., 1998). With the impedimetric technique, EIS is used to analyze the resistivity and capacitivity at the sensor surface based on the perturbation of the electrochemical system in equilibrium by a small-amplitude sinusoidal voltage signal as a function of frequency (Guan et al., 2004; Prodromidis, 2007).

EIS is an excellent technique for characterizing immunosensor surface fabrication and for monitoring biomolecular recognition events (Guan et al., 2004). EIS is a sensitive, accurate, non-destructive and label-free electrochemical technique used to investigate the electrical properties of electrode-electrolyte interfaces (Bahadır & Sezgintürk, 2016; Ding et al., 2005; Polese et al., 2014). Besides, it exhibits high potential to be integrated into a small, portable, and multi-analyte device (Guan et al., 2004). Therefore, it is widely employed in biosensor applications for the detection of bioaffinity reactions between target analytes and immobilized antibodies.

When the biorecognition events occur at the modified electrode surface, the change in interfacial properties (e.g., resistivity and capacitivity) of the electrode can be detected based on the electron transfers at the electrode surface. Nyquist plots obtained from EIS measurements are normally include a semicircle region followed by a linear line. Nyquist plots are analyzed by fitting with an equivalent circuit, which usually consists of resistances, capacitors, or constant phase elements either combined in parallel or in series arrangement (Bahadır & Sezgintürk, 2016). Darwish et al. (2016) reported an impedimetric immunosensor for direct detection of dengue virus NS1 biomarker in human serum. NS1 antigen in sample could specifically bind with the immobilized antibody, then the interfacial properties of the electrode would be altered. The increase in charge transfer resistivity of electrode surface was detected due to the

formation of the stable antigen-antibody complex on electrode surface, which blocked the electron transfers.

2.4 Target analyte detection mechanisms

Many types of target analyte detection mechanisms for immunosensors have been reported, for instance association, competitive inhibition, sandwich and displacement assays (Khor et al., 2011; Liu et al., 2011; Ricci et al., 2007). Selecting a detection mechanism is generally based on the molecular size of the target analyte and type of transducer used. Association assay is the simplest mechanism, whereby detection is based on the complexation between antigens and immobilized antibodies or vice versa (Figure 2.3a). With electrochemical or piezoelectric detection, the mechanism illustrated in Figure 2.3a(i) is more recommended for large molecule detection, because the binding of large molecules to the immobilized antibodies will yield a more substantial signal. An electrochemical immunosensor used to detect anti-biotin IgG antibody via an association was demonstrated by Liu et al. (2011). There are three types of competitive inhibition assays: (i) free antigens compete with labelled antigens for immobilized antibodies, (ii) free antigens compete with immobilized antigens for labelled antibodies and (iii) free antigens compete with immobilized antigens for primary antibodies, after which the labelled secondary antibodies bind to the surface-bound antibodies to give a detection signal (Ricci et al., 2007). With competitive inhibition assays, the detection signals decrease as the amount of target analyte increases. The mechanisms shown in Figures 2.3b(i) and 2.3b(iii) are more suitable for use in optical immunosensors. This is because the labelled antigens or labelled secondary antibodies are unnecessary for signaling in electrochemical and piezoelectric immunosensors. A competitive inhibition assay where surface-bound glycosylated pentapeptide and haemoglobin A1c (HbA1c, target analyte) in the sample compete for the anti-HbA1c IgG antibodies was reported by Liu et al. (2012). The similar mechanism is shown in Figure 2.3b(ii). In a sandwich

assay, the free antigens bind to immobilized antibodies and then the labelled secondary antibodies bind to the surface-bound antigens to generate a signal (Figure 2.3c) (Ghindilis et al., 1998). This detection mechanism is preferable in optical immunosensors. Ang et al. (2015) reported a colloidal gold-based lateral flow immunoassay, which is an optical immunosensor for detecting HbA1c via sandwich assay (Ang et al., 2015). In a displacement assay, detection is based on the dissociation of surface-bound antibodies from the immunosensor surface due to the competition for antibodies between free and immobilized antigens (Figure 2.3d) (Khor et al., 2011). A substantial detection signal is achievable when the large antibody molecules are dissociated from the immunosensor surface. Therefore, this mechanism is suitable for small molecule detection. Khor et al. (2011) and Khoo et al. (2016) employed this detection mechanism in an electrochemical immunosensors developed for small organic molecule detection (Khoo et al., 2016; Khor et al., 2011).

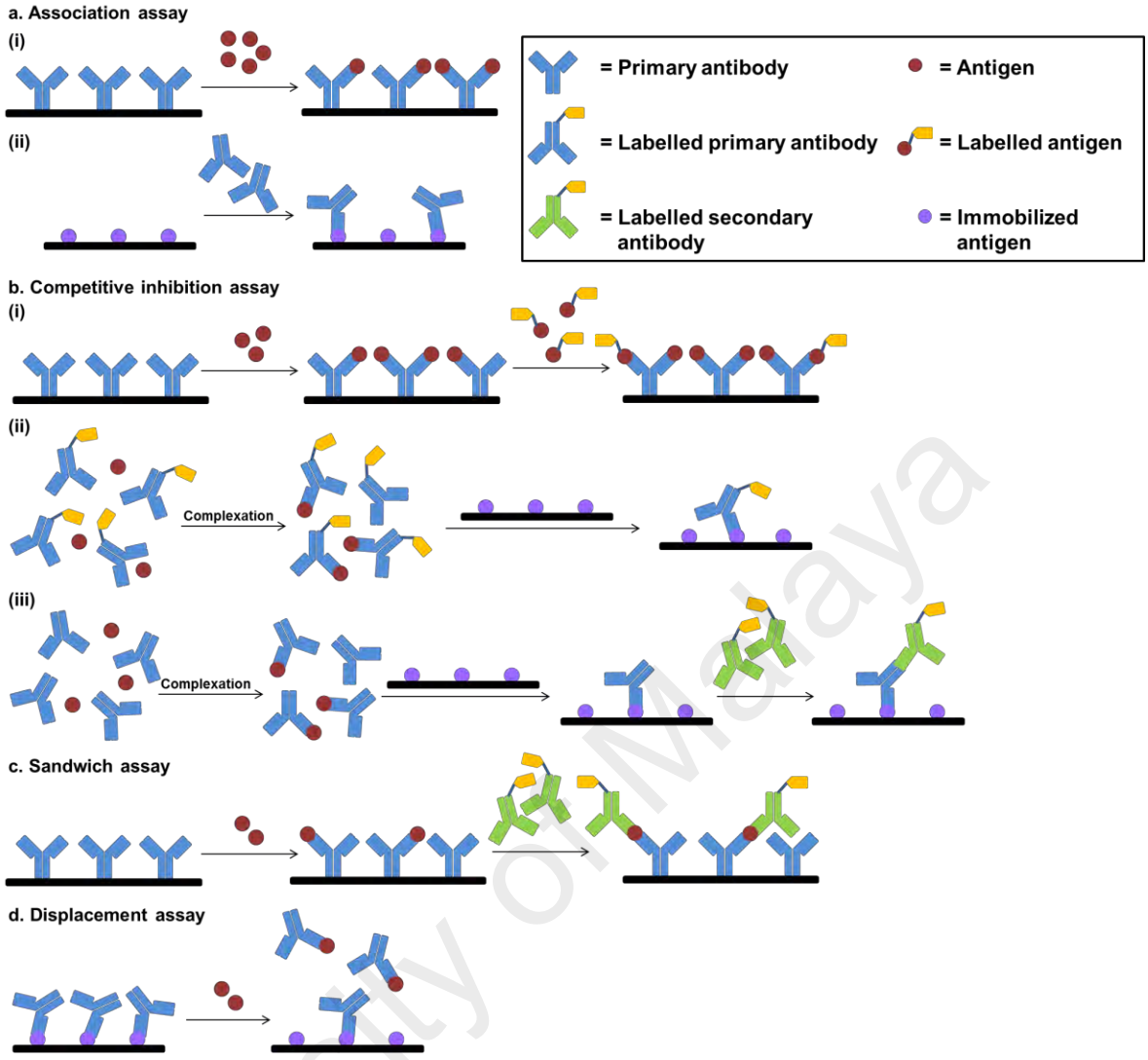

Figure 2.3: Schematic of target analyte detection mechanism in immunosensors. a. Association assays (i) with antibodies immobilized on immunosensor surface, and (ii) with antigens immobilized on immunosensor surface; b. Competitive inhibition assays based on (i) the competition for immobilized antibodies between free antigens and labelled antigens, (ii) the competition for labelled antibodies between free antigens and immobilized antigens, and (iii) the competition for primary antibodies between free antigens and immobilized antigens; c. Sandwich assay; d. Displacement assay (Khoo et al., 2016; Ricci et al., 2007).

2.5 Electrochemical immunosensor surface fabrication

A robust immunosensor interface with superior performance should be physically and chemically stable when exposed to biological media or atmosphere for long term, able to prevent non-specific protein adsorption on the immunosensor surface, and capable of converting the biorecognition into an accurate detection signal (Gui, 2011). Besides, the bioactivity of the immobilized bioreceptors must be retained to ensure accurate and specific detection. To fulfill all requirements, surface fabrication techniques have an important role in the development of immunosensor interfaces with multi-functionalities.

2.5.1 Electrode surface functionalization

Biomolecules such as enzymes, antibodies or nucleic acids are immobilized on the immunosensor surface for biorecognition purposes. Prior to the immobilization of the desired biomolecules, the surface is usually functionalized with organic molecules via physical adsorption, covalent bonding or biochemical interaction (Kim & Kang, 2008). The functionalized transducer surface can provide amino or carboxyl groups for biomolecule immobilization via amide bond formation. Besides, the non-specific interaction between the interferences (e.g., proteins) of a complex sample matrix and the biosensor interface can also be avoided by the zwitterionic functional groups on the electrode surface. The attachment of organic molecules onto a solid-state surface can form a SAMs, which is a nanometer-scale thin organic (Kim & Kang, 2008). Several types of SAMs modification approaches have been reported in previous studies, e.g. organosilane monolayer formation on a hydroxyl-terminated surface, organophosphonic acid monolayer formation on an indium tin oxide (ITO) surface, and alkanethiol monolayer formation on metal surfaces such as gold and silver (Gui, 2011; Kim & Kang, 2008). A well-defined alkanethiol monolayer may form on noble metal surfaces with simple preparation, but alkanethiol is mainly restricted to gold surface, which

increases immunosensor production costs, and has long-term stability problems when applied in biosensing devices (Gui, 2011; Ricci et al., 2012). Therefore, research effort has been aimed at functionalizing sensor surfaces with aryl diazonium salts, which are surprisingly compatible with a wide range of materials, like carbon allotropes, metals, semiconductors, ITO and polymers (Gui, 2011). In addition , aryl diazonium salt SAMs appear to be more stable than alkanethiol SAMs in thiol displacement, thermal treatments, electrochemical oxidation or reduction, and long-term exposure to atmosphere (Gui, 2011).

Electrode surface grafting with aryl diazonium salts can be achieved by applying reductive potentials to the surface. Upon electric potential application, the diazonium group splits from the aromatic ring to form dinitrogen and aryl radical; this radical then binds to the electrode surface through covalent bond formation (Figure 2.4) (Gui, 2011). Another method is the spontaneous adsorption of aryl diazonium salts, which is attained by the spontaneous electron transfer from the electrode surface to the aryl diazonium salt without electric potential application, after which deposition occurs (Gui, 2011). This process can widen the applicability range of aryl diazonium salts, especially in immunosensor commercialization.

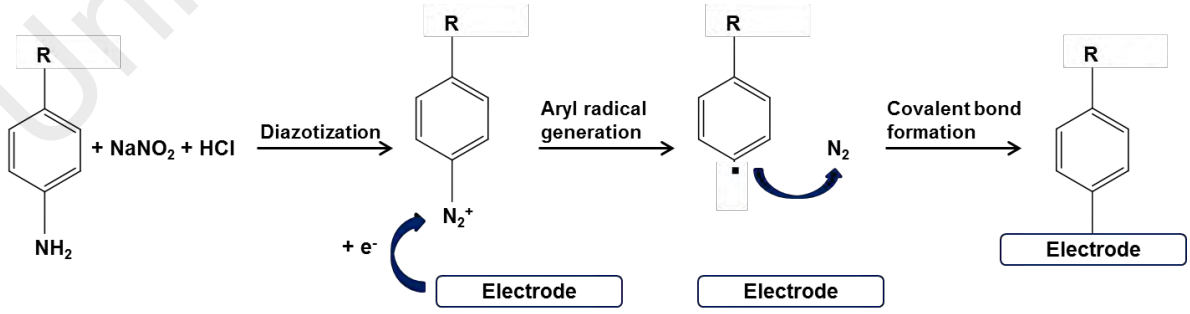

Figure 2.4: Electrode surface functionalization with aryl diazonium salts.

The design and fabrication of an electrode surface with a well-defined structure can significantly enhance immunosensor performance in terms of sensor sensitivity, selectivity and anti-fouling property. Mixed SAMs, which comprise a combination of two or more different organic molecules, facilitate the immunosensor surface with multi-functionalities (Gui, 2011). The properties of functionalized surfaces depend on the type of organic molecules grafted on the electrode surfaces. For example, an electrochemical immunosensor for detecting HbA1c in serum was demonstrated by Liu et al. (2012). In their study, a mixed SAM comprising an oligo(phenylethynylene) molecular wire (MW) and OEG was grafted on the GC surface, and then a redox probe 1,1'-di(aminomethyl)ferrocene (FDMA) was attached to the end of the MW. The OEG controls the non-specific protein adsorption to the immunosensor surface, the MW facilitates the electron transfer to the underlying GC surface, and the surface-bound FDMA generates an attenuated amperometric signal when the antibodies bind to the epitope (Khor et al., 2011; Liu et al., 2012). Besides, immunosensor sensitivity can also be improved by adjusting the ratio of MW to OEG in mixed SAMs (Khor et al., 2011). Because OEG, MW and FDMA were utilized in immunosensor surface fabrication, the electrochemical immunosensor developed by Liu et al. (2012) was found to have a strong anti-fouling property, high sensitivity and fast response.

The functional groups present on the surface of SAMs have their own indispensable roles in immunosensor surface design. For instance, amino groups ($-NH_2$) and carboxyl groups (-COOH) are linkers in the immobilization of biomolecules on the electrode surface via the 1-ethyl-3-[3-dimethylaminopropyl]-carbodiimide (EDC)-mediated reaction, N-hydroxysuccinimide (NHS)-mediated reaction, N,N'-dicyclohexylcarbodiimide (DCC)-mediated reaction and glutaraldehyde-mediated reaction (Khor et al., 2011; Kim & Kang, 2008; Liu et al., 2012). Besides, the amino groups and thiol groups (-SH) allow the covalent binding of AuNPs on the electrode

surface via incubation or electrochemical method (Liu et al., 2011). In addition, zwitterionic moieties and functional groups like $-SO_3^-$ and $-N(Me)_3^+$ can be used to prevent non-specific protein adsorption on the immunosensor surface (Gui et al., 2013). Positively-charged moieties repel positively-charged proteins, whereas negatively-charged moieties repel negatively-charged proteins.

2.5.2 Biomolecule immobilization methods

Other than surface functionalization, biomolecule immobilization on surfaces is also important because biomolecules are normally used for biorecognition where the interaction between target analytes and immobilized biomolecules occurs. Therefore, the 3D native structure of biomolecules must be retained following immobilization in order to maintain their biological activity and prevent inaccurate immunosensor detection (Kim & Kang, 2008). Biomolecular structure retention is fairly dependent on the biomolecule immobilization method. A range of biomolecule immobilization methods have been discussed and reported as shown in Table 2.3.

Table 2.3: Methods of biomolecule immobilization on functional surfaces.

Method	Description	Advantages	Disadvantages	Examples
Physical adsorption: electrostatic interaction	Interaction between charged biomolecules and oppositely charged surfaces	• Simple • Fast • Reversible • No linker molecule required • Retention of natural 3D structure	• Desorption by change in ionic strength or pH • Random orientation	A hydrogen peroxide sensor where the negatively charged DNA molecules were immobilized on a positively charged cysteamine-gold surface. (Song et al., 2006).
Physical adsorption: hydrophobic interaction	Direct adsorption of lipophilic biomolecules on hydrophobic surfaces	• Simple • Fast • No linker molecule required • Suitable for lipophilic biomolecules	• Desorption by detergent • Random orientation • Denaturation of soluble biomolecules	Lipophilic membrane-bound enzymes were immobilized on hydrophobic-functionalized gold electrodes by simple adsorption (Kim & Kang, 2008).
Covalent bonding	Formation of a covalent bond between biomolecules and functionalized surface	• Good stability • High binding strength • Suitable for long-term use	• Random orientation • Linker molecules needed • Slow • Irreversible	EDC and NHS-mediated reaction: Immobilization of N-glycosylated pentapeptide (GPP, analogue of HbA1c binding site) on NH_2-funtionalized surface for HbA1c detection (Liu et al., 2012).
Specific interaction (also known as 'lock-and-key' or 'ligand-receptor' interaction)	Use of biocompatible linkers between the surface and biomolecules	• Improved orientation • High specificity and functionality • Well-controlled • Reversible	• Biocompatible linker molecules needed • Expensive • Slow	A biotin immunosensor where monoclonal anti-biotin IgG antibodies were complexed with surface-bound epitope (sulfo-NHS-biotin) (Khoo et al., 2016).

2.5.3 Nanomaterial application in sensor interfacial design

Owing to the excellent properties of nanomaterials, such as carbon nanotubes (CNTs), graphene oxide (GO) and nanoparticles like AuNPs, nanomaterials are widely applied in the construction of novel sensing devices (Satvekar et al., 2014). Employing nanomaterials in sensor interfacial design can significantly enhance the analytical performance of biosensors in terms of response time, sensitivity, stability, and detection ability (Li et al., 2010; Satvekar et al., 2014; Vashist & Luong, 2015). The high surface-to-volume ratio of nanomaterials allows high biomolecule loading, thus imparting excellent detection sensitivity (Vashist & Luong, 2015). Besides, the superior electrical conductivity of nanomaterials facilitates the electron transfer between biomolecules and electrodes, resulting in rapid target analyte detection (Ng et al., 2015; Satvekar et al., 2014).

In electrochemical biosensors, AuNPs are often used as electron transfer wires, immobilization platforms and electrocatalysts (Li et al., 2010). The electrode surfaces are surrounded by SAMs of organic molecules and biomolecules, which therefore block the electron transfer between the electrode and bioreceptors. This can affect the performance of electrochemical biosensing devices. Due to the high electrical conductivity of AuNPs, AuNPs are always employed as electron transfer wires in order to enhance the electron transfer between the electrode and the bioreceptors (Liu et al., 2011). The excellent biocompatibility of AuNPs also allows biomolecule immobilization on their surfaces without causing loss of biological activity of the biomolecules (Li et al., 2010). Moreover, the electrocatalytic property of AuNPs can reduce the overpotential of many electrochemical reactions, enhance the reversibility of some redox reactions, and even allow the development of enzyme-free biosensors (Li et al., 2010). Therefore, AuNPs have attracted immense interest in the field of electrochemical biosensors.

2.5.4 Anti-fouling coatings for electrochemical immunosensors

Non-specific protein adsorption, or biofouling, is a serious concern in biosensor applications because it can affect the sensitivity and selectivity of biosensors, especially for immunosensors used in biological samples (e.g., serum, blood, saliva and urine) that contain many undesirable biological interferences (molecules other than the target analyte). The reason is that the immunosensor's detection signals can be influenced by unwanted proteins (molecules besides the target analyte) present in samples. For instance, the biotin-immunosensor can detect biotin in human serum, but the presence of proteins (unwanted interferences or proteins) in human serum may affect the signals for biotin detection. The detection signals are normally dependent on the specific interaction between antigens and antibodies. Such specific interactions, also known as 'lock-and-key' or 'ligand-receptor' interactions, are strong, but non-covalent bonds occur between two biomolecules like antigens and antibodies (Dhruv, 2009; Moina & Ybarra, 2012). Non-specific protein binding to the transducer surface will hinder or prevent the target analytes from accessing the binding sites on the immobilized bioreceptors, thus allowing biofouling, resulting in low sensor sensitivity (Gui, 2011). This is because the formation of a biofouling layer on the sensor surface increases the sensor surface impedance, resulting in sensor sensitivity loss. Moreover, the binding sites of the immobilized bioreceptors may also be occupied by unwanted proteins with a similar structure or composition as the target analyte (Dhruv, 2009). This would cause inaccurate detection signal obtained due to the non-specific protein adsorption on the immunosensor surface. For instance, biocytin, which has a similar structure as biotin, can occupy the binding sites of anti-biotin antibodies on biotin-immunosensors, resulting in inaccurate signals for biotin detection. Therefore, molecules with anti-fouling properties are in high demand in the field of biosensor application, especially for the fabrication of immunosensor surfaces.

A series of organic polymers appear to have anti-fouling properties, including OEG, PEG, poly(vinylalcohol) (PVA) and polyglycerols (PGs) (Gui, 2011). The anti-fouling properties of organic polymers depend on the formation of the hydration layer based on their hydrophilicity and steric repulsion caused by the flexible polymer chains (Zhang & Chiao, 2015). Among them, PEG is a well-known anti-fouling molecule in biomedical applications owing to its strong protein adsorption resistance, high biocompatibility and nontoxicity (Gui, 2011; Zhang & Chiao, 2015). Besides, many studies have demonstrated that enhance biosensor surface selectivity and better prevention of cell adhesion on biosensor surfaces are achievable by using OEG in biosensor surface fabrication (Gui, 2011). However, OEG and PEG are not chemically stable because they can be easily degraded by oxidation, especially in biological media (Gui, 2011; Lowe et al., 2015).

Other functionalities like zwitterionic polymers with equal amounts of positive and negative charges have been recognized to possess a certain degree of anti-fouling ability. PC moiety, a long-chain polymer composed of a negatively-charged phosphate group and a positively-charged choline group, seems to be a protein-resisting molecule but is readily prone to hydrolysis (Darwish et al., 2015; Gui, 2011; Zhang & Chiao, 2015). However, the surfaces of electrochemical biosensors functionalized with long-chain polymers can become high-impedance surfaces, leading to electrode sensitivity depletion (Darwish et al., 2015). In order to develop a chemically stable, anti-fouling immunosensor surface with low impedance, aryl diazonium salts with single-charge (e.g. $–SO_3^-$ or $–N(Me)_3^+$) or zwitterionic groups can be excellent alternative anti-fouling molecules replacing long-chain molecules (Darwish et al., 2015; Gui, 2011). Zwitterionic phenyl derivative systems have many advantages over long-chain polymer systems (e.g., OEG and PC systems) in terms of chemical stability and electrochemical properties. Applying molecular wires in zwitterionic phenyl derivative layers is

unnecessary, because the layers have shorter electron transfer pathways that can significantly reduce surface impedance (Gui, 2011).

2.6 Electrochemical immunosensor surface regeneration approaches for repeated use

Quantitative biosensors should have a wide dynamic range with high accuracy and signal resolution in order to obtain high signal-to-noise ratio in target analyte detection so the quantitative devices are able to monitor the specific interaction between biomolecules and the formation of specific biomolecular complexes (Choi, 2011). A series of calibration measurements are required for quantitative detection. Variations may occur due to batch-to-batch irreproducibility and unmanageable experimental conditions, if disposable devices are used to perform the calibration measurements (Choi, 2011). Therefore, the detection signals obtained may be inaccurate and unreliable. This has encouraged the development of reusable or regenerative biosensors for repeated measurements. A comparisons of disposable and reusable biosensors is presented in Table 2.4.

Table 2.4: Comparisons between disposable and reusable biosensors

(Khoo et al., 2016; Thévenot et al., 2001; Choi, 2011).

	Disposable biosensor	**Reusable biosensor**
Definition	• A type of single-use and non-regenerative device. • It is very difficult to regenerate.	• A type of multiple-use and regenerative device. • It can be used several times.
Advantages	• Simple and time-saving because no regeneration steps are required. • Suitable for samples that contain infectious bacteria (especially clinical samples).	• Multiple-use or for multiple measurements. • Regenerative. • Reproducible. • Low cost due to device reusability. • Environmentally friendly because less waste is produced.
Disadvantages	• Non-regenerative. • Non-reusable. • High cost for long-term use. • Not environmentally friendly.	• Loss of detection ability, sensitivity, and selectivity after multiple measurements if it is non-regenerative. • Limited sample types because it is not suitable for use on samples containing infectious bacteria.

Table 2.4: Continued.

	Disposable biosensor	**Reusable biosensor**
Limitations	• Single-use or one-time measurement. • Variation occurs if a disposable biosensor is used to perform a series of measurements for detailed calibration purpose, which may affect result accuracy and reliability.	• Not user-friendly due to regeneration steps required. • High technology is required to regenerate the sensor surface 100% so it can be reused.
Challenges	A challenge faced by the disposable biosensor industry is the environmental impact. It is difficult to replace the raw materials of disposable biosensors using biodegradable resources. Additionally, it is a challenge to maintain cost-effectiveness without compromising quality in terms of accuracy, sensitivity and selectivity.	The industry has the challenge of developing reusable biosensors that are capable of performing with minimal detection loss while maintaining high sensitivity and selectivity after multiple uses.

Table 2.4: Continued.

	Disposable biosensor	**Reusable biosensor**
Examples	• A glucose biosensor based on co-dispersion of a diffusional polymeric mediator and glucose oxidase (GOX) in a nanoparticulate membrane on a screen-printed carbon electrode (Gao et al., 2005). • A urea biosensor based on an ammonium-sensitive transducer (Eggenstein et al., 1999). • A DNA electrochemical biosensor used for the detection of metallic drugs, such as titanium and platinum drugs, titanocene dichloride and cisplatin (Santiago-Lopez et al., 2014). • A transcutaneous oxygen sensor based on the amperometric Clarke cell principle (Lam & Atkinson, 2002). • A multi-walled carbon nanotube (MWCNT)-based disposable biosensor for organophosphorus detection using the amperometric method (Jha & Ramaprabhu, 2009).	• A glucose biosensor developed by a robust radiofrequency-integrated passive device (Kim et al., 2015). • A cholesterol biosensor based on cholesterol oxidase immobilized onto a thioglycolic acid self-assembled monolayer modified with smart bio-chips (Rahman, 2014). • A laccase-based biosensor for the detection of ortho-substituted phenolic derivatives (Sarika et al., 2015). • A fiber optic biosensor for the detection of drugs and toxicants (Eldefrawi et al., 1993). • A potassium ion biosensor based on electrochemiluminescence resonance energy transfer (He et al., 2013). • A mercury(II) biosensor based on "turn on" resonance light scattering (Yue et al., 2013).

Immunosensor surface regeneration approaches can be categorized in two groups. The first approach is to remove the linker molecules that bind the bioreceptors to solid surfaces by chemical treatments using acids, bases or detergents (Choi, 2011). However, corrosive solutions may not only remove the linker molecules but could also slightly or extremely damage the surface (Choi, 2011). Therefore, the damaged surface cannot be reused anymore, leading to unsuccessful immunosensor surface regeneration. Besides, SAMs, which are a common linker used in immunosensors, are able to detach from metal surfaces by electrochemical desorption (Choi & Chae, 2009). When applying a negative potential to a gold surface, the SAMs is desorbed from the gold surface by one-electron reduction in the electrolyte (Choi & Chae, 2009). Hence, the gold surface can be regenerated for the next detection cycle. However, the high reductive potential applied for SAMs desorption can lead to metal electrode corrosion and hydrogen evolution reaction (Choi & Chae, 2009), potentially affecting biosensor sensitivity and accuracy as well as the structure of the regenerated SAMs for the next detection cycle. Additionally, detached SAMs re-adsorption is an issue in immunosensor regeneration, because accumulation caused by SAMs re-absorption can disturb the subsequent immobilization steps and then affect sensor sensitivity (Choi, 2011).

The second approach is to detach the target analyte from the immobilized biorecognition molecules using regeneration agents, like chaotropic reagents (e.g., ethanol, butanol and urea) or ionic solutions (e.g., $MgCl_2$ and Na_3PO_4) at high concentrations, detergents (e.g., Tween-20, Tween-80 and Triton X-100) or water-soluble organic solvents (e.g., acetonitrile, formic acid and dimethyl sulfoxide) (Andersson et al., 1999; Chung et al., 2006). The detection ability of the sensor can be significantly affected by surface regeneration, as the strong agents destroy the bioreceptors' bioactivity. In another case, antigens (target analyte) can be releases from the immobilized bioreceptors by using temperature-sensitive polymer-antibody

conjugates as bioreceptors (Liu et al., 2008). The temperature-sensitive polymer can switch reversibly between the collapsed form and extended form to control the binding or release of antigens (target analyte) (Liu et al., 2008). Nonetheless, the application of temperature-controlled surface regeneration approaches with immunosensors is limited by the fact that most biomolecules readily denature under extreme temperatures (≥40ºC).

Based on the reversible affinity interactions between antibodies and antigens, an analogue to the immobilized antigen (bioreceptor) can be used to displace the antibodies (target analyte) from the bioreceptors, allowing repeated sensor surface use (Yoon et al., 2002). High-affinity specific interactions between antibodies and antigens can provide high immunosensor sensitivity but slow reversibility, therefore it is difficult for the antigens to dissociate from the bound antibodies (Khoo et al., 2016; Oldham & Asanov, 1999). Additional force such as an electric field must be applied to speed up the reversibility of the antigen-antibody interactions so the immunosensor surface can rapidly regenerate (Khoo et al., 2016). Because a distinct correlation exists between immunosensor surface charge and biomolecule adsorption affinity, the dissociation of bound antibodies from the surface-bound epitope and the non-specific protein adsorption can be controlled by alternating the surface charge using electrochemical polarization technique (Holmlin et al., 2001; Khoo et al., 2016; Oldham & Asanov, 1999).

CHAPTER 3: EXPERIMENTAL PROCEDURES

3.1 Reagents and materials

1,3-Dicyclohexylcarbodiimide (DCC, 99%), 1,4-phenylenediamine (Ph-NH_2, ≥99%), 4-nitroaniline (Ph-NO_2, ≥99%), sodium nitrite ($NaNO_2$, ≥99%), 20 nm gold nanoparticles (AuNPs), 2-[2-(2-methoxyethoxy)ethoxy]acetic acid (OEG-COOH), monoclonal anti-biotin IgG antibody from goat, biotin, potassium phosphate dibasic (K_2HPO_4, ≥98%), potassium phosphate monobasic (KH_2PO_4, ≥99%), potassium chloride (KCl, ≥99%), sodium chloride (NaCl, ≥99%), sulfanilic acid (Ph-SO_3^-, 99%), cytochrome C (Cyt C, ≥95%), ascorbic acid, uric acid (≥99%), and guanine (98%) were purchased from Sigma-Aldrich (USA). Potassium ferricyanide ($K_3[Fe(CN)_6]$, ≥99%) and (4-aminophenyl) trimethylammonium iodide hydrochloride (PH-NMe_3^+, 94%) were purchased from Acros (USA). Sulfo-NHS-biotin was purchased from Thermo Scientific Company (USA). Di-sodium hydrogen phosphate dihydrate ($Na_2HPO_4.2H_2O$, ≥99.5%) and acetonitrile (≥99%) was purchased from Merck (Germany). Sodium hydroxide (NaOH, 48-50%), hydrochloric acid (HCl, 37%), and ethanol (EtOH, 99.7%) were purchased from R&M (UK). Human serum was purchased from Life Technologies Corporation, USA. Bovine serum albumin (BSA) was purchased from Amresco, USA. Micropolish alumina powder (1.0 µm, 0.3 µm and 0.05 µm) and microcloth pads were purchased from Buehler, USA. Purified nitrogen gas was purchased from Linde Sdn. Bhd. (Malaysia). All reagents were used as received, and all aqueous solutions were prepared with Milli-Q^{TM} water with resistivity of 18.2 MΩ•cm at 25ºC (Millipore, Sydney, Australia).

3.2 Glassy carbon (GC) electrode polishing

GC electrodes (BASi, USA) were polished successively with 1.0, 0.3, and 0.05 µm alumina slurries on microcloth pads. The electrodes were thoroughly rinsed with Milli-Q^{TM} water between polishing steps. Before electrode surface fabrication, the electrodes were dried with a stream of purified nitrogen gas.

3.3 Electrochemical measurements

All electrochemical measurements were made using an AutoLabIII potentiostat (Metrohm AutoLab, Netherlands) and a conventional three-electrode system comprising a GC working electrode, a platinum wire as the auxiliary electrode and Ag/AgCl (3.0 M KCl) as the reference electrode. A Plate Material Evaluating Cell consisting of a Teflon cell base and Teflon cell body was used to hold the GC electrode. An O-ring made of rubber was placed between the cell body and the GC electrode to avoid electrolyte solution leakage. Two 20 mm screws were used to attach the cell blocks. The platinum wire and reference electrode were inserted into the evaluating cell through the Teflon cap holes. All potentials applied were measured relative to the Ag/AgCl reference electrode at room temperature (25°C). Surface characterization of the GC electrode fabricated by CV and EIS was done in phosphate buffer solution (pH 7.0) containing 1 mM of $[Fe(CN)_6]^{4-/3-}$ redox species. The phosphate buffer solution was prepared with 0.05 M of KCl and 0.05 M of K_2HPO_4/KH_2PO_4 and adjusted to pH 7.0 with NaOH or HCl solution (Liu et al., 2012). CV and EIS were used to verify the deposition of the functionalized layers on the GC electrode surface. EIS also served as an electrochemical transducer to detect the specific interactions between biotin (target analyte) and surface-bound monoclonal anti-biotin IgG antibodies. The CV measurements for surface characterization were performed at a scan rate of 100 mV s^{-1} for 2 cycles between +0.6 V and -0.2 V versus Ag/AgCl. The EIS measurements were performed with DC potential of 0.200 V, frequency range of 0.1-10000 Hz and amplitude of 0.01 V. The

electrochemical reductive modification of the GC electrode was done by CV with a scan rate of 100 mV s^{-1} for 2 cycles between +0.2 V and -0.6 V versus Ag/AgCl. Immunosensor surface regeneration was carried out by chronoamperometry with potential of -800 mV for a duration of 600 s. Nova software was used to model the Nyquist plots obtained by EIS with an equivalent circuit and to determine the electrolyte solution resistivity (R_S), phase constant element (Q, n), and charge transfer resistivity (R_{CT}).

3.4 Two versions of immunosensor interface designs

In the first version of an immunosensor interface, OEG-COOH was applied as anti-fouling molecules; whereas in the second version, Ph-SO_3^- and Ph-NMe_3^+ were the anti-fouling molecules applied (Refer to Figure 3.1). As mentioned in the literature review, both OEG-fabricated and zwitterionic surfaces containing Ph-SO_3^- and Ph-NMe_3^+ displayed excellent anti-fouling properties. However, the structural difference between these anti-fouling molecules may yield different electrochemical characteristics, which could affect immunosensor performance. Therefore, the electrochemical characteristics of OEG- and Ph-SO_3^-/Ph-NMe_3^+-fabricated immunosensors are investigated in this study.

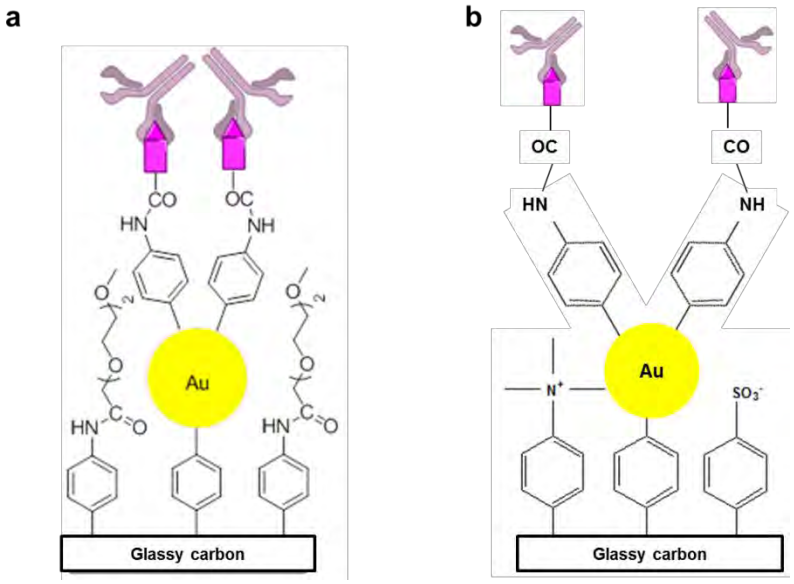

Figure 3.1: Immunosensor interfacial designs. (a) First version (OEG-COOH as anti-fouling molecules); (b) Second version (Ph-SO_3^- and Ph-NMe_3^+ zwitterionic molecules as anti-fouling molecules).

3.4.1 Stepwise immunosensor interface fabrication for the first interfacial design version

Figure 3.2 illustrates the bottom-up stepwise fabrication of an immunosensor interface for the direct detection of small molecule biotin. First, the well-polished GC electrode was passivated with a mixed monolayer of Ph-NH_2/Ph-NO_2 by CV at a scan rate of 100 mV s^{-1} for 2 cycles between +0.2 V and -0.6 V versus Ag/AgCl. To generate aryl diazonium salt, a 2.5 mM Ph-NH_2/Ph-NO_2 solution was prepared in 0.5 M of HCl containing 10 mM of $NaNO_2$. Then the diazonium cation solution was deaerated with purified nitrogen gas and allowed to react for at least 10 min prior to clean GC electrode derivatization. Prior to the next step, the fabricated electrode was rinsed with Milli-Q^{TM} water and dried under a stream of nitrogen gas. AuNPs were covalently bound to the aromatic rings on the electrode surface to produce AuNPs/Ph-NH_2:Ph-NO_2-fabricated GC electrode (Surface2, Figure 3.2) by scanning CV with a scan rate of 100 mV s^{-1} for 3 cycles between +0.6 V and -0.8 V versus Ag/AgCl. As Ph-NH_2 on the electrode

surface has been treated with $NaNO_2$ and HCl for diazotization, therefore the diazonium group splits from the aromatic ring to form dinitrogen and aryl radical when applying electric potential; the AuNPs can then bind to the radical through covalent bonding (Liu et al., 2011). Subsequently, the 4-nitrophenyl groups on the GC electrode surface were electrochemically reduced to 4-aminophenyl groups in a protic solution to form AuNPs/Ph-NH_2-fabricated GC electrode (Surface 3, Figure 3.2). The protic solution comprised 90:10 v/v H_2O-EtOH and 0.1 M of KCl. To prepare OEG/AuNPs/Ph-NH_2-fabricated GC electrode (Surface 4, Figure 3.2), OEG-COOH was attached to the amino groups on AuNPs/Ph-NH_2-fabricated GC electrode (Surface 3) through an amide bond by incubating AuNPs/Ph-NH_2-fabricated GC electrode (Surface 3) in an absolute EtOH solution containing 10 mM of OEG-COOH and 40 mM of DCC for 6 h at 25ºC. Subsequently, the AuNPs on OEG/AuNPs/Ph-NH_2-fabricated GC electrode (Surface 4, Figure 3.2) were further modified with Ph-NH_2 to produce Ph-NH_2/OEG/AuNPs/Ph-NH_2-fabricated GC electrode (Surface 5) by scanning at potential between +0.2 V and -0.6 V in a 0.5 M HCl solution containing 10 mM of $NaNO_2$ and 5 mM of Ph-NH_2 for 2 cycles at a scan rate of 100 mV s^{-1}. The overnight incubation of Ph-NH_2/OEG/AuNPs/Ph-NH_2-fabricated GC electrode (Surface 5, Figure 3.2) in 1 mg mL^{-1} of sulfo-NHS-biotin prepared in phosphate buffered saline (PBS), pH 7.4, at 4ºC resulted in the formation of specific binding sites for monoclonal anti-biotin IgG antibody on the fabricated electrode surface. PBS was prepared using 0.137 M of NaCl and 0.1 M of $NaH_2PO_4.2H_2O$ and adjusted to pH 7.4. Finally, the immunosensor interface (Ab/Biotin/Ph-NH_2/OEG/AuNPs/Ph-NH_2-fabricated GC electrode) used for biotin detection was formed by incubating the fabricated electrode in the monoclonal anti-biotin IgG antibody (50 µL, 0.5 µg mL^{-1}) prepared in PBS for 30 min at 25ºC.

The antibody-bound electrodes were used to carry out a series of calibration measurements with different concentrations of free biotin solution (100–2500 μg mL^{-1}, 50 μL) prepared in PBS at pH 7.4. EIS measurements were recorded for each electrode before and after the dissociation of the bound antibodies.

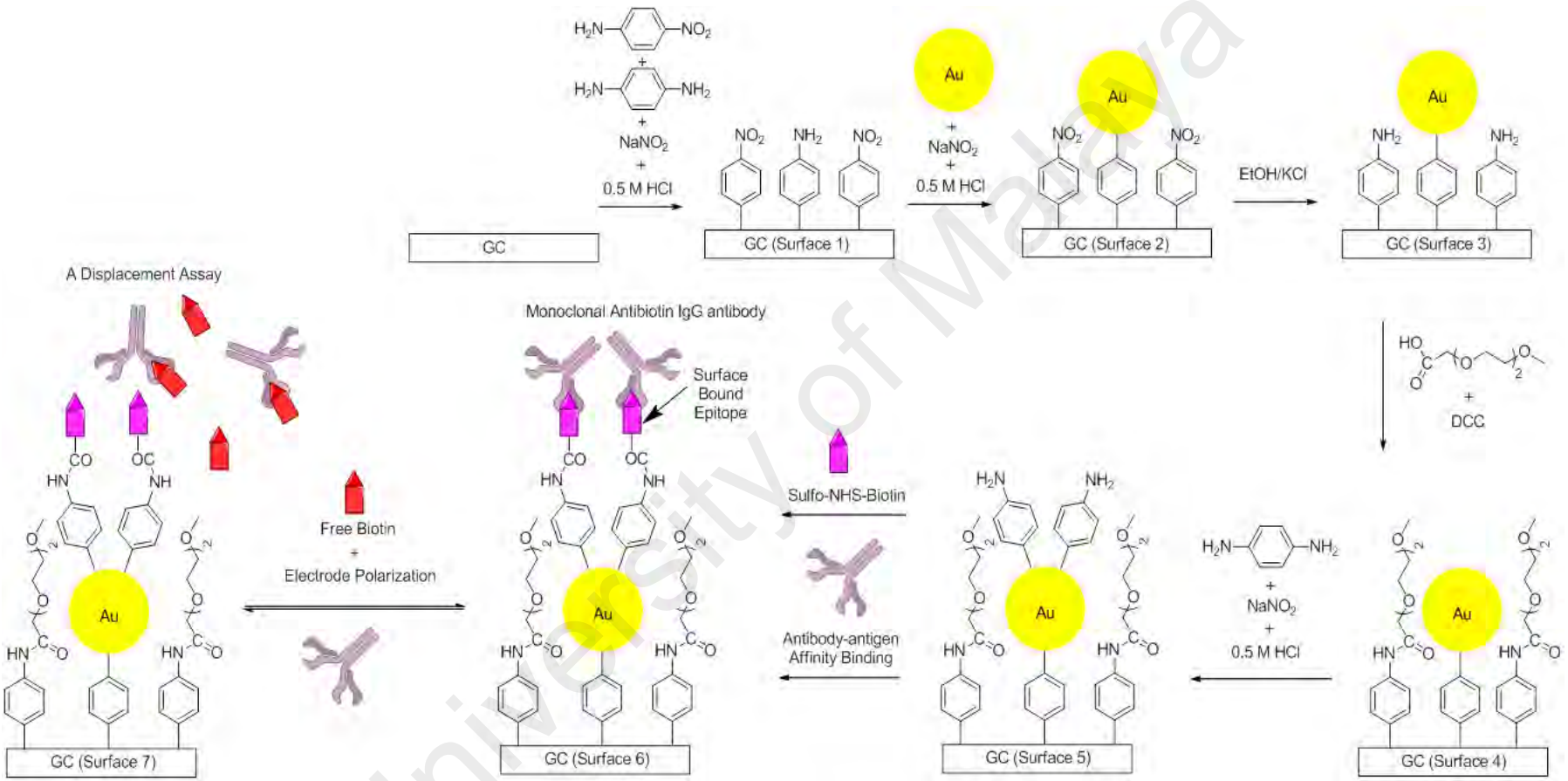

Figure 3.2: Stepwise fabrication of the first version of immunosensor interface.

The AuNPs/Ph-NH_2:Ph-NO_2–modified GC electrode surface (Surface 2 in Figure 3.2) and bare GC electrode surface were morphologically characterized by Hitachi SU8000 FE–SEM. FE-SEM analysis served to confirm the attachment and observe the distribution of AuNPs on the GC electrode.

All experiments involving FTIR were performed using Spectrum^{TM} 400 (Perkin Elmer, USA). An FTIR spectrometer covers both mid- and far-infrared spectral ranges. Starting from the bare GC electrode surface, the fabricated GC electrode was scanned with the FTIR spectrometer between each fabrication step. An FTIR study was used to investigate the functional groups of organic molecules present on the GC electrode surface through stepwise fabrication.

3.4.2 Stepwise immunosensor interface fabrication for the second interfacial design version

A clean GC electrode was fabricated according to the steps presented in Figure 3.3. The clean electrode was functionalized with a mixed monolayer of Ph-NH_2/Ph-SO_3^-/Ph-NMe_3^+ by electrochemical reduction. To produce the aryl diazonium cations, 2 mM of Ph-NH_2, 1.5 mM of Ph-SO_3^- and 1.5 mM of Ph-NMe_3^+ were dissolved in 0.5 M of HCl containing 10 mM of $NaNO_2$, followed by deaeration of the solution with purified nitrogen gas for 10 min. The electrode was functionalized with the in-situ generated aryl diazonium cations by scanning CV at a scan rate of 100 mV s^{-1} for two cycles between +0.2 V and -0.6 V versus Ag/AgCl. The functionalized electrode was then rinsed with Milli-Q^{TM} water and dried under a stream of nitrogen gas. Next, the AuNPs were coupled to the 4-amoniphenyl groups on the GC surface by electrochemical scanning at a scan rate of 100 mV s^{-1} for 3 cycles between +0.6 V and -0.8 V versus Ag/AgCl (3 M of KCl). After that, the AuNPs bound on AuNPs/Ph-NH_2:Ph-SO_3^-:Ph-NMe_3^+-fabricated GC electrode (Surface 2, Figure 3.3) were further functionalized with Ph-NH_2 by

scanning potential between +0.2 V and -0.6 V with 0.5 M of HCl solution containing 10 mM of $NaNO_2$ and 5 mM of Ph-NH_2 for 2 cycles at a scan rate of 100 mV s^{-1}. To generate Biotin/Ph-NH_2/AuNPs/Ph-NH_2:Ph-SO_3^-:Ph-NMe_3^+-modified GC electrode (Surface 4) as seen in Figure 3.3, the Ph-NH_2/AuNPs/Ph-NH_2:Ph-SO_3^-:Ph-NMe_3^+-modified electrode was then incubated in 1 mg mL^{-1} of sulfo-NHS-biotin prepared in PBS overnight at 4°C. Finally, the epitope-bound electrode was incubated in 50 µL of monoclonal anti-biotin IgG antibody solution (0.5 µg mL^{-1}) prepared in PBS for 30 min at 25ºC.

The antibody-bound electrodes were exposed to a series of free biotin solutions (5 – 250 µg mL^{-1}, 50 µL) prepared in PBS at pH 7.4. EIS measurements were recorded for each of the electrodes before and after the immobilized antibody dissociation.

During immunosensor interface characterization of the improved interfacial design version by FE-SEM, the AuNPs/Ph-NH_2:Ph-SO_3^-:Ph-NMe_3^+-fabricated GC electrode surface (Surface 2 in Figure 3.3) and bare GC electrode surface were morphologically characterized. Besides, the fabricated GC electrode was scanned with the FTIR spectrometer between each fabrication step, starting from the bare electrode surface.

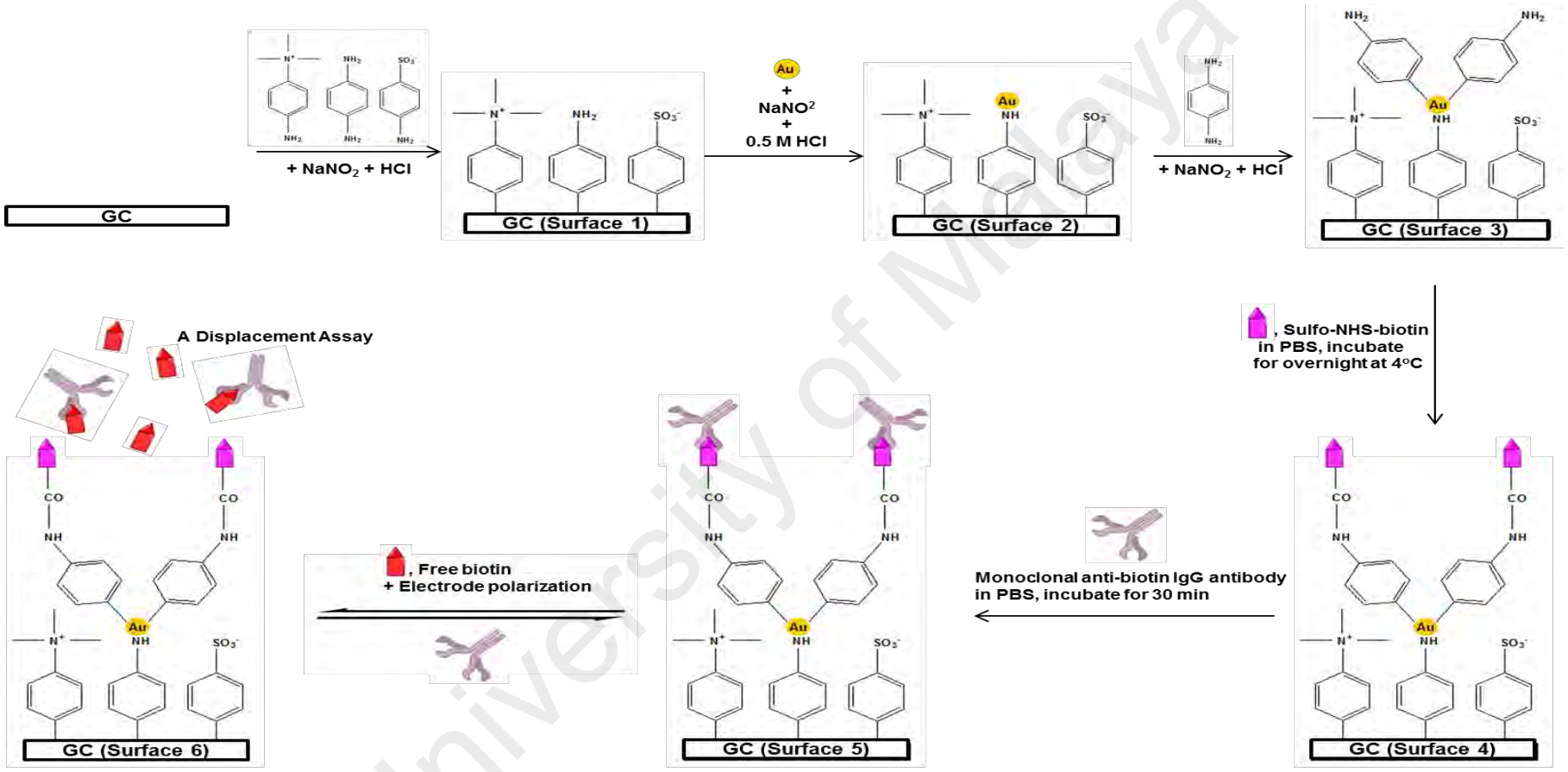

Figure 3.3: Stepwise fabrication of the second version of immunosensor interface.

3.5 Immunosensor surface regeneration (first version of immunosensor interface)

3.5.1 Immunosensor regeneration based on the reversible association-dissociation interactions between the antibody and surface-bound epitope

The epitope-modified immunosensor interface was first exposed to monoclonal anti-biotin IgG antibody solution (50 µL, 0.5 µg mL^{-1}) for 30 min, followed by free biotin solution (0.3 mg mL^{-1}) for 20 min to allow surface-bound antibody dissociation from the immunosensor interface. The original electrode was re-incubated in the antibody solution so the antibody could re-bind to the surface-bound epitope and the displacement assay could be performed again. This reversible interaction was repeated 5 times within 24 h. EIS measurements were taken before and after surface-bound antibody dissociation.

3.5.2 Voltage-induced surface-bound antibody dissociation for immunosensor regeneration

The biorecognition interface was regenerated by electrode polarization in the free biotin solution (0.3 mg mL^{-1}) to remove the surface-bound antibodies from the interface and then re-incubated in the antibody solution to allow antibody binding to the surface-bound epitope so that the displacement assay could be performed again (refer to Figure 3.4). A series of electrode polarizations at different potentials and time intervals were carried out to determine the optimal condition for the maximum dissociation of surface-bound antibodies. Electrode polarization can be conducted by chronoamperometry. Upon obtaining the optimal electrode polarization condition, immunosensor regeneration with applied voltage was conducted continuously 5 times within 24 h. EIS measurements were taken before and after surface-bound antibody dissociation. Furthermore, the passivation capacity of the grafted mixed layer of aryl diazonium salts

towards $Fe(CN)_6^{3-/4-}$ redox species was investigated by CV technique after the 1st, 5th, 10th and 15th cycles of surface regeneration.

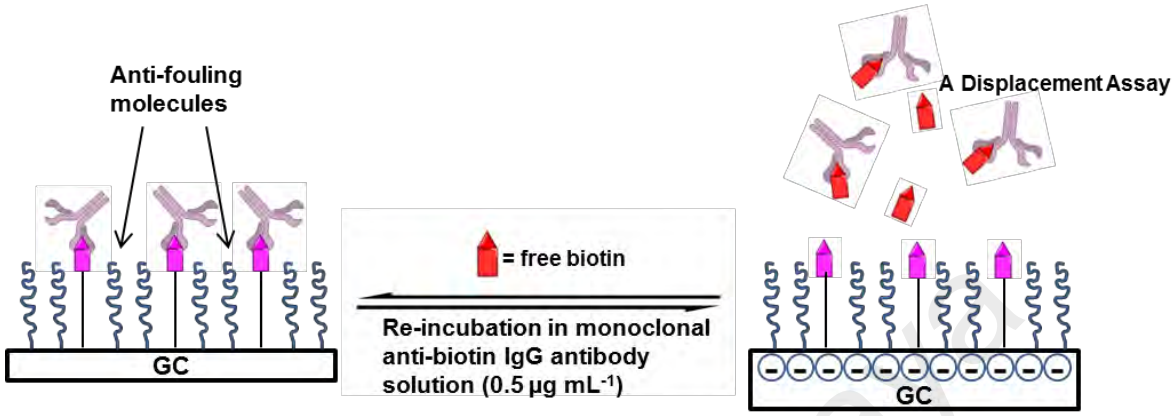

Figure 3.4: Mechanism of electrochemical immunosensor surface regeneration with the aid of induced voltage.

3.6 Anti-fouling and sensitivity studies of the $Ph\text{-}NH_2/Ph\text{-}SO_3^-/Ph\text{-}NMe_3^+$-fabricated GC electrodes with different molar ratios

The anti-fouling property and sensitivity of the immunosensor may be influenced by the different molar ratios of linker molecules ($Ph\text{-}NH_2$) and anti-fouling molecules ($Ph\text{-}SO_3^-$ and $Ph\text{-}NMe_3^+$) attached on the GC surface. Therefore, the GC electrodes were fabricated with $Ph\text{-}NH_2$:$Ph\text{-}SO_3^-$:$Ph\text{-}NMe_3^+$ at different molar ratios of 4:0.5:0.5 (Mix 1), 3:1:1 (Mix 2), 2:1.5:1.5 (Mix 3) and 1:2:2 (Mix 4) for anti-fouling and sensitivity studies. Prior to investigating the anti-fouling property of $Ph\text{-}NH_2/Ph\text{-}SO_3^-/Ph\text{-}NMe_3^+$-fabricated GC electrodes, the anti-fouling properties of $Ph\text{-}NH_2$-, $Ph\text{-}SO_3^-$-, $Ph\text{-}NMe_3^+$- and $Ph\text{-}SO_3^-/Ph\text{-}NMe_3^+$-fabricated electrodes with a molar ratio of 1:1 were initially investigated. The experiment was conducted by exposing the bare GC surface and the aryl diazonium molecule-fabricated GC surfaces to 1 mg mL^{-1} of BSA solution for 1 h at 25ºC. EIS measurements were recorded before and after exposing the bare GC electrode and functionalized GC electrode to the BSA solution. The experiment was

repeated by replacing BSA with 2 mg mL^{-1} of Cyt–C and 0.2 g mL^{-1} of infant formula (Dutch Lady). PBS served as the control in the experiment. Next, the anti-fouling property of Ph-NH_2/Ph-SO_3^-/Ph-NMe_3^+-fabricated GC electrodes was investigated with the same method mentioned above.

To study the sensitivity of immunosensors fabricated with different molar ratios of Ph-NH_2 and Ph-SO_3^-/Ph-NMe_3^+, the GC electrodes were first made with a combination of Ph-NH_2/Ph-SO_3^-/Ph-NMe_3^+ at various molar ratios (Mix 1, Mix 2, Mix 3 and Mix 4), followed by attaching the AuNPs on top of the linker molecule Ph-NH_2, sulfo-NHS-biotin and monoclonal anti-biotin IgG antibody. The antibody-bound electrodes were pulsed at -800 mV for 10 min in 100 μg mL^{-1} biotin solution prepared in PBS (Khor et al., 2011). EIS measurements were recorded before and after exposing the fabricated electrodes to biotin solution.

3.7 Performance of the second immunosensor version in terms of reproducibility, selectivity, stability and intra-day/inter-day precision

In order to guarantee good quality in the mass production for product commercialization, a reproducibility study must be conducted to investigate the performance of the immunosensor interface developed. A reproducibility study of the immunosensor was carried out using 10 fabricated GC electrodes. The electrodes were exposed to free biotin solution (75 μg mL^{-1}, 50 μL) prepared in PBS. Subsequently, the electrodes were rinsed with PBS solution to remove the dissociated antibodies. EIS measurements were recorded for each electrode before and after the dissociation of the immobilized antibodies.

A selectivity study was carried out to ensure that the immunosensor interface produced is highly specific to biotin and has no response to other molecules. Six

different types of small organic molecules (biotin, sucrose, citric acid, ascorbic acid, uric acid and guanine) were tested in the study. EIS measurements were recorded before and after exposing the fabricated electrodes to the small organic molecule solutions.

In ensuring the long-term stability of the surface-bound biomolecules on the immunosensor interface, a stability test had to be performed to ensure the detection ability of the immunosensor. The GC electrodes produced were kept in PBS solution for 1, 3, 5, 7, 14, 21, and 28 days, respectively, at 4ºC. EIS measurements were taken before and after exposing the fabricated electrodes to 75 μg mL^{-1} free biotin solution for 1, 3, 5, 7, 14, 21, and 28 days, respectively.

Intra-day and inter-day precision studies were done to ensure there were no significant variations between the immunosensor results within a day or in different days. For the intra-day precision study, 50 μg mL^{-1}, 75 μg mL^{-1}, and 100 μg mL^{-1} of free biotin solutions prepared in PBS were tested with the developed electrodes. Each concentration was tested 4 times with different immunosensor electrodes within the same day. In the inter-day precision study, the fabricated electrodes were tested in 50 μg mL^{-1}, 75 μg mL^{-1}, and 100 μg mL^{-1} of free biotin solutions within the same day. The experiment was repeated for 5 days with newly-prepared electrodes.

3.8 Analytical performance of electrochemical immunosensor with the second interfacial design version in real samples

3.8.1 Quantification of biotin in infant formulas with the second electrochemical immunosensor version using a standard addition method

Two types of infant formulas (Dutch Lady and Friso Gold) were selected for testing. Dutch Lady is a product of Malaysia, while Friso Gold is a product of The Netherlands. The two formulas contain different amounts of biotin. In order to eliminate the matrix effect, the standard addition method was applied to quantify biotin in the infant formulas. Both formula samples (Dutch Lady and Friso Gold) were prepared as follows. Six vials of 1.5 mL infant formula (1 g infant formula was dissolved in 5 mL Milli-Q^{TM} water) were prepared, and 5 μg mL^{-1} of biotin solution were added to the vials in varying amounts: 0, 5, 10, 15, 20, and 25 μL. No other pre-treatment steps, it only involves a simple dissolvation of infant formula in Milli-Q^{TM} water. Before exposing the fabricated electrode surface in the infant formula solution, a Nyquist plot of the electrode surface (Ab/Biotin/Ph-NH_2/OEG/AuNPs/Ph-NH_2-fabricated GC elctrode) was recorded. After exposing the fabricated electrode surface into the infant formula solution, the electrode surface was rinsed with copious amount of Milli-Q^{TM} water to remove the interferences (e.g., white particles) from the electrode surface before the imunosensor surface was tested in $[Fe(CN)6]^{4-/3-}$ solution to obtain the EIS measurement after the displacement assay, so that the EIS measurement won't be affected by the interferences.

3.8.2 Method validation by HPLC in the quantification of biotin in infant formulas using a standard addition method

About 5–10 g of infant formula were dispersed into 20 mL of 70% ethanol. The solution was sonicated for 30 min, followed by centrifugation at 4000 rpm for 10 min. The upper solution layer was transferred to a 25 mL volumetric flask, which was filled to the mark with 70% ethanol. The solution was filtered through a 0.45 μm syringe filter (regenerated cellulose, RC). Standard addition was performed as described below. Seven vials of 1.0 mL infant formula were prepared. 1000 μg mL^{-1} of biotin solution was added to the vials in the amounts of 0, 20, 40, 60, 80, 100, and 150 μL. The prepared samples were transferred to an HPLC vial and injected into the HPLC system according to the analytical conditions stated in Tables 3.1 and 3.2.

Table 3.1: HPLC setup for the analysis of infant formulas, biotin-containing supplements and serum.

Instrument	Waters HPLC with photodiode array detector
Absorbance	Infant formulas and serum: 190 nm Supplements: 200 nm
Mobile phase A	20 mM phosphate buffer at pH 2.5
Mobile phase B	Acetonitrile
Column	Merck Chromolith high resolution RP-18e encapped, 100 × 4.6 mm HPLC column
Injector	Infant formulas: full loop at 100 μL Serum: full loop at 50 μL Supplements: full loop at 20 μL

Table 3.2: Mode gradient setup for HPLC.

Time, min	Flow, mL min^{-1}	% A	% B
0.00	0.7	95	5
1.00	0.7	95	5
10.0	0.7	50	50
15.0	0.7	50	50
20.0	0.7	95	5
24.0	0.7	95	5

3.8.3 Direct detection of biotin in biotin-containing supplements using the second electrochemical immunosensor version

Two types of effervescent tablets (Guardian and Berocca) and B-complex capsules (21^{ST} Century) were investigated in this study. The mass of the tablets and capsules was recorded before solubilization. For the capsules (21^{ST} Century), the capsule caps were first dismantled to obtain the powder for mass measurement. 1 Guardian brand tablet was dissolved in 2.5 mL of Milli-Q^{TM} water, 1 Berocca brand tablet was dissolved in 3 mL of Milli–Q^{TM} water, and 5 capsules of 21^{ST} Century brand were dissolved in 4 mL of Milli–Q^{TM} water. The antibody-bound electrode was pulsed in the prepared sample solution (750 µL) at -800 mV for 10 min. EIS measurements were carried out before and after exposing the antibody-bound electrode to the sample solution. External calibration method was applied to determine the biotin concentration in the samples.

3.8.4 Method validation by HPLC for direct detection of biotin in biotin–containing supplements

An external calibration method was used to determine the biotin concentration in biotin-containing supplement samples. A calibration plot for a series of biotin solutions with concentrations of 2.5 - 40.0 µg mL^{-1} prepared in 80% acetonitrile was obtained using HPLC with a photodiode array detector. The biotin-containing supplements were pre-treated as follows. The effervescent tablet samples (Guardian and Berocca) were first mortared and pestled into fine powder. The sample powder (0.5 – 1 g) was dispersed in 10 mL of 80% acetonitrile. The solution was sonicated for 30 min to eliminate carbon dioxide, followed by centrifugation at 4000 rpm for 5 min. The solution was filtered through a 0.45 µm syringe filter (RC). The B-complex capsule covers (21^{ST} Century) were dismantled to obtain the powder. This sample powder (0.1 – 0.3 g) was dispersed in 5 mL of 80% acetonitrile. The mixture was vortexed for 5 min to disperse the powder, followed by centrifugation at 4000 rpm for 5 min. The solution was filtered through a 0.45 µm syringe filter (RC). The prepared samples were transferred into HPLC vials and injected into the HPLC system according to the analytical conditions stated in Tables 3.1 and 3.2.

3.8.5 Correlation between the detection signals obtained by electrochemical immunosensor and HPLC with photodiode array detector for human serum

10% human serum was prepared in PBS, pH 7.4. 1500 µg mL^{-1} of biotin solution was added to the vials, which contained 2.0 mL prepared serum, in amounts of 20, 40, 60, 80, and 100 µL. Electrochemical immunosensor and HPLC with photodiode array detector were used to detect the biotin in the samples at different concentrations.

CHAPTER 4: RESULTS AND DISCUSSION

4.1 First electrochemical immunosensor version used for direct detection of biotin molecule

4.1.1 Electrochemical characterization of the immunosensor interface with OEG as anti-fouling molecule

The CV technique was employed to investigate the electrochemical characteristics of the modified biosensor interface using $Fe(CN)_6^{3-/4-}$ redox-active species after every single step of GC electrode surface fabrication. Figure 4.1 shows cyclic voltammograms of bare GC electrode surface and GC electrode surfaces after the attachment of a mixed layer of Ph-NH_2/Ph-NO_2, AuNPs, OEG-COOH, Ph-NH_2, sulfo-NHS-biotin and monoclonal anti-biotin IgG antibody. A pair of well-defined Faradaic peaks for $Fe(CN)_6^{3-/4-}$ species was clearly visible on the reversible cyclic voltammogram of bare GC surface (Figure 4.1(i)), because the redox species had directly access to the GC electrode. Before attaching the Ph-NH_2 and Ph-NO_2 on electrode surface, a mixture of Ph-NH_2 and Ph-NO_2 was treated with $NaNO_2$ and HCl for diazotization. Upon electric potential application, the diazonium group splits from the aromatic ring to form dinitrogen and aryl radical; this radical then attaches on electrode surface through covalent bonding (Gui, 2011). Therefore, no Faradaic peaks for the redox species were noted between +0.6 V and -0.4 V after the electrochemical deposition of Ph-NH_2/Ph-NO_2 (Figure 4.1(ii)), because redox species access to the electrode surface was inhibited by a mixed Ph-NH_2/Ph-NO_2 layer. After the electrochemical attachment of AuNPs, an increase in the peak current of redox species was evident on the cyclic voltammogram (Figure 4.1(iii)) of AuNPs/Ph-NH_2:Ph-NO_2-fabricated GC electrode (Surface 2, Figure 3.2) due to the conductivity of AuNPs. The enhanced electron transfer rate caused by the attachment of AuNPs was attested in the previous review study reported by Li et al. (2010). There was no significant change in the peak current of $Fe(CN)_6^{3-/4-}$ species

indicated (refer to Figure 4.1(iv)) after the electrochemical reduction of nitro groups on AuNPs/Ph-NH_2:Ph-NO_2-fabricated GC electrode (Surface 2, Figure 3.2). A slight decrease in the peak current of $Fe(CN)_6^{3-/4-}$ redox species was observed (Figure 4.1(v)) after OEG-COOH molecules were bound to the amino groups of the Ph-NH_2-modified GC electrode. The redox species were blocked from the OEG-modified GC electrode due to the long-chain OEG-COOH molecules. The Faradaic peaks of the redox species on Ph-NH_2/OEG/AuNPs/Ph-NH_2-fabricated GC surface (Surface 5, Figure 3.2) disappeared again as seen in Figure 4.1(vi), because redox species access to the Ph-NH_2/AuNPs-modified GC electrode was absolutely inhibited. Then, the sulfo-NHS-biotin (surface-bound epitope) attached on the AuNPs surface via linker molecules (Ph-NH_2), resulting in a small restriction in redox-active species access from solution to the AuNPs-modified electrode. Finally, the specific binding of monoclonal anti-biotin IgG antibodies to the sulfo-NHS-biotin on the AuNPs-modified GC surface led to the formation of an electrochemical immunosensor surface (Ab/Biotin/Ph-NH_2/AuNPs-modified GC surface, Surface 6 in Figure 3.2) for biotin detection. The specific binding covered the immobilized AuNPs with proteins and hindered $Fe(CN)_6^{3-/4-}$ species access to the electron transfer mediators (AuNPs) on the GC electrode, thus resulting in decreased peak current of the redox species (Figure 4.1(viii)).

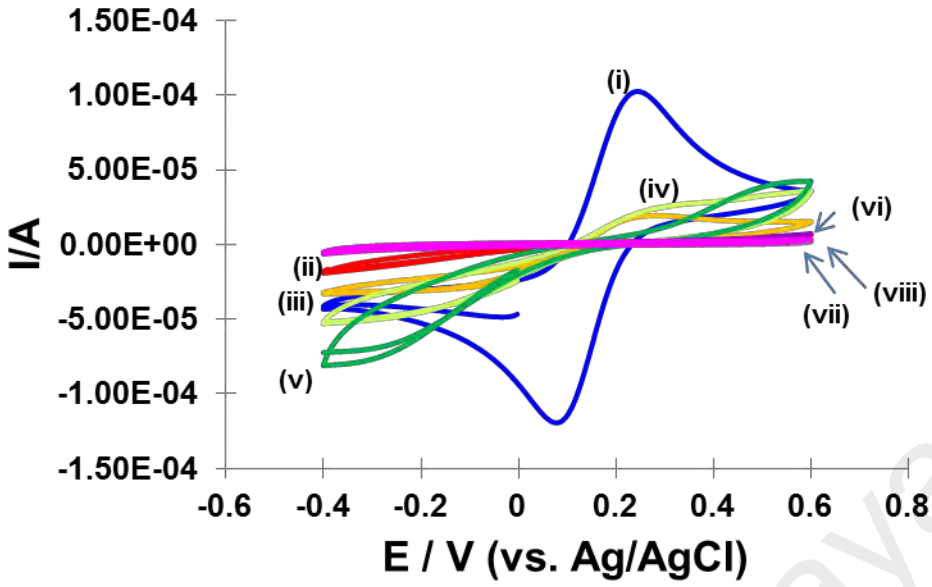

Figure 4.1: Stepwise surface characterization of the first immunosensor interface version by CV technique. Cyclic voltammograms recorded for (i) bare GC electrode (blue), (ii) Surface 1 (red), (iii) Surface 2 (orange), (iv) Surface 3 (light green), (v) Surface 4 (green), (vi) Surface 5 (purple), (vii) Surface 6 (grey), and (viii) Surface 7 (pink).

The EIS technique was used to study the GC surfaces characteristics after every step of GC electrode surface fabrication. Figure 4.2 presents the Nyquist plots of EIS measurements for bare and modified GC surface (Surface 1 to Surface 7). The parameters (e.g., R_{CT}, R_S, Q and n) as given in Table 4.1 can be determined by fitting the Nyquist plots with an equivalent electric circuit (inset of Figure 4.2). R_S, which refers to the resistivity between the Ag/AgCl reference electrode (3 M KCl) and the GC working electrode, is influenced by the ion type, ionic concentration, temperature and geometry of current flowing between the working electrode and reference electrode (Gheorghe-Constantin & Petru, 2011). The geometry of current flowing between the working and reference electrodes caused a slight attenuation in the R_S obtained from the experiment (Table 4.1). This means that the varying R_S values in Table 4.1 were not due to the stepwise immunosensor surface fabrication, but were indeed caused by the uneven current flow in the electrolyte (Gheorghe-Constantin & Petru, 2011). When the

current flows between the working electrode and reference electrode, the current flow in the electrolyte is usually non-uniform (Khoo et al., 2016). The capacitance (C_{dl}) was calculated with Equation 4.1 (Abouzari et al., 2009).

$$C_{dl} = R_{CT}^{\frac{1-n}{n}} \times Q^{\frac{1}{n}} \qquad \text{Equation 4.1}$$

C_{dl} and R_{CT} are represented by the impedance semicircle, which is correlated to electrical properties like the dielectric and insulating features of the electrode/electrolyte interface. Therefore, stepwise electrode surface fabrication can strongly influence C_{dl} and R_{CT} (Radi et al., 2009). Even so, the changes in C_{dl} obtained from the experiment were not as significant as the changes in R_{CT} caused by the electrode surface fabrication (Table 4.1). In addition, a constant phase element was used to replace the capacitor in the normal Randles equivalent circuit due to the broadening or deformation of the impedance semicircle (Abouzari et al., 2009). This was provoked by the inhomogeneous distribution of defects in the grain boundary vicinity or the roughness of the modified electrode surface (Abouzari et al., 2009). Fortunately, a parallel connection of a resistor and a constant phase element was investigated in this study as an appropriate solution to solve the problem. Additionally, the values of n shown in Table 4.1 were close to 1, indicating there were few defects in the layer fabricated on the GC electrode surface. Ultimately, R_{CT} was deemed the most suitable parameter for studying the interfacial properties of the fabricated GC surface throughout all surface fabrication steps and for monitoring the specific interaction between free biotin and surface-bound IgG antibody.

The changes in R_{CT} were monitored by EIS after each electrode surface fabrication step, where the changes in R_{CT} were completely consistent with the result obtained by CV. After the electrochemical deposition of Ph-NH_2/Ph-NO_2 on the GC surface, the mixed layer of Ph-NH_2/Ph-NO_2 inhibited the $Fe(CN)_6^{3-/4-}$ redox species from

approaching the GC surface, therefore the R_{CT} increased (Figure 4.2(ii)). A significant decrease in R_{CT} was noted after the AuNPs were covalently bound to the amino groups of Ph-NH_2 modified on the electrode surface (Figure 4.2(iii)), because the conductive AuNPs acted as an electron transfer mediator between electrolyte and electrode (Liu et al., 2011). The attachment of long-chain OEG-COOH molecules to the amino groups on AuNPs/Ph-NH_2-fabricated GC surface (Surface 3, Figure 3.2) led to the increase in R_{CT} (Figure 4.2(v)). Subsequently, the attachment of Ph-NH_2 on the AuNPs surface resulted in blocking the $Fe(CN)_6^{3-/4-}$ species from the AuNPs surface, thus increasing the R_{CT} (Figure 4.2(vi)). To generate the immunosensor surface (Ab/Biotin/Ph-NH_2/AuNPs-modified GC surface, Surface 6 in Figure 3.2), the sulfo-NHS-biotin was bound to the AuNPs on the GC electrode through Ph-NH_2 linker molecules, after which the monoclonal anti-biotin IgG antibody was specifically bound to the surface-bound biotin. These led to the obvious increase in R_{CT} (Figure 4.2(vii)), because the AuNPs on the electrode surface were surrounded by a layer of macromolecules like the anti-biotin antibody. As reported by Khor et al. (2011), the crystallographic dimensions of anti-biotin IgG antibody is A_{front} = 85.1 nm^2, A_{side} = 65.8 nm^2 and A_{top} = 57.9 nm^2. The dimensions of each binding domain of the anti-biotin antibody are approximately 4 nm × 2.5 nm × 2.5 nm.

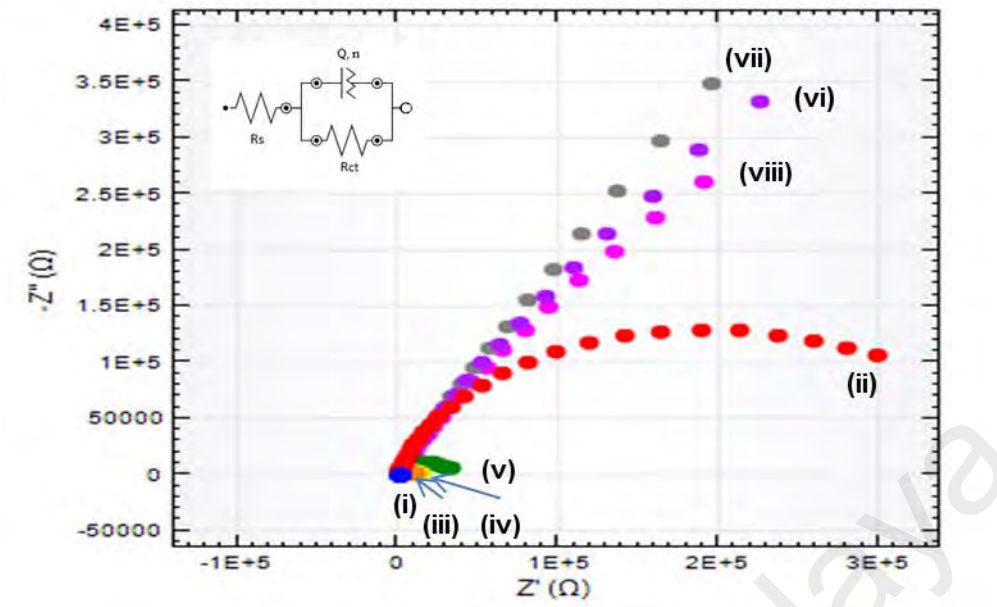

Figure 4.2: Stepwise surface characterization of the first immunosensor interface version by EIS. Nyquist plots recorded for EIS measurements of (i) bare GC electrode (blue), (ii) Surface 1 (red), (iii) Surface 2 (orange), (iv) Surface 3 (light green), (v) Surface 4 (green), (vi) Surface 5 (purple), (vii) Surface 6 (grey), and (viii) Surface 7 (pink) with DC potential of 0.200 V, frequency range of 0.1 – 10000 Hz and amplitude of 0.01 V. Inset of Figure 4.2: Equivalent circuit of Nyquist plots obtained from EIS.

Table 4.1: Equivalent circuit parameter values for the fitting curves of the bottom-up stepwise fabrication of the first immunosensor interface version by NOVA software.

Electrodes	R_S (Ω)	R_{CT} (Ω)	Q (Mho)	n	C_{dl} (F)
Bare GC	50.62	9.29×10^{2}	1.69×10^{-5}	0.802	6.095×10^{-6}
Ph-NH_2:Ph-NO_2-fabricated GC (Surface 1)	55.32	3.06×10^{5}	1.15×10^{-6}	0.884	1.001×10^{-6}
AuNPs/Ph-NH_2:Ph-NO_2-fabricated GC (Surface 2)	92.08	8.11×10^{3}	1.74×10^{-6}	0.852	8.309×10^{-7}
AuNPs/Ph-NH_2-fabricated GC (Surface 3)	110.41	1.25×10^{4}	3.95×10^{-6}	0.818	2.022×10^{-6}
OEG/AuNPs/Ph-NH_2-fabricated GC (Surface 4)	143.15	3.22×10^{4}	7.56×10^{-6}	0.827	5.630×10^{-6}
Ph-NH_2/OEG/AuNPs/Ph-NH_2-fabricated GC (Surface 5)	93.02	8.89×10^{5}	2.66×10^{-6}	0.808	3.266×10^{-6}
Ab/Biotin/Ph-NH_2/OEG/AuNPs/Ph-NH_2-fabricated GC (Surface 6)	243.37	1.34×10^{6}	2.96×10^{-6}	0.787	4.296×10^{-6}
Biotin/Ph-NH_2/OEG/AuNPs/Ph-NH_2-fabricated GC (Surface 7)	207.50	7.71×10^{5}	3.32×10^{-6}	0.781	4.316×10^{-6}

The electrochemical immunosensor surface developed (Ab/Biotin/Ph-NH_2/AuNPs-modified GC surface, Surface 6 in Figure 3.2) was used to detect the small molecule biotin present in PBS solution via a displacement assay. The immunosensor surface was pulsed with a negative potential of -800 mV in free biotin solution for 10 min to enhance the dissociation of monoclonal anti-biotin IgG antibodies from the sulfo-NHS-biotin (surface-bound epitope), because the carboxylate groups ($-COO^-$) of monoclonal anti-biotin IgG antibody acting as surface-active functional groups were readily repelled from the negatively-charged GC surface when the electrode is purposely pulsed at a cathodic potential (-800 mV) based on the concept of electrostatic interaction. The dissociated anti-biotin antibodies were bound to the free biotin (Biotin/Ph-NH_2/OEG/AuNPs/Ph-NH_2-fabricated GC surface, Surface 7 in Figure 3.2). This led to the greater access of $Fe(CN)_6^{3-/4-}$ redox-active species to the immunosensor surface, therefore a decrease in R_{CT} from 1.34×10^6 Ω to 7.71×10^5 Ω was detected (Table 4.1). In addition, the difference in R_{CT} [$R_{CT(b)} - R_{CT(a)}$] seemed to be directly proportional to the concentration of free biotin in PBS solution, falling in the linear range of 700 to 1500 μg mL^{-1} (Figure 4.3). $R_{CT(b)}$ and $R_{CT(a)}$ represent the R_{CT} before and after the dissociation of bound antibodies in the presence of free biotin, respectively. This observation indicates that the electrochemical immunosensor surface produced is able to detect small molecule biotin.

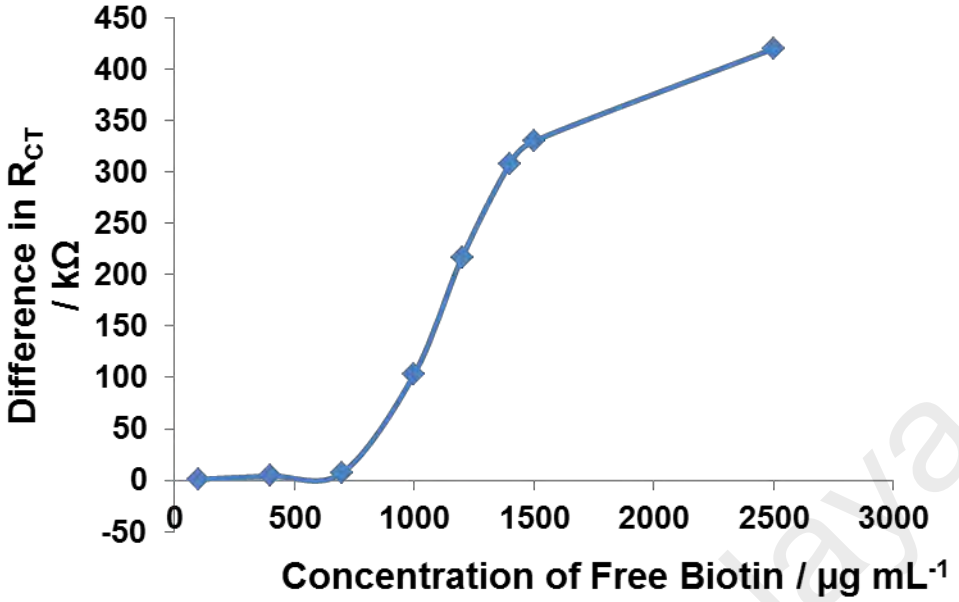

Figure 4.3: Calibration plot of biotin detection in PBS solution using first immunosensor interface version.

4.1.2 Characterization of the first immunosensor interface version by FE-SEM and FTIR

FE-SEM images of the bare GC surface and AuNPs/Ph-NH_2:Ph-NO_2-fabricate GC surface (Surface 2, Figure 3.2) are shown in Figure 4.4. The clean and dark surface in Figure 4.4a denotes the clean GC surface and no AuNPs residue present on the GC surface after polishing. A lot of small white dots on the dark surface (Figure 4.4b) illustrate that the AuNPs were successfully bound to the amino groups on the GC surface. Besides, the uniform and homogeneous distribution of AuNPs on the Ph-NH_2/Ph-NO_2-modified GC electrode illustrated in Figure 4.4b indirectly indicates that the Ph-NH_2 and Ph-NO_2 on electrode surface were evenly-distributed, as AuNPs was only attached to Ph-NH_2. The density of AuNPs on AuNPs/Ph-NH_2:Ph-NO_2-fabricate GC surface (Surface 2, Figure 3.2) was found to be approximately 1.75×10^7 AuNPs cm^{-2}. The size of AuNPs determined was approximately 20 nm.

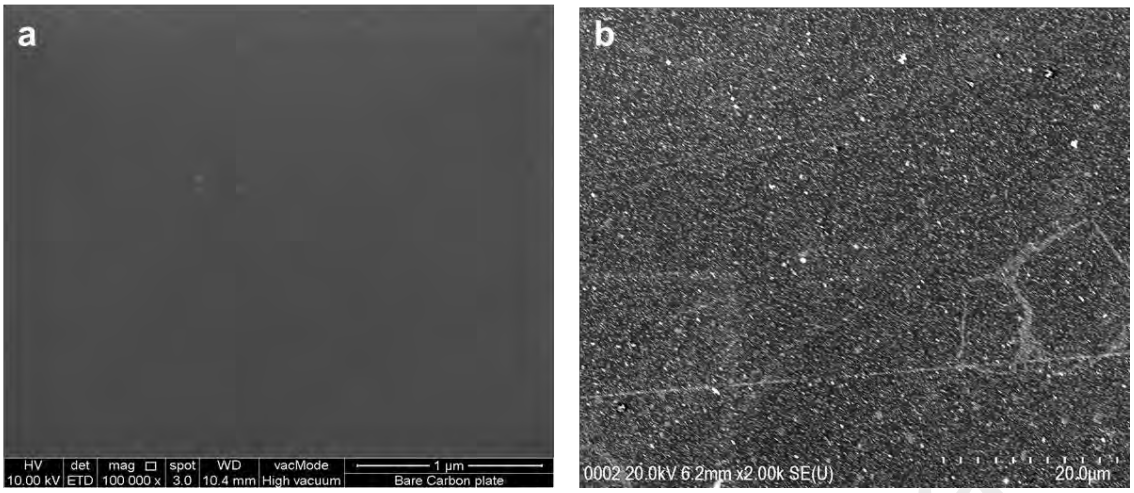

Figure 4.4: Immunosensor surface characterization for the first immunosensor interface version by FE-SEM. FE-SEM images of GC for (a) bare surface and (b) after the covalent attachment of AuNPs (AuNPs/Ph-NH_2:Ph-NO_2-fabricate GC surface, Surface 2 in Figure 3.2) with a magnification of 100 K. The image was taken at an angle of 40° to the surface.

Furthermore, FTIR technique was employed to characterize the electrode surfaces after every step of surface fabrication. No specific peak appeared in the FTIR spectrum for the bare GC surface (Figure 4.5a), because the GC surface was properly cleaned and no organic molecules deposited thereupon. The specific peaks for amino groups (at approximately 3700 cm^{-1}), aromatic rings (at 1548 cm^{-1}) and nitro groups (at 1209 cm^{-1}) are clearly visible in the spectrum for the Ph-NH_2/Ph-NO_2-fabricated electrode surface (Figure 4.5b). This indicates the successful attachment of Ph-NH_2 and Ph-NO_2 on the clean GC surface. The signal for the amino groups was significantly reduced (Figure 4.5c), because the amino groups were substituted by AuNPs that were bound to the aromatic rings through covalent bonds. However, the peak for amino groups in the spectrum became sharper (Figure 4.5d) when the nitro groups were electrochemically reduced to amino groups. After the attachment of OEG–COOH molecules to the amino groups via amide bonds, a peak for N-H stretching (at 3316 cm^{-1}) for the amide bonds, a peak for carbonyl groups (at 1626 cm^{-1}) and a broad band for ether groups (1000 –

1300 cm^{-1}) were observed in the spectrum (Figure 4.5e). The peak for amino groups re-appeared at 3641 cm^{-1} in the spectrum (Figure 4.5f) after the electrochemical attachment of Ph-NH_2 to the AuNPs. The spectra for Biotin/Ph-NH_2/OEG/AuNPs/Ph-NH_2-fabricate GC surface and Ab/Biotin/Ph-NH_2/OEG/AuNPs/Ph-NH_2-fabricate GC surface in Figures 4.5g and 4.5h could not be analyzed due to the complicated structures of sulfo-NHS-biotin and monoclonal anti-biotin IgG antibody, thus a reasonable assignment of FTIR peaks was not possible.

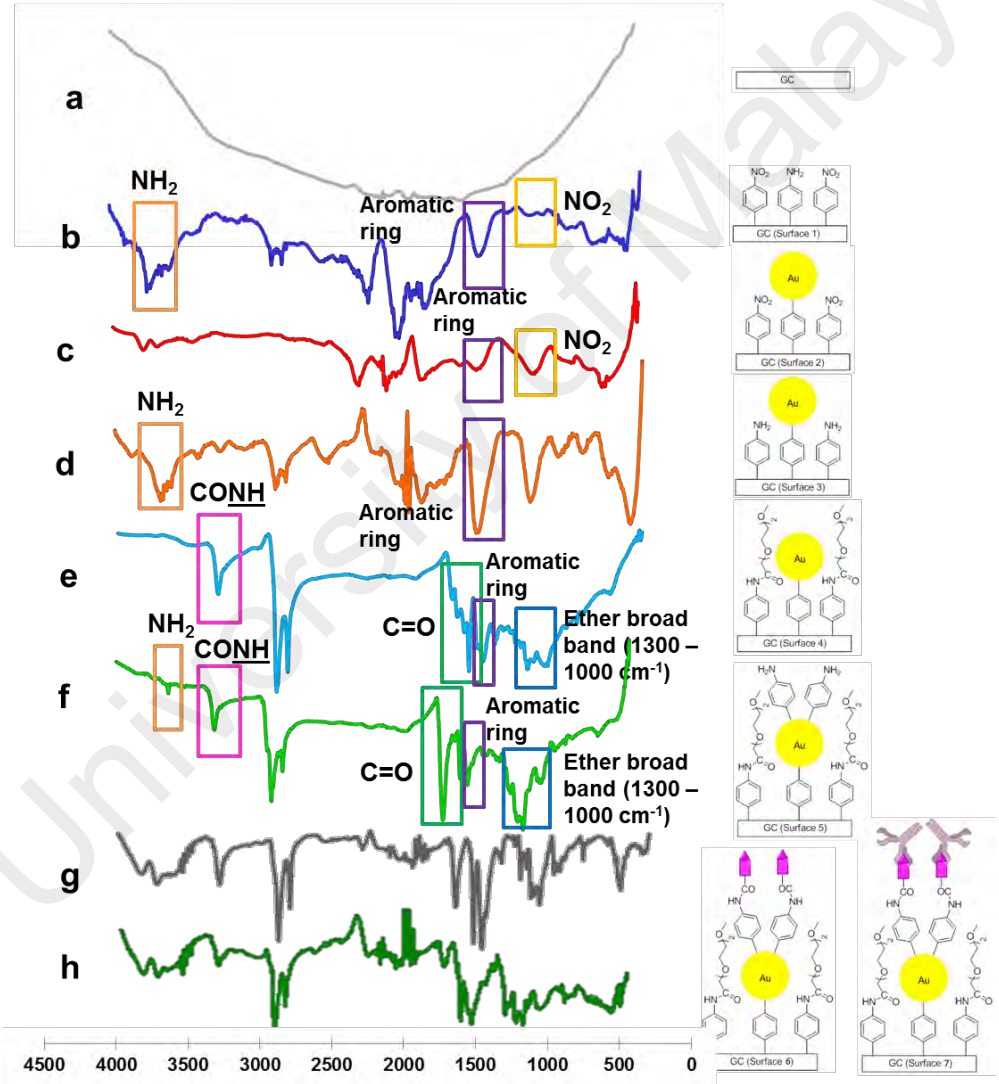

Figure 4.5: Immunosensor surface characterization for the first immunosensor interface version by FTIR. FTIR surface characterization of (a) bare GC electrode; (b) Surface 1, (c) Surface 2, (d) Surface 3, (e) Surface 4, (f) Surface 5, (g) Surface 6, and (h) Surface 7.

4.2 Second electrochemical immunosensor version used for sensitive detection of biotin molecules

4.2.1 Electrochemical characterization of the immunosensor interface with Ph-SO_3^- and Ph-NMe_3^+ as anti-fouling molecules

Figure 4.6 displays cyclic voltammograms of the bare and fabricated GC surface after every step of surface fabrication. Owing to the complete access of $Fe(CN)_6^{3-/4-}$ redox species to the bare GC surface, a pair of cathodic and anodic peaks appeared on the reversible cyclic voltammogram (Figure 4.6(i)). The well-defined peaks disappeared after the successful attachment of Ph-NH_2, Ph-SO_3^- and Ph-NMe_3^+ onto the clean GC surface (Figure 4.6(ii)), because this mixed layer of Ph-NH_2/Ph-SO_3^-/Ph-NMe_3^+ prevented the $Fe(CN)_6^{3-/4-}$ redox species from approaching the GC surface. Interestingly, the electrochemical attachment of AuNPs on the electrode surface led to the re-appearance of the cathodic and anodic peaks in cyclic voltammogram (Figure 4.6(iii)) because of the high conductivity of AuNPs. A clear suppression of current peaks was evident after the attachment of Ph-NH_2 on the AuNPs, because the access of redox species to the AuNPs-modified GC electrode was hindered. The successful attachment of sulfo-NHS-biotin on the AuNPs surface through Ph-NH_2 linker molecules resulted in a slight decrease in redox species peak current. After that, the monoclonal anti-biotin IgG antibody was bound to the surface-bound biotin through a 'lock-and-key' interaction. This caused a significant decrease in $Fe(CN)_6^{3-/4-}$ redox species peak current, because the AuNPs were surrounded by epitope-antibody complexes, hence preventing the redox species from approaching the electron transfer mediator (AuNPs).

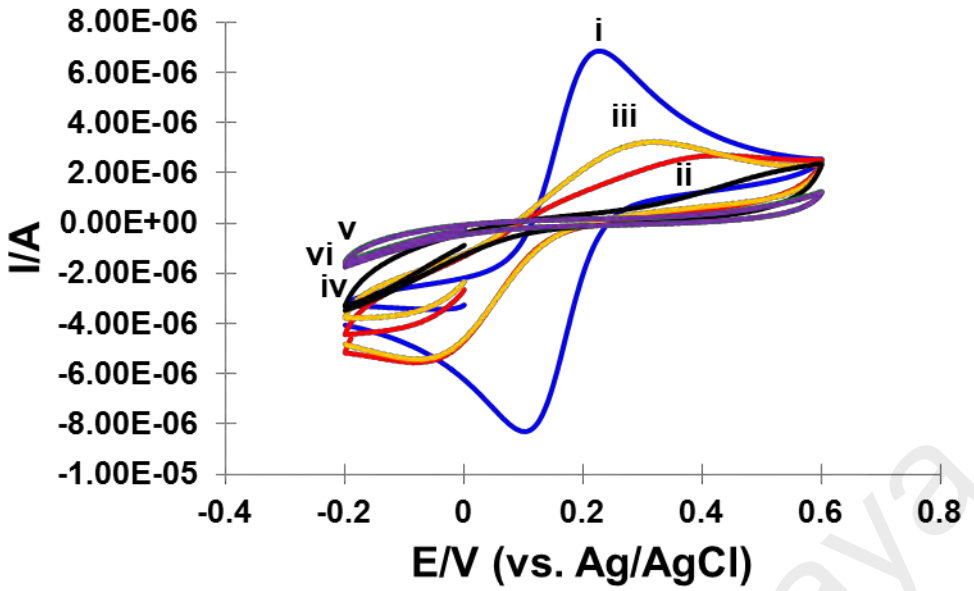

Figure 4.6: Stepwise surface characterization of the second immunosensor interface version by CV technique. Cyclic voltammograms recorded for (i) bare GC electrode (blue), (ii) Surface 1 (red), (iii) Surface 2 (orange), (iv) Surface 3 (black), (v) Surface 4 (green), (vi) Surface 5 (purple).

The stepwise immunosensor surface fabrication was further characterized by EIS. The experimental EIS results are in complete accord with the results obtained by CV. Figure 4.7 presents the Nyquist plots obtained from EIS measurements of the bare GC electrode and Surface 1 to Surface 5 (Figure 3.3). The equivalent circuit in the inset of Figure 4.7 was employed to fit the Nyquist plots in order to determine the electronic component parameters as given in Table 4.2. As discussed in Section 4.1.1, R_{CT} was used to study the changes in resistivity at the modified GC electrode surface and to detect the specific interaction between free biotin and surface-bound antibodies. The bare GC electrode had the lowest R_{CT} (Table 4.2), because the $Fe(CN)_6^{3-/4-}$ redox species faced no resistance when approaching the GC surface. The electrochemical deposition of a mixed Ph-NH_2/Ph-SO_3^-/Ph-NMe_3^+ layer blocked the redox species from reaching the electrode surface, thus the R_{CT} for Ph-NMe_3^+:Ph-SO_3^-:Ph-NH_2-fabricated GC surface (Surface 1, Figure 3.3) greatly increased (refer to Figure 4.7(ii)). Following electrochemical deposition of AuNPs on the GC surface, a substantial reduction in R_{CT}

was noted (Figure 4.7(iii)) due to the high electrical conductivity of AuNPs, which helped enhance the electron transfer between redox active species and GC electrode (Liu et al., 2011). The attachment of linker molecules (Ph-NH_2) on the AuNPs surface reduced the R_{CT} for Ph-NH_2/AuNPs/Ph-NMe_3^+:Ph-SO_3^-:Ph-NH_2-fabricated GC surface (Surface 3, Figure 3.3). Then sulfo-NHS-biotin was bound on the AuNPs surface through the Ph-NH_2 linker molecules, resulting in the decrease in R_{CT} (Figure 4.7(v)). To fabricate the immunosensor surface (Ab/Biotin/Ph-NH_2/AuNPs/Ph-NMe_3^+:Ph-SO_3^- :Ph-NH_2-fabricated GC surface, Surface 5 in Figure 3.3), the monoclonal anti-biotin IgG antibody was specifically complexed with the surface-bound biotin, thus increasing the R_{CT} again (Figure 4.7(vi)). This is because the insulation from the epitope-antibody complexes embraced the conductive AuNPs, hence the redox species were unable to approach the AuNPs on the modified GC electrode surface.

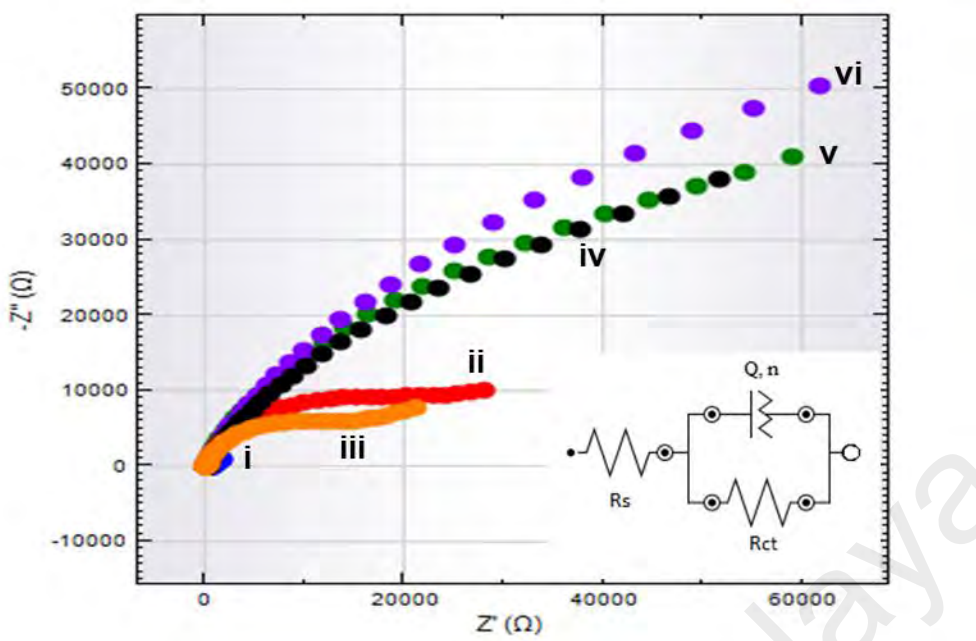

Figure 4.7: Stepwise surface characterization of the second immunosensor interface version by EIS. Nyquist plots recorded for EIS measurements of (i) bare GC electrode (blue), (ii) Surface 1 (red), (iii) Surface 2 (orange), (iv) Surface 3 (black), (v) Surface 4 (green), and (vi) Surface 5 (purple) with DC potential of 0.200 V, frequency range of 0.1 – 10000 Hz and amplitude of 0.01 V.

Table 4.2: Equivalent circuit parameter values for the fitting curves of the bottom-up stepwise fabrication of the second electrochemical immunosensor interface version by NOVA software.

Electrodes	R_S (Ω)	R_{CT} (Ω)	Q (Mho)	n	C_{dl} (F)
Bare GC	46.96	8.32×10^{2}	9.49×10^{-6}	0.904	5.675×10^{-6}
Ph-NMe_3^+:Ph-SO_3^-:Ph-NH_2-fabricated GC (Surface 1)	37.88	8.38×10^{4}	9.90×10^{-6}	0.753	9.312×10^{-6}
AuNPs/Ph-NMe_3^+:Ph-SO_3^-:Ph-NH_2-fabricated GC (Surface 2)	32.21	5.82×10^{4}	1.03×10^{-5}	0.733	8.548×10^{-6}
Ph-NH_2/AuNPs/Ph-NMe_3^+:Ph-SO_3^-:Ph-NH_2-fabricated GC (Surface 3)	28.35	1.82×10^{5}	1.03×10^{-5}	0.717	1.320×10^{-5}
Biotin/Ph-NH_2/AuNPs/Ph-NMe_3^+:Ph-SO_3^-:Ph-NH_2-fabricated GC (Surface 4)	27.13	2.37×10^{5}	8.85×10^{-6}	0.741	1.147×10^{-5}
Ab/Biotin/Ph-NH_2/AuNPs/Ph-NMe_3^+:Ph-SO_3^-:Ph-NH_2-fabricated GC (Surface 5)	38.46	2.44×10^{5}	8.84×10^{-6}	0.751	1.141×10^{-5}
Biotin/Ph-NH_2/AuNPs/Ph-NMe_3^+:Ph-SO_3^-:Ph-NH_2-fabricated GC (Surface 6)	32.63	1.05×10^{5}	1.28×10^{-5}	0.749	1.413×10^{-5}

As discussed in Section 4.1.1, transduction is achieved by the dissociation of surface-bound antibodies from the immunosensor surface in the presence of free biotin. As such, a decrease in R_{CT} was detected from 2.44×10^5 Ω to 1.05×10^5 Ω (Table 4.2). A linear relationship between the difference in R_{CT} and the free biotin concentration was determined within the dynamic range of 50 µg mL^{-1} to 200 µg mL^{-1} (Figure 4.8). Therefore, the electrochemical immunosensor with the second interfacial design version is believed to be capable of detecting biotin molecules at low concentration.

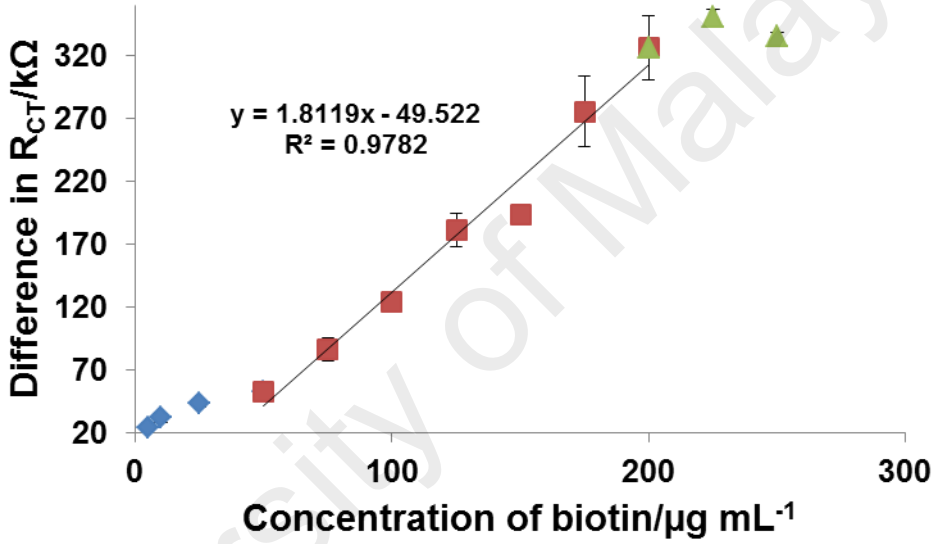

Figure 4.8: Calibration plot of biotin detection in PBS solution using second immunosensor interface version.

4.2.2 Characterization of the second immunosensor interface version by FE-SEM and FTIR

The FE–SEM image in Figure 4.9a shows a clean GC electrode surface with no AuNPs residue attached to the GC surface after polishing. The small white dots on the GC surface (Figure 4.9b) indicate the successful attachment of AuNPs onto the GC surface, denoted by AuNPs/Ph-NMe_3^+:Ph-SO_3^-:Ph-NH_2-fabricated GC surface (Surface 2, Figure 3.3). The number of AuNPs attached on the GC surface was counted manually. The calculated density of AuNPs attached on the GC surface was approximately 1.68×10^7 AuNPs cm^{-2}.

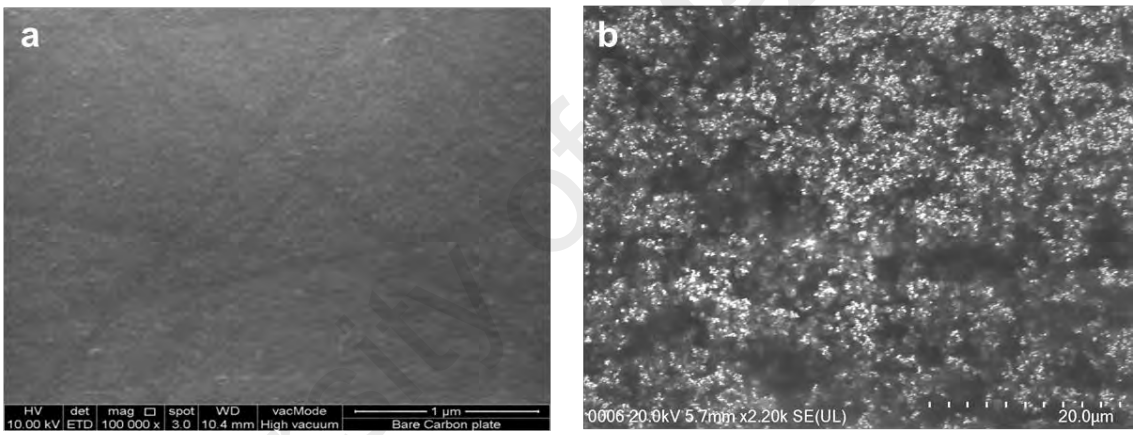

Figure 4.9: Immunosensor surface characterization for the second immunosensor interface version by FE–SEM. FE–SEM images of GC for (a) bare surface and (b) after the attachment of AuNPs (Surface 2 in Figure 3.3) at magnification of 100 K. The image was taken at an angle of 40° to the surface.

Additionally, the FTIR spectra in Figure 4.10 were used to qualitatively detect the presence of functional groups on Surface 1 to Surface 5. No specific peak is visible in the bare GC surface spectrum (Figure 4.10a). The presence of specific peaks for the primary amino groups (at approximately 3700 cm^{-1}), sp^2 carbon and sp^3 carbon (at 3000 cm^{-1} and 2866.7 cm^{-1}, respectively), aromatic rings (at 1600 cm^{-1}), S=O asymmetrical stretching (at 1433.3 cm^{-1}), C-N stretching (at 1200 cm^{-1}), N-H out-of-plane bending

(at approximately 800 cm^{-1}), and S-O stretching (at 633.3 cm^{-1}) was clearly determined on the spectrum for Ph-NMe_3^+:Ph-SO_3^-:Ph-NH_2-fabricated GC surface (Surface 1, refer to Figure 4.10b). Therefore, the electrochemical deposition of Ph-NH_2, Ph-SO_3^- and Ph-NMe_3^+ on the GC surface was proven to be successful. After the attachment of AuNPs to amino groups by covalent bonding, the peak for amino groups disappeared in the FTIR spectrum for AuNPs/Ph-NMe_3^+:Ph-SO_3^-:Ph-NH_2-fabricated GC surface (Surface 2, refer to Figure 4.10c). However, the specific peaks for other functional groups on Ph-NH_2/AuNPs/Ph-NMe_3^+:Ph-SO_3^-:Ph-NH_2-fabricated GC surface (Surface 3) remained almost the same as the peaks in Figure 4.10b. The attachment of Ph-NH_2 onto the AuNPs surface led to the re-appearance of peaks for the amino groups (at approximately 3700 cm^{-1}) and N-H bending (at about 800 cm^{-1}) in the spectrum for Ph-NH_2/AuNPs/Ph-NMe_3^+:Ph-SO_3^-:Ph-NH_2-fabricated GC surface (Surface 3, refer to Figure 4.10d). The FTIR spectra for Biotin/Ph-NH_2/AuNPs/Ph-NMe_3^+:Ph-SO_3^-:Ph-NH_2-fabricated GC surface (Surface 4, refer to Figure 4.10e) and Ab/Biotin/Ph-NH_2/AuNPs/Ph-NMe_3^+:Ph-SO_3^-:Ph-NH_2-fabricated GC surface (Surface 5, refer to Figure 4.10f) could not be analyzed due to the complicated structures of sulfo-NHS-biotin and monoclonal anti-biotin IgG antibody. Therefore, it was not possible to assign specific peaks.

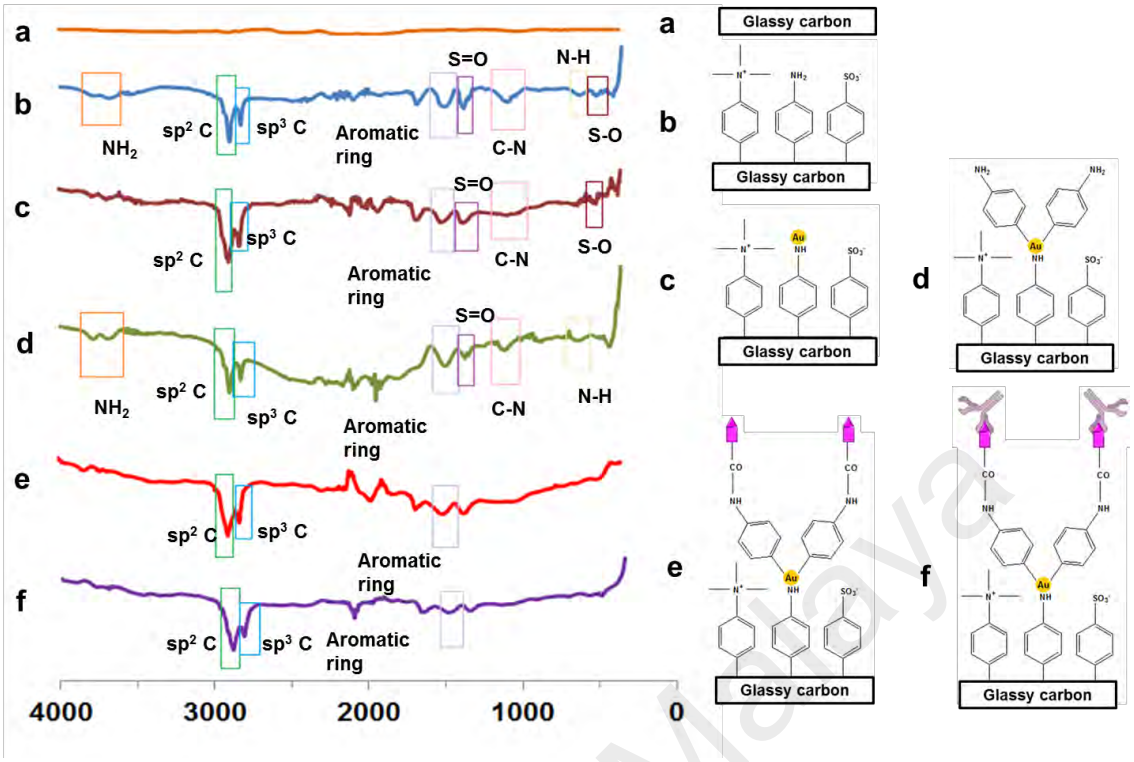

Figure 4.10: Immunosensor surface characterization for the second immunosensor interface version by FTIR. FTIR surface characterization of (a) bare GC electrode; (b) Surface 1, (c) Surface 2, (d) Surface 3, (e) Surface 4, and (f) Surface 5.

4.3 Electrochemical immunosensor surface regeneration

4.3.1 Immunosensor regeneration based on the reversible interactions between monoclonal anti-biotin IgG antibody and sulfo-NHS-biotin

In order to regenerate the immunosensor interface for repeated sensor use, a repeatability study was conducted. The same electrode surface produced was subjected to the association of monoclonal anti-biotin IgG antibody to the surface-bound epitope and the dissociation of surface-bound antibody in the presence of free biotin for 5 replicate continuous cycles within 24 h. Figure 4.11a shows the R_{CT} obtained before and after the dissociation of surface-bound antibody for the 5 regeneration cycle repetitions. Figure 4.11b shows the increment in R_{CT} after the association of monoclonal anti-biotin IgG antibody to the surface-bound epitope, while Figure 4.11c shows the decrement in R_{CT} following the surface-bound antibody displacement initiated by the presence of free

biotin in standard solution. Evidently, the electrode fabricated with first interfacial design version did not produce consistent electrochemical signals (ΔR_{CT}) for the 5 regeneration cycle repetitions, especially for the fourth and fifth cycles. A significant increment in R_{CT} after antibody association was observed for the fourth and fifth regeneration cycles (Figure 4.11b). This indicates that the amount of anti-biotin antibodies immobilized on the electrode surface greatly increased, leading to antibody saturation due to limited binding sites for the surface-bound epitope on the electrode surface. Besides, the decrement of R_{CT} after the dissociation of bound antibodies during the displacement assay in the fourth regeneration cycle was found to be approximately zero (Figure 4.11c), because only a small amount of antibodies was dissociated from the antibody-saturated immunosensor surface. The reason is the high binding affinity of anti-biotin antibody to the surface-bound biotin, which could restrict the antibody dissociation from the immunosensor surface after a long period of epitope-antibody complexation. Therefore, the surface-bound antibody could not be completely dissociated from the fabricated electrode surface, although the exposure time for the fabricated electrode to free biotin solution was extended from 20 min to 30 min. Furthermore, a negative R_{CT} decrement value ($R_{CT(a)} - R_{CT(b)}$ = negative value) was obtained after the displacement assay for the fifth regeneration cycle (Figure 4.11c). This signifies that no surface-bound antibodies were dissociated from the immunosensor surface (no displacement assay occurred) for the fifth regeneration cycle; however, only epitope-antibody complex accumulation occurred on the immunosensor surface. Hence, the saturation condition or the remaining epitope-antibody complexes restricted the free binding sites for the next antibody complexation cycle. Due to the high binding affinity of anti-biotin antibody to surface-bound biotin, the reversible interaction between antibody and surface-bound biotin was restricted. Therefore, this non-ideal regeneration

method is not suitable for immunosensor surface regeneration, because it prompts the degradation of immunosensor sensitivity for repeated measurements.

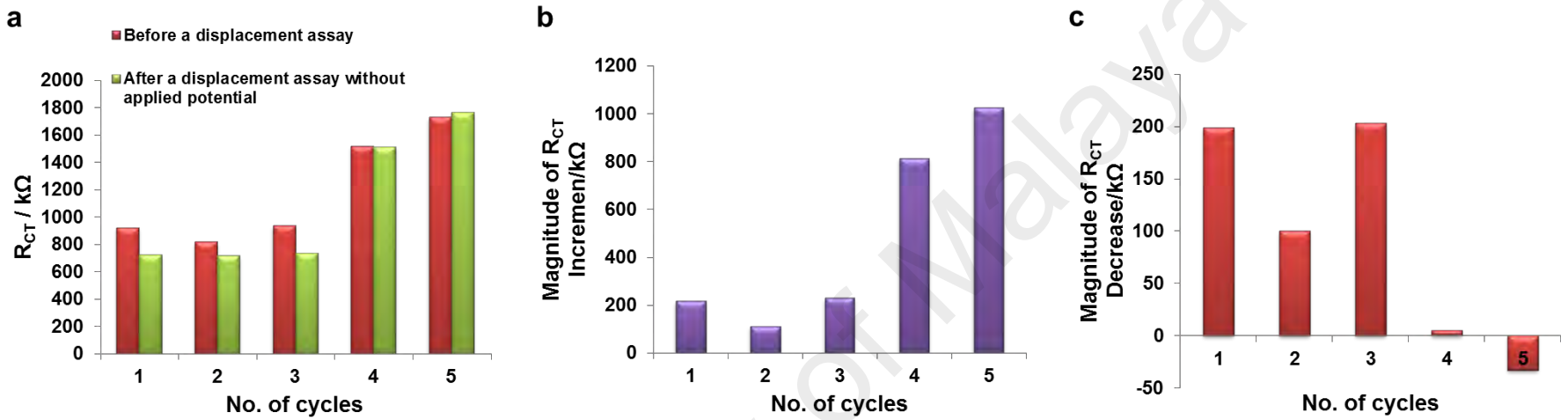

Figure 4.11: Immunosensor repeatability study based on the reversible interactions between the antibody and surface-bound epitope. a. Repetition process of the association of monoclonal anti-biotin IgG antibody to surface-bound epitope and the dissociation of surface-bound antibody in the presence of free biotin; b. Increment in R_{CT} after exposing the fabricated electrode surface to 0.5 µg mL^{-1} of monoclonal anti-biotin IgG antibody solution; c. Decrement in R_{CT} following a displacement assay in free biotin solution.

4.3.2 Voltage-induced dissociation of surface-bound antibody for the regeneration of first immunosensor surface version

The cathodic polarization technique was applied to enhance the dissociation of surface-bound proteins rather than anodic polarization, because protein adsorption on the electrode surface is possible in anodic condition. At anodic potential, the carboxylate groups ($-COO^-$) of proteins function as surface-active functional groups (Jackson et al., 2000). Therefore, protein adsorption on the electrode surface may be a result of the interaction between the negatively-charged carboxylate groups of proteins and the electrode surface in anodic condition (Omanovic & Roscoe, 1999). Therefore, the dissociation of surface-bound anti-biotin IgG antibodies from surface-bound epitopes was investigated under different conditions of cathode polarization (varying potentials and time intervals). Based on a detailed study with the results presented in Figure 4.12a, the potential magnitude and time interval used for electrochemical polarization appeared to have a strong impact on the amount of antibody dissociating from the surface-bound epitope, hence indirectly affecting immunosensor sensitivity. Thus, electrochemical polarization of -800 mV at a 10 min interval was found to be the optimum condition for immunosensor regeneration, because the immunosensor surface achieved a maximum dissociation of surface-bound antibodies via a displacement assay under these conditions. Therefore, the maximum decrement in R_{CT} was detected after the dissociation of surface-bound antibodies from the surface-bound epitope in optimum electrode polarization condition (-800 mV, 10 min), which yielded the highest immunosensor sensitivity. However, the surface-bound antibody could not be dissociated from the surface-bound epitope in the presence of free biotin at a less negative polarization potential, and the R_{CT} obtained after cathodic polarization was even higher than before. By extending the duration of potential application from 10 min to 20 min at -800 mV, the decrements in R_{CT} after a displacement assay appeared to be

lower than the decrement in R_{CT} obtained in optimum condition (-800 mV, 10 min). This indicates that the cathodic polarization at -800 mV from 15 min being extended to 20 min intervals did not improve the amount of surface bound antibody dissociated from the immunosensor surface. Moreover, applying a more negative potential (-900 mV) to the immunosensor surface for a 10 min interval also did not enhance the dissociation of surface-bound antibody compared to the optimum cathodic polarization condition (-800 mV, 10 min).

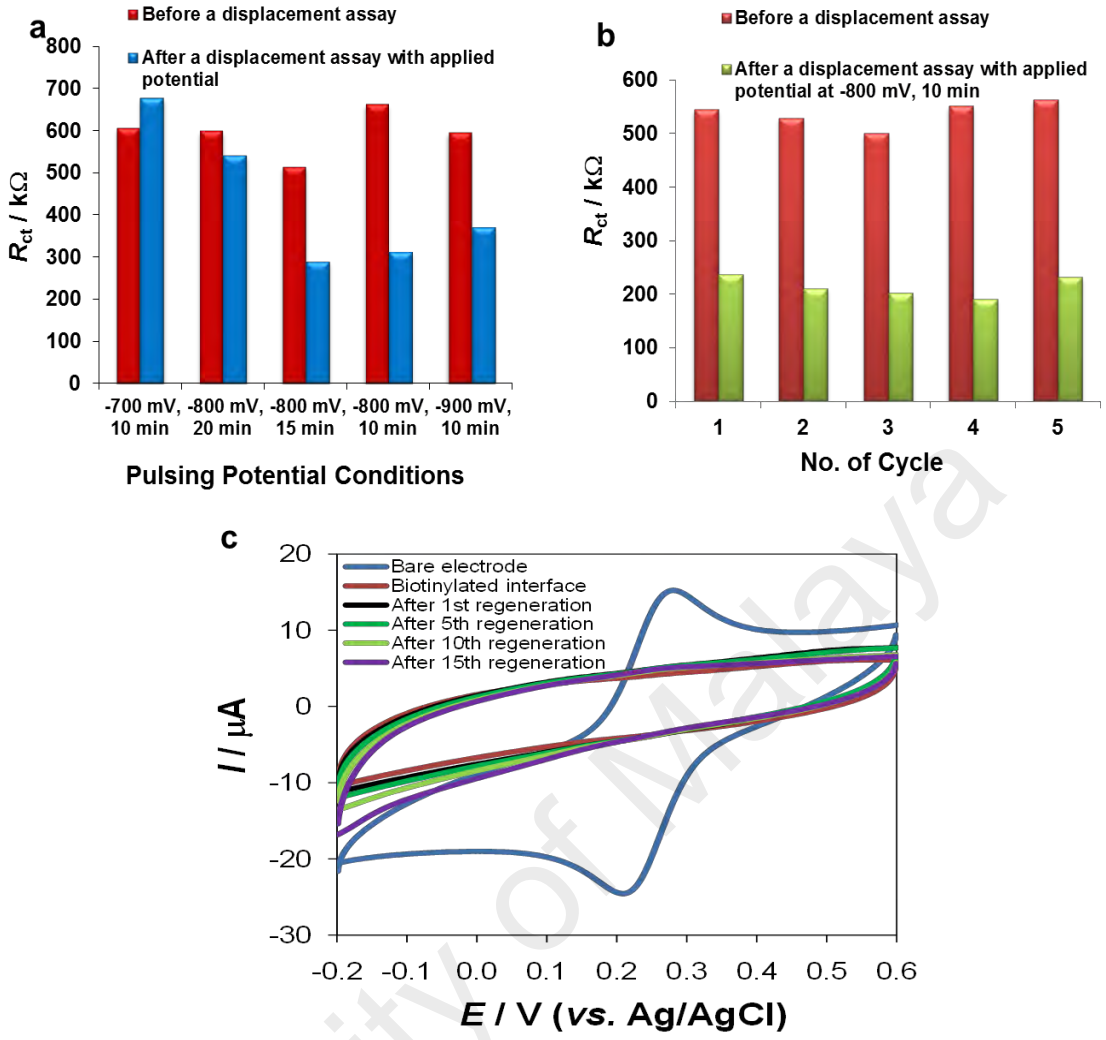

Figure 4.12: Immunosensor regeneration study based on the voltage-induced dissociation of bound anti-biotin antibody from the surface-bound epitope. a. Optimization for the maximum dissociation of surface-bound antibody via displacement assay at varying potentials and time intervals; b. Five repeated processes of the association of monoclonal anti-biotin IgG antibody and dissociation of surface-bound antibody in optimum cathodic polarization condition; c. Passivation capability of the grafted mixed layer of *in situ*-generated aryl diazonium salts towards $Fe(CN)_6^{3-/4-}$ redox species upon multiple electrode polarization cycles (-800 mV, 10 min).

In addition, a set of control experiments were performed with the absence of free biotin and using the same cathodic polarization condition as shown in Figure 4.12a. The difference in R_{CT} for the control experiments was found in the range of 0.3 kΩ to 1.03 kΩ. This is considered a non-significant change in R_{CT} obtained before and after a displacement assay for the control experiments compared to the decrement in R_{CT} displayed in Figure 4.12a. This observation signifies that the dissociation of bound

antibodies was practically driven by the electrochemical polarization condition and the presence of free biotin that prevented the re-complexation of the dissociated antibody on the surface-bound epitope. The reason is that the binding affinity between the free biotin and dissociated antibody is greater than the binding affinity between the surface-bound biotin and dissociated antibody.

According to the results obtained from the optimization study of the maximum dissociation of bound antibody in different electrode polarization conditions, a repeatability study was carried out next in the optimum electrode polarization condition (-800 mV, 10 min) to ensure the regeneration ability of the immunosensor surface and the stability of the grafted layer on the GC surface upon multiple cycles of surface regeneration. To non-invasively regenerate the immunosensor, the biorecognition surface was first exposed to 0.5 μg mL^{-1} monoclonal anti-biotin IgG antibody, followed by a displacement assay in 0.3 mg mL^{-1} of free biotin solution with the aid of electrode polarization. Figure 4.12b presented the R_{CT} obtained before and after bound antibody displacement with the aid of electrode polarization of -800 mV at a 10 min interval for 5 repeated cycles. By applying a negative potential (-800 mV) to the immunosensor surface for 10 min, the surface-bound antibody was removed from the surface-bound epitope as much as possible in the presence of free biotin during a displacement assay in order to empty out the surface-bound biotin binding sites for the next antibody-epitope complexation. This experiment was repeated for 5 continuously cycles within 24 h at 25ºC. Compatible to a study reported by Oldham et al. (1999), the specific interaction between monoclonal anti-biotin IgG antibody and surface-bound biotin seemed to be reversible with the aid of electrochemical polarization. After 5 regeneration cycles, the electrochemical signal for the displacement assay exhibited only a small variation with a relative standard deviation (RSD) of 9.14%. The association of monoclonal anti-biotin

IgG antibody to surface-bound biotin after 5 continuous regeneration cycles determined was over 98.8% compared to the initial value. The repeatability study indicated that no obvious loss in sensor detection ability was caused by the incomplete dissociation of antibodies or antibody saturation.

For repeated immunosensor use, the electrochemical polarization technique applied to enhance the dissociation of surface-bound antibodies must be non-invasive to the layer fabricated on the GC electrode surface so the detection ability of the immunosensor can be guaranteed for repeated use. In this case, the passivation capability of the grafted layer of aryl diazonium salts towards $Fe(CN)_6^{3-/4-}$ redox species was investigated to ensure the stability of the grafted layer on the electrode surface after multiple surface regeneration cycles. The cyclic voltammograms in Figure 4.12c indicate that redox species penetration was blocked successfully by the grafted layer after the 1^{st}, 5^{th}, 10^{th} and 15^{th} surface regeneration cycles. In other words, the immunosensor interface was considered stable and no significant changes occurred after being subjected to multiple cycles of electrode polarization. Therefore, the electrode polarization applied to enhance the dissociation of surface-bound antibodies from the immunosensor interface can be indirectly considered a non-invasive method of controlling the specific interaction between monoclonal anti-biotin IgG antibody and surface-bound biotin. The cathodic polarization approach is suitable for developing a reusable immunosensor because a stable and reproducible condition was attained at the biotinylated interface after multiple regeneration cycles.

4.4 Comparison between first and second immunosensor surface versions

For the first immunosensor interfacial design, OEG-COOH was employed as anti-fouling molecule in the immunosensor, while Ph-SO_3^- and Ph-NMe_3^+ were employed as anti-fouling molecules in the second immunosensor interfacial design. Due to the difference in the chemical structure of OEG–COOH versus aryl diazonium anti-fouling molecules (with different terminal charges), the R_{CT} of these two different interfacial designs of an immunosensor interface (Surface 6 in Figure 3.2 and Surface 5 in Figure 3.3) was investigated by EIS technique. Figure 4.13 shows that the Nyquist plots (a, b and c) for the antibody-bound interfaces containing OEG–COOH as anti-fouling molecule are obviously bigger and wider than the Nyquist plots (d, e and f) for the antibody-bound interfaces containing Ph-SO_3^- and Ph-NMe_3^+ as anti-fouling molecules. This observation is in line with a previous surface modification study, showing that an OEG-Ph-modified GC surface has higher impedance than a Ph-SO_3^-/Ph-NMe_3^+-modified GC surface (Gui, 2011). The average R_{CT} calculated for Nyquist plots (a, b and c) was $(1.25 \pm 0.17) \times 10^6$ Ω, whereas the average R_{CT} calculated for Nyquist plots (d, e and f) was $(4.10 \pm 0.14) \times 10^5$ Ω. In other words, the immunosensor surface fabricated with Ph-SO_3^- and Ph-NMe_3^+ (Surface 5 in Figure 3.3) has lower impedance than the first immunosensor surface version fabricated with OEG-COOH (Surface 6 in Figure 3.2). This is because the zwitterionic phenyl layer formed by Ph-SO_3^- and Ph-NMe_3^+ consists of both the positive charge and negative charge, while the OEG phenyl layer is an electrical insulating layer, therefore the zwitterionic phenyl layer show low resistance to electron transfer. Besides, the lower electrical insulation of the zwitterionic phenyl layer improved the electron transfer rate from the biorecognition molecule to the underlying electrode due to the presence of positively- and negatively-charged moieties (Gui, 2011). These led to the formation of a low-impedance coating of Ph-SO_3^- and Ph-NMe_3^+ at the antibody-bound electrode surface (Surface 5 in Figure 3.3). Moreover, the

high impedance layer formed by OEG-COOH caused a loss of immunosensor sensitivity (Darwish et al., 2015), because the electrochemical signals were not delivered efficiently from the immunosensor interface to the underlying electrode. Thus, the second immunosensor interface version is preferable for use in electrochemical immunosensor construction.

Additionally, the dynamic range of biotin detection in PBS using the Ph-SO_3^-/Ph-NMe_3^+-fabricated immunosensor surface (second version) was found to be in the range of 50 μg mL^{-1} to 200 μg mL^{-1} (Figure 4.8), whereas the dynamic range obtained with the OEG–fabricated immunosensor surface (first version) was in the range of 700 μg mL^{-1} to 1500 μg mL^{-1} (Figure 4.3). This signifies that the Ph-SO_3^-/Ph-NMe_3^+-fabricated immunosensor was more sensitive in a lower biotin concentration range than the OEG–fabricated immunosensor. The reason is that the low impedance feature of the Ph-SO_3^-/Ph-NMe_3^+-fabricated immunosensor reduced the signal-to-noise ratio, at which the electrochemical detection signal appeared to be significant even if only a small amount of bound antibody was dissociated from the immunosensor surface at low biotin concentration. The dissociation of bound antibody from surface-bound epitope was attributed to the relatively higher binding affinity of the anti-biotin antibody to free biotin and the aid of electrode polarization, which enhanced the dissociation of bound antibody from the immunosensor surface. The Ph-SO_3^-/Ph-NMe_3^+-fabricated immunosensor facilitates high signal-to-noise when used at a low biotin concentration range, and it is thus preferable for biotin monitoring in clinical diagnosis and the food industry because the biotin in clinical and food samples usually presents at low concentrations one the ppm or ppb scale (Höller et al., 2006; Staggs et al., 2004). Therefore, the analytical performance of the second immunosensor surface version was further investigated in this study.

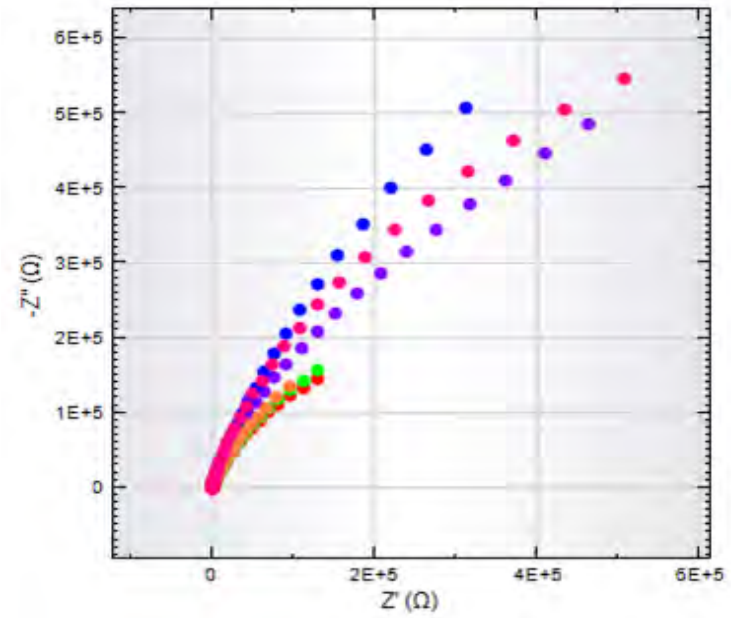

Figure 4.13: Comparison of electrochemical characteristics between OEG-fabricated GC surfaces and Ph-SO_3^-/Ph-NMe_3^+-fabricated GC surfaces. Nyquist plots recorded for antibody-bound GC surfaces (Surface 6 in Figure 3.2) containing OEG-COOH as anti-fouling molecules: a. blue, b. pink and c. purple; and for antibody-bound GC surfaces (Surface 5 in Figure 3.3) containing Ph-SO_3^- and Ph-NMe_3^+ as anti-fouling molecules: d. orange, e. green and f. red.

4.5 Performance of low impedance electrochemical immunosensor (second version) used for biotin molecule detection

4.5.1 Effects of different molar ratios of Ph-NH_2 and Ph-SO_3^-/Ph-NMe_3^+-fabricated immunosensor interfaces on the anti-fouling property and sensitivity of the immunosensor

Prior to investigating the influence of immunosensor interfaces fabricated with different molar ratios of Ph-NH_2 and Ph-SO_3^-/Ph-NMe_3^+ on the anti-fouling property of the immunosensor, the Ph-NH_2-, Ph-SO_3^--, Ph-NMe_3^+- and Ph-SO_3^-/Ph-NMe_3^+-fabricated GC electrodes with a ratio of 1:1 were prepared for the anti-fouling study. The control experiment was conducted by exposing the bare GC surface and the aryl diazonium molecule-fabricated GC surfaces to PBS solution for 1 h at 25ºC. The anti-fouling property of GC surfaces was dependent on the increment in R_{CT} after exposing the GC surfaces to PBS, BSA, Cyt-C and infant formula (Dutch Lady) for 1 h at 25ºC. The larger the increment in R_{CT} value after GC electrode exposure to the 4 solutions mentioned above, the weaker the anti-fouling property of the GC modified surfaces was. No decrement or increment in R_{CT} was detected after exposing the modified GC surfaces to PBS solution, indicating that the bare GC surface and the aryl diazonium molecule-fabricated GC surfaces had no response to the ions present in PBS solution. As shown in Figure 4.14a, the Ph-SO_3^-/Ph-NMe_3^+-fabricated GC surfaces with a ratio of 1:1 have nearly 0 values for the changes in R_{CT} recorded before and after exposure to BSA (negatively-charged protein), Cyt-C (positively-charge protein) and infant formula (Dutch Lady) for 1 h at 25ºC. Ph-SO_3^- and Ph-NMe_3^+ (1:1) formed a hydrophilic zwitterionic mixed layer on the GC surface. Thus, the water hydration layer formed could resist against protein adsorption (Gui, 2011). Besides, a mixture of Ph-SO_3^-/Ph-NMe_3^+ with a ratio of 1:1 was used to make an anti-fouling layer in order to achieve electrical neutrality, which inhibited the electrostatic interaction between the

zwitterionic-modified GC surface and the charged proteins (Lowe et al., 2015). Therefore, the Ph-SO_3^-/Ph-NMe_3^+ (1:1)-fabricated GC surface was found to have the strongest anti-fouling capability. In contrast to Ph-SO_3^-/Ph-NMe_3^+ (1:1)-fabricated GC surface, the Ph-NH_2-fabricated GC surface exhibited the greatest significant change in R_{CT} value compared to the Ph-SO_3^-/Ph-NMe_3^+ (1:1)-fabricated GC surfaces. This was because Ph-NH_2 is a linker molecule that can bind with any protein through amide bonding, therefore Ph-NH_2 was not able to resist against protein adsorption. The anti-fouling capability of the Ph-SO_3^--fabricated GC surface seemed better than the Ph-NH_2-fabricated GC surface, because Ph-SO_3^- formed a negatively-charged layer on GC that could repel the negatively-charged protein (BSA). However, the negatively-charged surface had no resistance to the positively-charge protein (Cyt–C) and some other molecules (e.g., proteins, carbohydrates and vitamins) present in the infant formula (Dutch Lady). Apart from that, the Ph-NMe_3^+-fabricated GC surface was found to have a high degree of anti-fouling capability, as the protein adsorption on the positively-charged layer formed by Ph-NMe_3^+ was not obvious. This may be due to the steric hindrance caused by the presence of three methyl groups in each Ph-NMe_3^+ molecule, therefore both positively- and negatively-charged proteins were prevented from adsorbing on the Ph-NMe_3^+-fabricated surface (Lowe et al., 2015). An unexpectedly excellent anti-fouling capability was presented on the bare GC surface (Figure 4.14a). There was no functional group on the bare GC surface, thus the protein molecule could only physically absorb on the GC surface but not chemically bind to the GC surface, so the protein could be easily washed off by Milli-Q^{TM} water. However, the bare GC surface is not recommended for the specific detection of biotin although it possesses excellent anti-fouling capability, because there is no specific interaction between free biotin and the bare GC surface due to the absence of anti-biotin antibody (the

immobilized biorecognition molecule for specific biotin detection) on the GC surface, hence producing no detection signal.

In order to maintain the electrical neutrality of the zwitterionic immunosensor surface, the molar ratio of Ph-SO_3^- and Ph-NMe_3^+ must be 1:1. Therefore, only the molar ratio between Ph-NH_2 and Ph-SO_3^-/Ph-NMe_3^+ on the immunosensor interfaces was investigated. The anti-fouling properties of Ph-NH_2/Ph-SO_3^-/Ph-NMe_3^+-fabricated GC electrodes (Mix 1, Mix 2, Mix 3 and Mix 4) towards BSA, Cyt–C and infant formula (Dutch Lady) are shown in Figure 4.14b. This figure generally indicates that the anti-fouling property of the Ph-NH_2/Ph-SO_3^-/Ph-NMe_3^+-fabricated GC electrodes increases when the amount of anti-fouling molecules attached on the GC surfaces increases.

The Ph-NH_2/Ph-SO_3^-/Ph-NMe_3^+-fabricated GC electrode with a molar ratio of 4:0.5:0.5 (Mix 1) was determined to have the highest increment in R_{CT} after being exposed to BSA (13.0 kΩ), Cyt-C (4.9 kΩ) and infant formula (Dutch Lady) (37.3 kΩ) for 1 h. Therefore, GC surfaces fabricated with Mix 1 exhibited the weakest anti-fouling property compared to other Ph-NH_2/Ph-SO_3^-/Ph-NMe_3^+-fabricated GC electrodes. The reason is that the amount of anti-fouling molecules (Ph-SO_3^- and Ph-NMe_3^+) attached on the GC surfaces was too small, so the anti-fouling capacity of the GC surfaces fabricated with Mix 1 was not strong enough to resist the adsorption of proteins on the GC surfaces.

According to Figure 4.14b, the Ph-NH_2/Ph-SO_3^-/Ph-NMe_3^+-fabricated GC electrodes with a molar ratio of 3:1:1 (Mix 2) exhibited lower values in R_{CT} increment because more anti-fouling molecules were attached on these surfaces, so they had a better anti-fouling property than GC electrodes fabricated with Mix 1. However, there was no significant electrochemical signal detected for the protein absorption on the Ph-NH_2/Ph-

SO_3^-/Ph-NMe_3^+-fabricated GC electrodes with molar ratios of 2:1.5:1.5 (Mix 3) and 1:2:2 (Mix 4). Hence, the GC surfaces fabricated with Mix 3 and Mix 4 appeared to have an excellent anti-fouling property towards BSA, Cyt–C and infant formula (Dutch Lady).

Immunosensor surface sensitivity was dependent on the decrement in R_{CT} according to a displacement assay performed in 100 μg mL^{-1} of free biotin solution with the aid of electrode polarization (-800 mV, 10 min) at 25ºC. The larger the decrement in R_{CT} after exposing the immunosensor surfaces to 100 μg mL^{-1} of free biotin solution, the higher the immunosensor surface sensitivity was. As observed in Figure 4.14c, the decrement in R_{CT} after exposing the antibody-bound electrodes to 100 μg mL^{-1} of free biotin solution increased as the amount of linker molecules (Ph-NH_2) attached on the GC electrodes increases. This is because when there were more linker molecules attached on the GC surfaces, the amount of AuNPs attached to the amino groups on the GC surfaces could increase, therefore leading to high anti-biotin antibody loading on the immunosensor surfaces. This was able to improve the sensitivity of the immunosensor. Therefore, after exposure to 100 μg mL^{-1} of free biotin solution, the Ph-NH_2/Ph-SO_3^-/Ph-NMe_3^+-fabricated GC surfaces with a molar ratio of 4:0.5:0.5 (Mix 1) exhibited the greatest decrement in R_{CT} (the highest sensor sensitivity), whereas the immunosensor surfaces fabricated with a molar ratio of 1:2:2 (Mix 4) exhibited the lowest decrement in R_{CT} (the lowest sensor sensitivity).

Based on the results obtained from both anti-fouling and sensitivity studies of the Ph-NH_2/Ph-SO_3^-/Ph-NMe_3^+-fabricated GC surfaces, the GC surface fabricated with Mix 3 was selected for further investigation. This surface possessed an excellent anti-fouling property along with good sensor sensitivity, which is considered important features for an immunosensor to be used in real sample analysis. In addition, the immunosensor

surface fabricated with Mix 3 exhibited higher sensor sensitivity than the immunosensor surface fabricated with Mix 4, therefore the surface made with Mix 3 was deduced as the most suitable candidate for real sample analysis. Nonetheless, the immunosensor surface fabricated with Mix 4 also exhibited an excellent anti-fouling property.

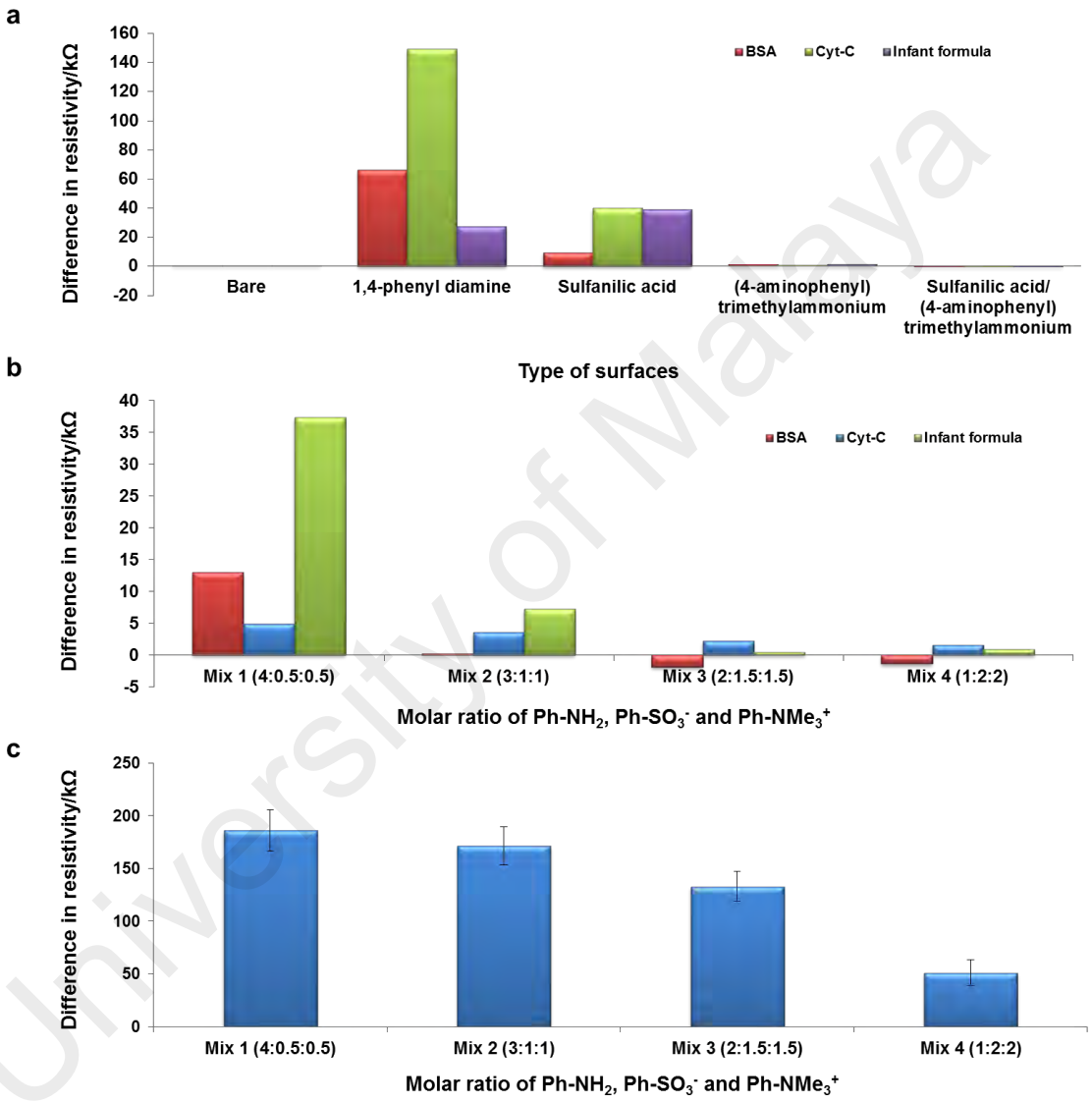

Figure 4.14: Anti-fouling and sensitivity studies of Ph-NH_2/Ph-SO_3^-/Ph-NMe_3^+-fabricated GC surfaces with different molar ratios (Mix 1, Mix 2, Mix 3 and Mix 4). a. Anti-fouling study of bare GC electrodes, Ph-NH_2-fabricated electrodes, Ph-SO_3^--fabricated electrodes, Ph-NMe_3^+-fabricated electrodes and Ph-SO_3^-/Ph-NMe_3^+-fabricated electrodes; b. Anti-fouling study of the GC electrodes fabricated with different molar ratios of Ph-NH_2/Ph-SO_3^-/Ph-NMe_3^+ (Mix 1, Mix 2, Mix 3 and Mix 4); c. Sensitivity study of GC electrodes fabricated with different molar ratios of Ph-NH_2/Ph-SO_3^-/Ph-NMe_3^+ (Mix 1, Mix 2, Mix 3 and Mix 4).

4.5.2 Reproducibility study of the second version of biotin immunosensor

High reproducibility of the developed immunosensor is essential to the mass production for immunosensor commercialization. Thus, the reproducibility of the immunosensor was examined by exposing 10 different immunosensor surfaces to 75 μg mL^{-1} of free biotin solution prepared in PBS. The decline in R_{CT} for the 10 immunosensor surfaces after the displacement assay is presented in Figure 4.15. The RSD calculated for the decrement in R_{CT} was 8.44% for all 10 immunosensor surfaces. The excellent reproducibility of the developed immunosensor can be attributed to the immunosensor interface design and the fabrication procedure (Darwish, 2016). The zwitterionic anti-fouling layer formed by Ph-SO_3^- and Ph-NMe_3^+ on the GC surface can effectively resist against non-specific protein adsorption (Gui, 2011). Besides, the highly-specific monoclonal antibody used for biotin detection allows only the specific binding between the biotin and monoclonal antibody. Therefore, the grafting of anti-fouling molecules (e.g., Ph-SO_3^- and Ph-NMe_3^+) on the GC electrode surface and the specific interaction between monoclonal anti-biotin IgG antibody and free biotin have a potentially strong impact on immunosensor reproducibility.

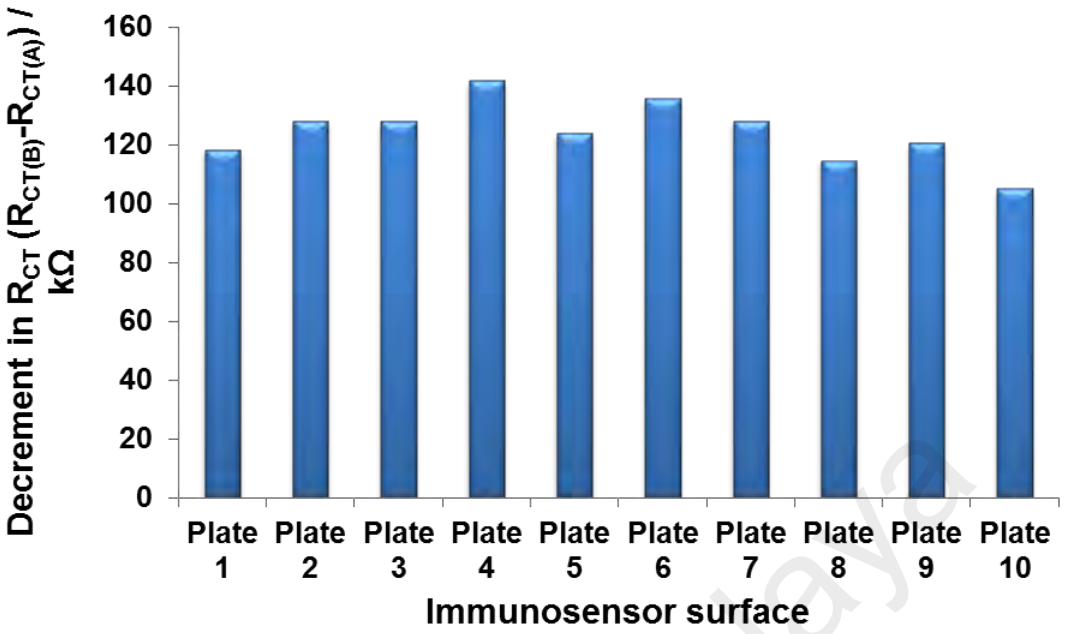

Figure 4.15: Reproducibility study of the developed immunosensor.

4.5.3 Selectivity study of the second biotin immunosensor version

A selectivity study was undertaken to investigate the specificity of the immunosensor surface towards biotin molecule by exposing the immunosensor surface to different types of small organic molecules (e.g., biotin, sucrose, citric acid, ascorbic acid, uric acid and guanine). These small organic molecules were selected for testing in this study, because they may be present in real samples, such as infant formulas and biotin-containing supplements. The antibody-bound electrodes were individually exposed to a single type of small organic molecule interference. As presented in Figure 4.16, a significant decrease in R_{CT} was obtained after a displacement assay with the aid of electrode polarization (-800 mV, 10 min) was performed in free biotin solution. In contrast, the immunosensor surface did not show an obvious change in electrochemical signal after immunosensor surface exposure to sucrose, citric acid, ascorbic acid, uric acid and guanine. The reason is that the monoclonal anti-biotin IgG antibody was highly specific to the biotin molecule, hence there was not obvious amount of anti-biotin

antibodies dissociated from the immunosensor surface after exposing the immunosensor surface to sucrose, citric acid, ascorbic acid, uric acid and guanine. Therefore, the R_{CT} values obtained before and after exposing the immunosensor surface to these small interferent organic molecules displayed no significant change. The high selectivity of the developed immunosensor surface was mainly attributed to the high specificity of the monoclonal anti-biotin IgG antibody towards the biotin molecule as well as the anti-fouling capability of the fabricated immunosensor surface.

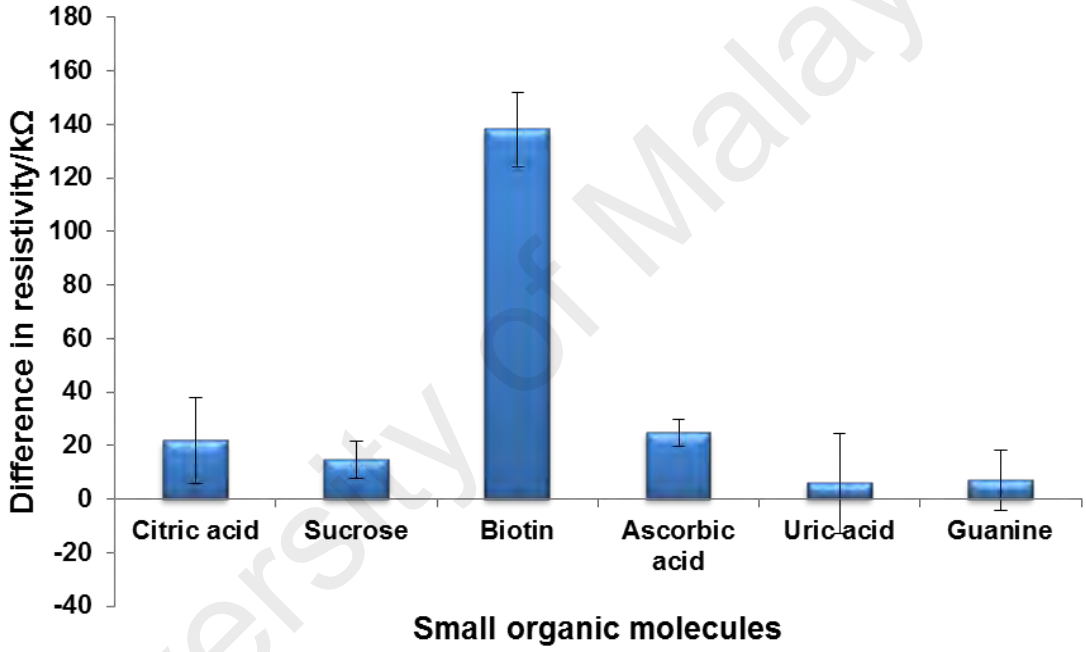

Figure 4.16: Selectivity study of the developed immunosensor.

4.5.4 Stability study of the second biotinylated interface version

In order to investigate the long-term stability of the layers fabricated on the GC electrode surface, the immunosensor surfaces kept in PBS solution at 4ºC were used to detect free biotin prepared in PBS solution on Days 1, 3, 5, 7, 14, 21 and 28, respectively. As shown in Figure 4.17, there was no obvious loss in the detection ability of the developed immunosensor after being stored for 28 days at 4ºC. The detection

signal obtained by the immunosensor on Day 28 was retained at 95.2% of the initial signal. Therefore, the immunosensor surface could be considered stable for 28 days in PBS solution stored at 4ºC. The long-term stability of the layers fabricated on GC surface was attributed to the immunosensor interfacial design and the surface fabrication technique (Darwish, 2016); for instance, aryl diazonium salt attachment on the GC surface through covalent bonding by electrochemical reduction and AuNP binding to the aromatic rings on the electrode surface through covalent bonding by electrochemical deposition. The AuNPs were homogeneously distributed on the GC surface and strongly bound on the GC surface, hence producing a stable immunosensor surface (Liu et al., 2011; Wang et al., 2014).

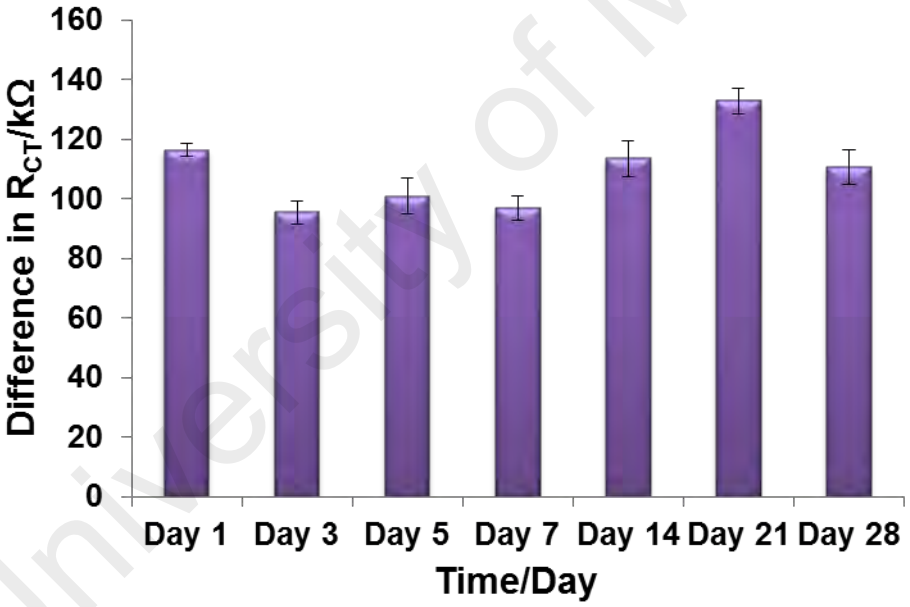

Figure 4.17: Long-term stability study of the developed immunosensor.

4.5.5 Intra-day and inter-day precision test for biotin detection using the second immunosensor surface version

Biotin solutions with concentrations of 50 μg mL^{-1}, 75 μg mL^{-1}, and 100 μg mL^{-1} were prepared in PBS solution at pH 7.4. In the intra-day precision study, each concentration was tested 4 times with different immunosensor surfaces within the same day (Figure 4.18a). The RSD calculated based on the results obtained from 4 replicates of biotin detection with biotin concentrations of 50 μg mL^{-1}, 75 μg mL^{-1}, and 100 μg mL^{-1} were 10.67%, 8.37%, and 9.97%, respectively. In the inter-day precision study, biotin detection for biotin concentrations of 50 μg mL^{-1}, 75 μg mL^{-1}, and 100 μg mL^{-1} was tested one time on different immunosensor surfaces on the same day. The experiment was repeated for 5 continuous days (Figure 4.18b). The RSD calculated based on the results obtained for the biotin concentrations of 50 μg mL^{-1}, 75 μg mL^{-1}, and 100 μg mL^{-1} over 5 continuous days were 12.98%, 5.45%, and 9.04%, respectively. The RSD in both intra-day and inter-day precision studies were found in an acceptable range (≤20%) according to CODEX Guidelines[ii] (European Medicines Agency, 2009). These results indicated the immunosensor was able to produce a high-precision detection signal for quantitative biotin detection. In terms of the quantitative detection of biotin, the high immunosensor precision may boost the reliability of the results obtained to a certain level.

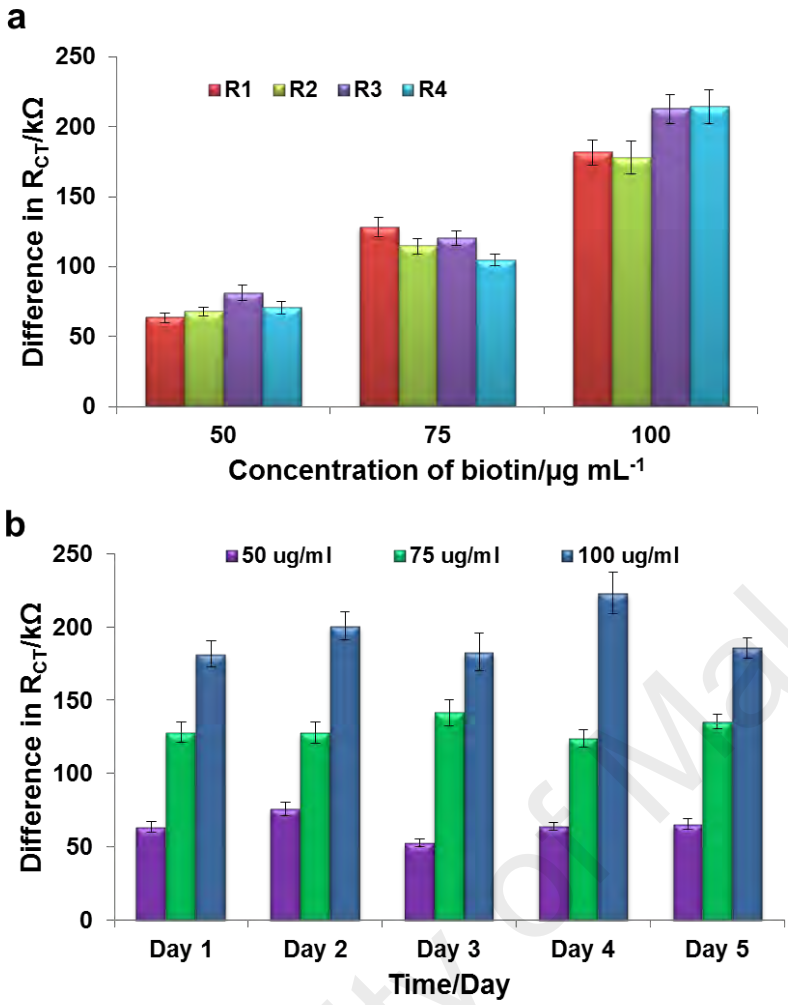

Figure 4.18: Intra-day and inter-day precision studies of biotin immunosensor. a. Intra–day precision of the developed immunosensor tested using 3 biotin concentrations (i.e., 50 µg mL^{-1}, 75 µg mL^{-1}, and 100 µg mL^{-1}). Each concentration was tested 4 times (R1, R2, R3 and R4) using different immunosensor surfaces. b. Inter–day precision of the developed immunosensor tested for 3 biotin concentrations (i.e., 50 µg mL^{-1} (purple), 75 µg mL^{-1} (green), and 100 µg mL^{-1} (blue)) for 5 continuous days.

4.6 Analytical performance of the second electrochemical immunosensor version in real sample analysis

4.6.1 Method validation of the developed immunosensor by HPLC with photodiode array detector to detect biotin in infant formulas using standard addition method

In immunosensor biotin quantification, the infant formula samples were not subjected to any sample pre-treatment. Hence, the standard addition method was applied in the quantitative detection of biotin in infant formulas. The presence of various interferences in infant formulas could result in the matrix effect, which can affect biotin detection accuracy. In biotin detection using the developed immunosensor, the free biotin concentrations in infant formulas (Dutch Lady and Friso Gold) (Table 4.3) were calculated from the standard addition plots shown in Figures 4.19a and 4.19b, respectively. In order to ascertain the data reliability of the developed immunosensor in free biotin quantification in infant formulas, standard addition method was also applied in HPLC biotin detection, although the samples were treated prior to biotin detection. Biotin quantification was done on infant formulas with different dilution factors using HPLC as shown in Figure 4.20a for Dutch Lady infant formula and Figure 4.20b for Friso Gold infant formula. Dilution factor refers to the ratio of the volume of water to the mass of infant formula. The concentrations of biotin in Dutch Lady and Friso Gold determined using HPLC (Table 4.3) were calculated from the standard addition plots in Figures 4.20a and 4.20b, respectively. The biotin concentration found with the developed immunosensor in Dutch Lady was 11.3 μg/100 g and 11.9 μg/100 g with HPLC. The biotin concentration found with the immunosensor in Friso Gold was 11.9 μg/100 g and 12.6 μg/100 g with HPLC. The biotin concentration recoveries in infant formulas using both techniques were determined based on the biotin concentration stated on the packaging. The biotin concentration recovery determined by the

immunosensor in Dutch Lady was 93.9% and 99.0% with HPLC, while the biotin concentration recoveries determined with the immunosensor in Friso Gold was 91.3% and 96.6% with HPLC. The biotin concentration recoveries achieved with the electrochemical immunosensor were slightly lower than with the HPLC technique, because no pre-treatment was conducted on the infant formula samples analyzed using the immunosensor, leading to the presence of interference in infant formulas. Nevertheless, the biotin concentration recoveries attained with both techniques were still in an acceptable range (80%-120%). In short, biotin quantification using the electrochemical immunosensor is preferable, because a highly accurate detection signal can be obtained without sample pre-treatment, which resulted in short analysis time. The tedious sample pre-treatment prior to biotin quantification using HPLC is time-consuming (about 30-40 min per sample).

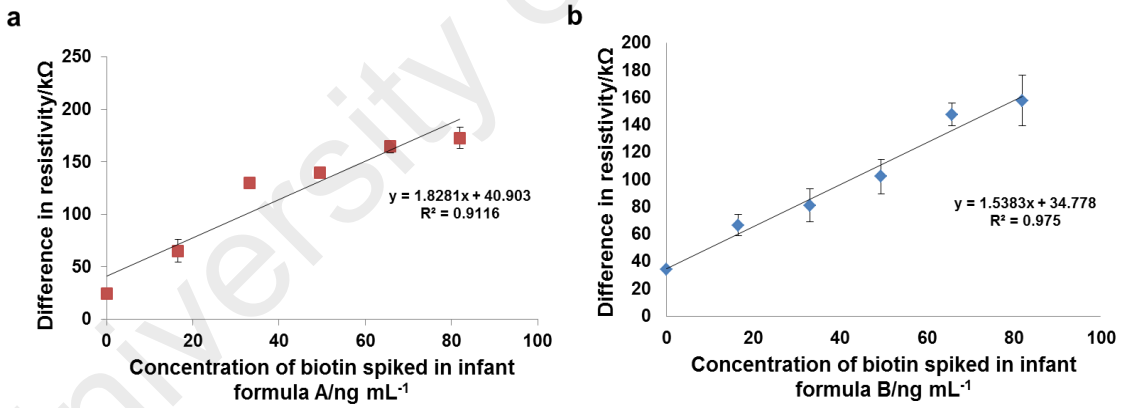

Figure 4.19: Biotin concentration quantification in infant formulas using the developed immunosensor with the standard addition method. Standard addition plots for the quantitative detection of biotin in (a) Dutch Lady and (b) Friso Gold using the electrochemical immunosensor. Each sample measurement with a dilution factor of 5 was repeated 3 times.

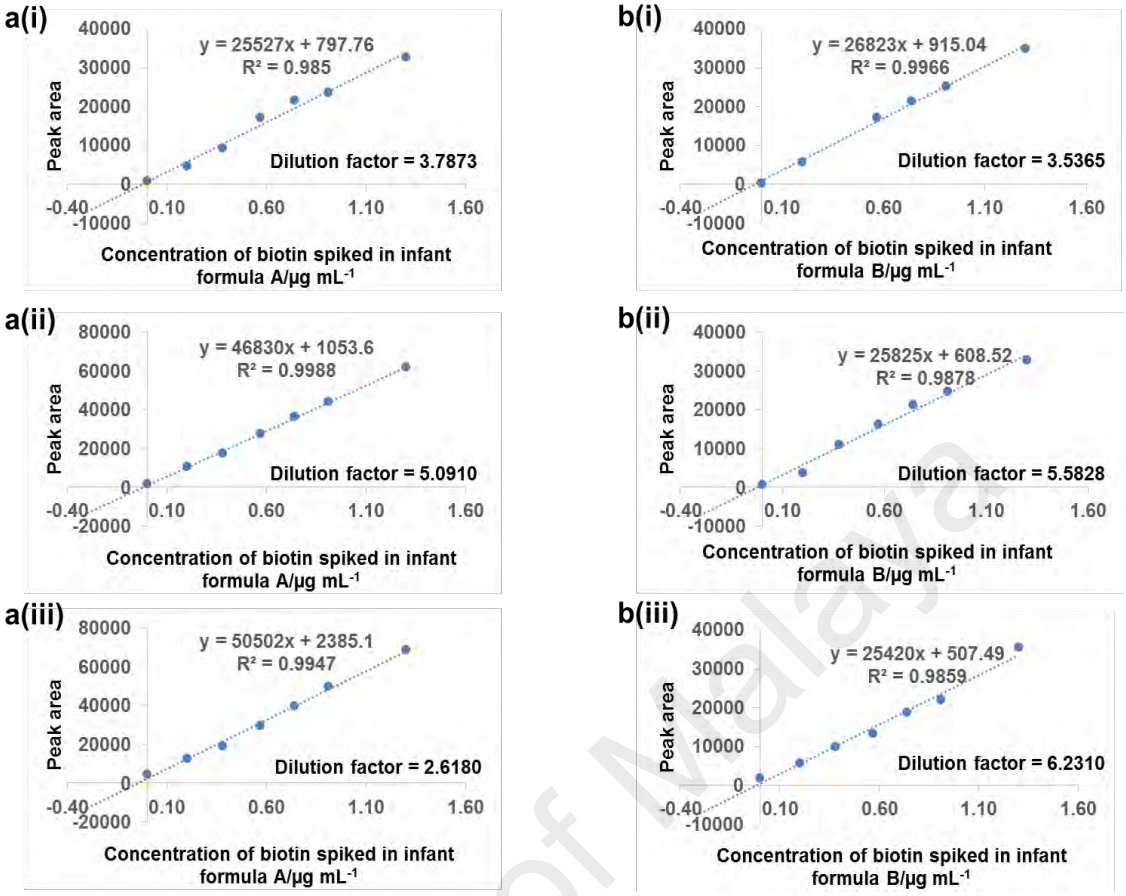

Figure 4.20: Biotin concentration quantification in infant formulas using HPLC technique with the standard addition method. Standard addition plots for the quantitative detection of biotin in (a) Dutch Lady and (b) Friso Gold using HPLC with a photodiode array detector. Biotin detection in each infant formula was repeated with 3 dilution factors (i, ii and iii).

Table 4.3: Biotin concentration in infant formulas (Dutch Lady and Friso Gold) obtained using an electrochemical immunosensor and HPLC with photodiode array detector.

Infant formula	**Biotin concentration as stated on packaging, µg/100 g**	**[1]Concentration obtained, µg/100 g**		**[1]Recovery, %**	
		Electrochemical immunosensor	HPLC	Electrochemical immunosensor	HPLC
Dutch Lady	12	11.3±1.9	11.9±0.5	93.9±16.2	99.0±3.8
Friso Gold	13	11.9±4.6	12.6±0.6	91.3±35.1	96.6±4.3

[1]Results based on 3 replicate analyses with a standard error in the 95% confidence limit.

4.6.2 Method validation of the developed immunosensor by HPLC in the direct detection of biotin in biotin-containing supplements

For three rational reasons, an external calibration method was selected for the quantification of biotin in biotin-containing supplements rather than the standard addition or internal standard method. The first reason is the high specific binding of anti-biotin antibody to free biotin (target analyte), which is an important immunosensor feature. Hence, the free biotin in sample solutions can be specifically detected via a displacement assay and the matrix effect can be neglected. Second, the standard addition method would be an inappropriate option because the aim was to investigate the performance of the developed immunosensor in biotin detection in un-spiked real samples. Furthermore, the internal standard method is not suitable in this study, because it is difficult to find an adequate internal standard for biotin detection. The third reason is the lower complexity of the studied samples since the biotin-containing supplements were only solubilized in Milli-Q^{TM} water. This exhibits lower complexity than intricate matrices such as serum and infant formula samples (an external standard method is not appropriate for serum and infant formula samples). Therefore, an external calibration method was employed to quantitatively detect the biotin in biotin-containing supplements (Guardian, Berocca and 21ST Century). The calibration plot of biotin detection by HPLC technique in 80% acetonitrile is presented in Figure 4.17. With the detection signals obtained by the developed immunosensor and HPLC, the biotin concentration of supplements can be determined based on the calibration plots in Figures 4.8 and in 4.21, respectively. The concentrations of biotin in supplements (Guardian, Berocca and 21ST Century) determined by electrochemical immunosensor and HPLC are stated in Table 4.4. The biotin concentration found in Guardian effervescent tablets was 139.4 µg/tablet by immunosensor and 130.3 µg/tablet by HPLC; the biotin concentration found in Berocca effervescent tablets was 159.8

μg/tablet by immunosensor and 151.3 μg/tablet by HPLC; and the biotin concentration found in 21ST Century B-complex capsule was 40.0 μg/capsule by immunosensor and 39.1 μg/capsule by HPLC. The recoveries of biotin concentration in supplements determined by electrochemical immunosensor and HPLC were calculated based on the biotin concentrations stated on packaging (Table 4.4). The recoveries of biotin in supplements (Guardian, Berocca and 21ST Century) detected by electrochemical immunosensor were 92.9%, 106.5% and 100.0%, respectively. The recoveries of biotin in supplements (Guardian, Berocca and 21ST Century) detected by HPLC technique were 86.9%, 100.9% and 97.8%, respectively. The accuracy of both techniques used in the quantification of biotin in supplements seems promising, as the biotin detection recoveries obtained from the experiments were in an accepted range (80%–120%). Nevertheless, the electrochemical immunosensor is preferable for used in the detection of biotin in real samples, because no tedious sample pre-treatment steps are needed. Unlike HPLC, sample pre-treatment steps like sonication, centrifugation and filtration are required to solubilize the sample and remove the undissolved substances and macromolecules from samples, so it is possible to avoid HPLC column blockage by undissolved substances and macromolecules. Due to the simple and fast detection, the development of electrochemical immunosensors for use in target analyte detection in complex matrices has become prominent.

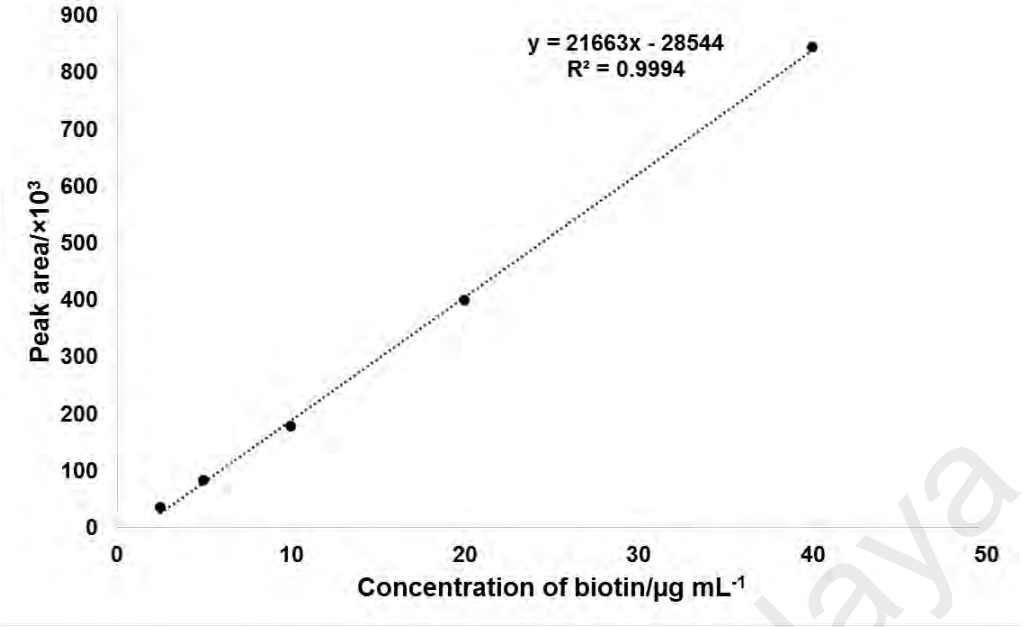

Figure 4.21: Calibration plot of peak area versus biotin concentration obtained by HPLC.

Table 4.4: Biotin concentration in biotin-containing supplements (Guardian, Berocca and 21ST Century) determined using the developed immunosensor and HPLC with photodiode array detector.

Brand	**Biotin concentration as stated on packaging, µg/tablet**	**[1]Concentration obtained, µg/tablet**		**[1]Recovery, %**	
		Electrochemical immunosensor	HPLC	Electrochemical immunosensor	HPLC
Guardian	150	139.4±4.7	130.3±0.5	92.9±3.1	86.9±0.3
Berocca	150	159.8±13.5	151.3±1.9	106.5±9.0	100.9±1.3
21ST Century	40	40.0±7.4	39.1±0.5	100.0±18.5	97.8±1.3

[1]Results based on 3 replicate analyses with a standard error in the 95% confidence limit.

4.6.3 Correlation between the signals obtained in the quantification of biotin in human serum by electrochemical immunosensor and HPLC

Human serum is among the biological fluids that contain biotin. Therefore, human serum may be collected for biotin monitoring in the human body. However, several interferences exist, such as proteins (e.g., antibodies/antigens and albumin), electrolytes (e.g., bicarbonate, calcium, sodium and magnesium), hormones, and other substances (e.g., uric acid, cholesterol, globulin and glucose) (U.S. Food and Drug Administration, 2017). Hence, a test was conducted to confirm that the correlation between the detection signals obtained by electrochemical immunosensor and HPLC would not be affected by the matrix effects or interferences present in human serum. In other words, this test may be used to investigate the influence of interferences in human serum on the detection signal obtained by an immunosensor. In order to investigate the correlation between the two techniques, the biotin solution (1500 μg mL^{-1}) in the human serum was spiked with 20, 40, 60, 80, and 100 μL. For biotin detection in human serum, a linear relationship between the detection signals obtained by the immunosensor and by HPLC was obtained within a biotin concentration range of 10 μg mL^{-1} – 90 μg mL^{-1} (Figure 4.22). This signifies that the detection signals obtained by both techniques increase with the biotin concentration in human serum. The high linearity with R^2 of 0.9702 proves that the detection ability of the developed immunosensor is not affected by interferences present in serum samples. Therefore, this finding indirectly indicates that the biotin concentration in real samples can be quantified using the developed electrochemical immunosensor without requiring sample pre-treatment.

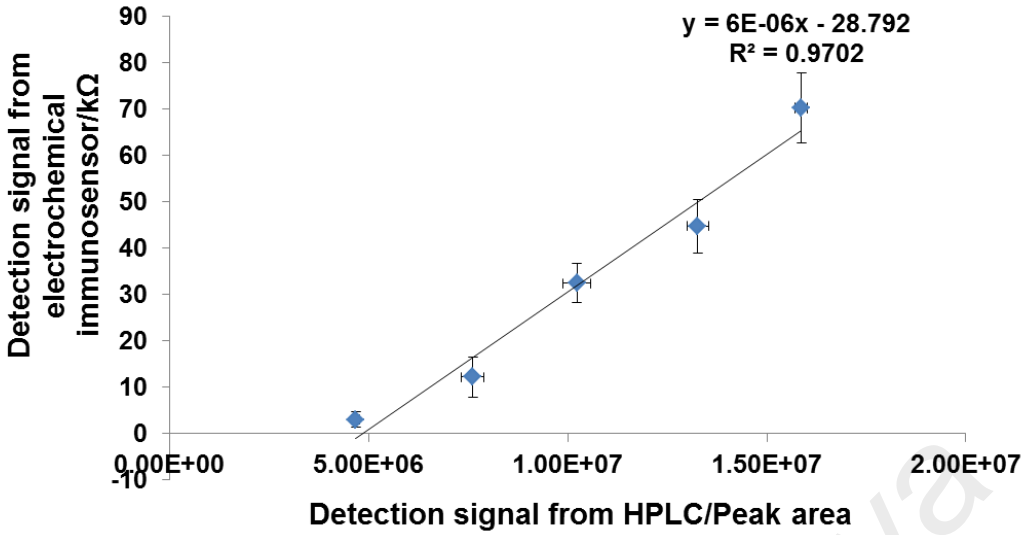

Figure 4.22: Correlation between immunosensor and HPLC in biotin detection in human serum.

CHAPTER 5: CONCLUSIONS AND FUTURE PERSPECTIVES

The bottom-up immunosensor interface fabrication of an OEG-modified immunosensor and Ph-SO_3^-/Ph-NMe_3^+-modified immunosensor was successfully characterized by CV, EIS, FE-SEM and FTIR. Both immunosensor surface versions were used to detect free biotin present in PBS solution (pH 7.4) via a displacement assay, in which the surface-bound anti-biotin antibody was dissociated from the immunosensor surface and complexed with free biotin in PBS solution. The dynamic range determined for the OEG-modified immunosensor was 700 μg mL^{-1} to 1500 μg mL^{-1}, whereas the dynamic range determined for the Ph-SO_3^-/Ph-NMe_3^+-modified immunosensor was 50 μg mL^{-1} to 200 μg mL^{-1}. The Ph-SO_3^-/Ph-NMe_3^+-modified immunosensor was selected for further investigation, because it could detect biotin in low concentration ranges sensitively, as most real samples contain low biotin concentrations at the ppm or ppb scale.

For the purpose of repeated immunosensor use, electrode polarization of -800 mV for a 10 min interval was applied to regenerate the immunosensor interface in order to yield the highest sensitivity of the developed immunosensor. Surface-bound antibody dissociation was enhanced by applying a negative potential (-800 mV) to the GC electrode for 10 min. This consequently improved the sensor sensitivity. No significant degradation in immunosensor detection ability was observed after applying electrode polarization for 5 regeneration cycles. Besides, the aryl diazonium layer appeared to be stable and robust after being subjected to multiple cycles of electrode polarization, because $Fe(CN)_6^{3-/4-}$ redox species penetration was blocked successfully by the grafted layer after the 1st, 5th, 10th and 15th surface regeneration cycles. This indicates that an immunosensor interface can be used multiple times without the need to re-fabricate the entire immunosensor interface.

Based on anti-fouling and sensitivity investigations of Ph-NH_2/Ph-SO_3^-/Ph-NMe_3^+-fabricated GC surfaces with different molar ratios (Mix 1, Mix 2, Mix 3 and Mix 4), the GC surface containing Mix 3 was selected for further investigation. The reason is that it possesses an excellent anti-fouling property besides good sensor sensitivity, which are considered important characteristics of an immunosensor for use in real sample analysis. The low-impedance Ph-SO_3^-/Ph-NMe_3^+-modified immunosensor was proven to be highly reproducible, with RSD of 8.44% obtained after 10 different immunosensors were exposed to 75 μg mL^{-1} of biotin solution. The developed immunosensor exhibited high selectivity only to biotin, as the immunosensor did not show a significant response to ascorbic acid, uric acid, citric acid, sucrose and guanine. The immunosensor surface grafted with a mixture of Ph-SO_3^-/Ph-NMe_3^+ had a high anti-fouling property, since no protein adsorption was identified on the immunosensor surface after exposure to BSA, Cyt–C and infant formula A. The good stability of the developed immunosensor was confirmed, with no obvious loss in immunosensor detection ability discovered after being stored for 28 days at 4ºC. With RSD obtained in the range of 5% to 13% in intra-day and inter-day precision studies, the developed immunosensor was proven to be able to produce high-precision detection signals in biotin quantification. Therefore, the Ph-SO_3^-/Ph-NMe_3^+-modified immunosensor reported herein is reproducible, selective, resistive to non-specific protein adsorption, stable and precise.

In the quantitative detection of biotin in real samples, the high biotin concentration recoveries determined in infant formulas (Dutch Lady and Friso Gold) were 93.9% and 91.3%, respectively, by the developed electrochemical immunosensor with no sample pre-treatment necessary. Besides, the direct biotin detection in biotin-containing supplements (Guardian, Berocca and 21ST Century) by the developed immunosensor without sample pre-treatment yielded high recoveries of 92.9%, 106.5% and 100.0%,

respectively. These results indicate that the immunosensor performance was not affected by interferences present in infant formulas and supplements. A standard instrument (HPLC with photodiode array detector) was used to validate the performance of the developed immunosensor, in which sample pre-treatment was required to prevent interferences (in infant formulas and supplements) from blocking the HPLC column. The highly linear relationship (linearity of 0.97) when the biotin concentrations in human serum measured using the immunosensor and HPLC were compared, confirms that the developed immunosensor can make precise and accurate measurements of biotin concentrations in human serum. The linearity with $R^2 \geq 0.98$ of the correlation plot also proves that the detection ability of the developed immunosensor is not influenced by interferences present in serum samples. Therefore, the electrochemical immunosensor reported herein is proven to be capable of producing reliable and accurate detection signals in biotin detection in real samples.

As future perspectives, in addition to the electrochemical biotin detection by the second immunosensor version, biotin detection using the second immunosensor surface version (sulfo-NHS-biotin/Ph-NH_2/AuNPs/Ph-NH_2:Ph-SO_3^-:Ph-NMe_3^+-fabricated GC surface) can not only be done by electrochemical technique but also by optical technique. In other words, the second immunosensor surface version is recommended for use in both electrochemical and optical detection of biotin. To achieve this goal, fluorescent dye-conjugated anti-biotin antibody must be used to generate the optical signal. In the presence of biotin, the surface-bound anti-biotin antibody is dissociated from the immunosensor surface with the aid of induced voltage, therefore an electrochemical signal is generated based on the decrease in charge transfer resistivity following displacement assay and an optical signal will be generated based on the decrease in surface-bound antibody fluorescent intensity following a displacement assay. An immunosensor comprising dual-detectors may provide the results based on

the changes in electrochemical signal and fluorescent intensity at the immunosensor surface, whereby the results obtained are complementary to each other and more convincing for immunosensor users. In terms of device commercialization, the manufacturer can decide which detection mode should be selected based on the budget presented after a detailed cost calculation, or depending on the market demand of end users on different continents. Thus, they can recommend whether an electrochemical or optical biosensor is preferable and more acceptable.

In order to expand the versatility of the developed immunosensor surface, the second version is suggested for use in the detection of other small organic molecules such as 2,4-dinitrophenol (2,4-DNP). 2,4-DNP is aimed as the analyte for a future study, because it is a highly toxic chemical. It was used by the French as an explosive during the First World War and then it was also used in the manufacturing of dye, wood preservers, herbicides, antiseptics, pesticides and photographic developers as well as in anti-obesity drugs. Besides, it is well-absorbed through the skin, by inhalation, and oral as well as eye exposure due to its solubility and biochemical activity. Therefore, the 2,4-DNP content in environmental, food and clinical samples has to be monitored from time to time. 2,4-DNP detection using the developed immunosensor is achievable by simply replacing the sulfo-NHS-biotin with 2-amino-4,6-dinitrophenol (surface-bound epitope for 2,4-DNP). Other than that, the anti-2,4-DNP antibody can be applied in the immunosensor to specifically capture the target analyte (2,4-DNP) in the detection of 2,4-DNP. This could prevent the analogues of 2,4-DNP (e.g., 3,4-dinitrophenol, 2-methyl-4,6-dinitrophenol and 4-methyl-2,6-dinitrophenol) from occupying the binding sites of the anti-2,4-DNP antibody, resulting in selective detection due to the high immunosensor specificity. Furthermore, displacement or sandwich assays are suggested for application in small organic molecule detection in order to generate a significant detection signal; hence, the detection mechanism functioning in 2,4-DNP detection must

be investigated. However, the detection signal produced is principally based on the interaction between 2,4-DNP and anti-2,4-DNP antibody, therefore detection mechanism selection may be influenced by the binding affinity between 2,4-DNP and its antibody. In addition, the analytical performance of the immunosensor used for 2,4-DNP detection must be investigated further.

REFERENCES

Abouzari, M. S., Berkemeier, F., Schmitz, G., & Wilmer, D. (2009). On the physical interpretation of constant phase elements. *Solid State Ionics, 180*(14), 922-927.

Ahuja, T., Tanwar, V. K., Mishra, S. K., Kumar, D., & Biradar, A. M. (2011). Immobilization of uricase enzyme on self-assembled gold nanoparticles for application in uric acid biosensor. *Journal of Nanoscience and Nanotechnology, 11*(6), 4692-4701.

Albarracin, C. A., Fuqua, B. C., Evans, J. L., & Goldfine, I. D. (2008). Chromium picolinate and biotin combination improves glucose metabolism in treated, uncontrolled overweight to obese patients with type 2 diabetes. *Diabetes/metabolism Research and Reviews, 24*(1), 41-51.

Andersson, K., Hämäläinen, M., & Malmqvist, M. (1999). Identification and optimization of regeneration conditions for affinity-based biosensor assays. A multivariate cocktail approach. *Analytical Chemistry, 71*(13), 2475-2481.

Ang, S. H., Yu, C. Y., Ang, G. Y., Chan, Y. Y., Yatimah Alias, & Khor, S. M. (2015). A colloidal gold-based lateral flow immunoassay for direct determination of haemoglobin A1c in whole blood. *Analytical Methods, 7*(9), 3972-3980.

Asanov, A. N., Wilson, W. W., & Oldham, P. B. (1998). Regenerable biosensor platform: a total internal reflection fluorescence cell with electrochemical control. *Analytical Chemistry, 70*(6), 1156-1163.

Bahadır, E. B., & Sezgintürk, M. K. (2015). Applications of commercial biosensors in clinical, food, environmental, and biothreat/biowarfare analyses. *Analytical Biochemistry, 478*, 107-120.

Bahadır, E. B., & Sezgintürk, M. K. (2016). A review on impedimetric biosensors. *Artificial Cells, Nanomedicine, and Biotechnology, 44*(1), 248-262.

Bi, L., Dong, J., Xie, W., Lu, W., Tong, W., Tao, L., & Qian, W. (2013). Bimetallic gold–silver nanoplate array as a highly active SERS substrate for detection of streptavidin/biotin assemblies. *Analytica Chimica Acta, 805*, 95-100.

Choi, S. (2011). *Advancing microfluidic-based protein biosensor technology for use in clinical diagnostics* (Doctoral dissertation, Arizona State University).

Choi, S., & Chae, J. (2009). *A regenerative biosensing surface using electrochemical desorption of self-assembled monolayer in microfluidics.* Paper presented at the Solid-State Sensors, Actuators and Microsystems Conference, 2009. TRANSDUCERS 2009. International.

Chung, J. W., Kim, S. D., Bernhardt, R., & Pyun, J. C. (2006). Additive assay for the repeated measurements of immunosensor without regeneration step. *Sensors and Actuators B: Chemical, 114*(2), 1007-1012.

Darwish, N. T. (2016). *An electrochemical immunosensor for dengue virus NS1 protein detection* (Doctoral dissertation, University of Malaya).

Darwish, N. T., Yatimah Alias, & Khor, S. M. (2015). Indium tin oxide with zwitterionic interfacial design for biosensing applications in complex matrices. *Applied Surface Science, 325*, 91-99.

Dhruv, H. D. (2009). *Controlling nonspecific adsorption of proteins at bio-interfaces for biosensor and biomedical applications* (Doctoral dissertation, Utah State University).

Ding, S. J., Chang, B. W., Wu, C. C., Lai, M. F., & Chang, H. C. (2005). Electrochemical evaluation of avidin–biotin interaction on self-assembled gold electrodes. *Electrochimica Acta, 50*(18), 3660-3666.

Eggenstein, C., Borchardt, M., Diekmann, C., Gründig, B., Dumschat, C., Cammann, K., Spener, F. (1999). A disposable biosensor for urea determination in blood based on an ammonium-sensitive transducer. *Biosensors and Bioelectronics, 14*(1), 33-41.

Eldefrawi, M. E., Eldefrawi, A. T., Anis, N. A., & Valdes, J. J. (1993). Reusable fiber optic biosensors for detection of drugs and toxicants. *Uses of Immobilized Biological Compounds* (pp. 387-395): Springer.

European Medicines Agency. (2009). *Guidelines for the validation of analytical methods used in residue depletion studies.* Retrieved from http://www.ema.europa.eu/ema/pages/includes/document/open_document.jsp?webContentId=WC500040499. Last accessed on 25 Feb 2016.

Gao, Z., Xie, F., Shariff, M., Arshad, M., & Ying, J. Y. (2005). A disposable glucose biosensor based on diffusional mediator dispersed in nanoparticulate membrane on screen-printed carbon electrode. *Sensors and Actuators B: Chemical, 111*, 339-346.

Gheorghe-Constantin, I., & Petru, C. (2011). Brief survey on electrochemical impedance spectroscopy evaluation and its application on nickel corrosion in chloride solutions. *Journal of Applied Engineering Sciences, 1(14)*(4).

Ghindilis, A. L., Atanasov, P., Wilkins, M., & Wilkins, E. (1998). Immunosensors: electrochemical sensing and other engineering approaches. *Biosensors and Bioelectronics, 13*(1), 113-131.

Gholivand, M. B., Jalalvand, A. R., Goicoechea, H. C., Gargallo, R., & Skov, T. (2015). Chemometrics: an important tool for monitoring interactions of vitamin B7 with bovine serum albumin with the aim of developing an efficient biosensing system for the analysis of protein. *Talanta, 132*, 354-365.

Guan, J. G., Miao, Y. Q., & Zhang, Q. J. (2004). Impedimetric biosensors. *Journal of Bioscience and Bioengineering, 97*(4), 219-226.

Gui, A. L. (2011). *Stable and Low Impedance Anti-fouling Coating Formed from the Reductive Adsorption of Aryl Diazonium Salts on Electrode Surfaces* (Doctoral dissertation, The University of New South Wales Sydney 2052, Australia).

Gui, A. L., Luais, E., Peterson, J. R., & Gooding, J. J. (2013). Zwitterionic phenyl layers: finally, stable, anti-biofouling coatings that do not passivate electrodes. *ACS Applied Materials & Interfaces, 5*(11), 4827-4835.

He, L. J., Wu, M. S., Xu, J. J., & Chen, H. Y. (2013). A reusable potassium ion biosensor based on electrochemiluminescence resonance energy transfer. *Chemical Communications, 49*(15), 1539-1541.

He, Y., Hower, J., Chen, S., Bernards, M. T., Chang, Y., & Jiang, S. (2008). Molecular simulation studies of protein interactions with zwitterionic phosphorylcholine self-assembled monolayers in the presence of water. *Langmuir, 24*(18), 10358-10364.

Höller, U., Wachter, F., Wehrli, C., & Fizet, C. (2006). Quantification of biotin in feed, food, tablets, and premixes using HPLC–MS/MS. *Journal of Chromatography B, 831*(1), 8-16.

Holmlin, R. E., Chen, X., Chapman, R. G., Takayama, S., & Whitesides, G. M. (2001). Zwitterionic SAMs that resist nonspecific adsorption of protein from aqueous buffer. *Langmuir, 17*(9), 2841-2850.

Indyk, H. E., Evans, E. A., Caselunghe, M. C. B., Persson, B. S., Finglas, P. M., Woollard, D. C., & Filonzi, E. L. (2000). Determination of biotin and folate in infant formula and milk by optical biosensor-based immunoassay. *Journal of AOAC International, 83*(5), 1141-1148.

Jackson, D. R., Omanovic, S., & Roscoe, S. G. (2000). Electrochemical studies of the adsorption behavior of serum proteins on titanium. *Langmuir, 16*(12), 5449-5457.

Jha, N., & Ramaprabhu, S. (2009). Development of MWNT based disposable biosensor on glassy carbon electrode for the detection of organophosphorus nerve agents. *Journal of Nanoscience and Nanotechnology, 9*(9), 5676-5680.

Kergaravat, S. V., Gómez, G. A., Fabiano, S. N., Chávez, T. I. L., Pividori, M. I., & Hernández, S. R. (2012). Biotin determination in food supplements by an electrochemical magneto biosensor. *Talanta, 97*, 484-490.

Khoo, M. M., Zarina Rahim, Darwish, N. T., Yatimah Alias, & Khor, S. M. (2016). Non-invasive control of protein-surface interactions for repeated electrochemical immunosensor use. *Sensors and Actuators B: Chemical, 224*, 683-691.

Khor, S. M., Liu, G., Fairman, C., Iyengar, S. G., & Gooding, J. J. (2011). The importance of interfacial design for the sensitivity of a label-free electrochemical immuno-biosensor for small organic molecules. *Biosensors and Bioelectronics, 26*(5), 2038-2044.

Kim, D. C., & Kang, D. J. (2008). Molecular recognition and specific interactions for biosensing applications. *Sensors, 8*(10), 6605-6641.

Kim, N. Y., Adhikari, K. K., Dhakal, R., Chuluunbaatar, Z., Wang, C., & Kim, E. S. (2015). Rapid, sensitive, and reusable detection of glucose by a robust radiofrequency integrated passive device biosensor chip. *Scientific Reports, 5*.

Lam, L. Y. Z., & Atkinson, J. (2002). Disposable screen-printed biosensor for transcutaneous oxygen measurement. *Measurement Science and Technology, 13*(12), 2074.

Lee, B. Q., Mohamed, C. W. J. B. W., & Khor, S. M. (2016). A simultaneous derivatization of 3-monochloropropanediol and 1, 3-dichloropropane with hexamethyldisilazane–trimethylsilyl trifluoromethanesulfonate at room temperature for efficient analysis of food sample analysis. *Journal of Chromatography A, 1432*, 101-110.

Li, Y., Schluesener, H. J., & Xu, S. (2010). Gold nanoparticle-based biosensors. *Gold Bulletin, 43*(1), 29-41.

Liu, G., Iyengar, S. G., & Gooding, J. J. (2012). An electrochemical impedance immunosensor based on gold nanoparticle–modified electrodes for the detection of HbA1c in human blood. *Electroanalysis, 24*(7), 1509-1516.

Liu, G., Khor, S. M., Iyengar, S. G., & Gooding, J. J. (2012). Development of an electrochemical immunosensor for the detection of HbA1c in serum. *Analyst, 137*(4), 829-832.

Liu, G., Liu, J., Davis, T. P., & Gooding, J. J. (2011). Electrochemical impedance immunosensor based on gold nanoparticles and aryl diazonium salt functionalized gold electrodes for the detection of antibody. *Biosensors and Bioelectronics, 26*(8), 3660-3665.

Liu, G., Luais, E., & Gooding, J. J. (2011). The fabrication of stable gold nanoparticle-modified interfaces for electrochemistry. *Langmuir, 27*(7), 4176-4183.

Liu, Y., Meng, S., Mu, L., Jin, G., Zhong, W., & Kong, J. (2008). Novel renewable immunosensors based on temperature-sensitive PNIPAAm bioconjugates. *Biosensors and Bioelectronics, 24*(4), 710-715.

Lowe, S., O'Brien-Simpson, N. M., & Connal, L. A. (2015). Antibiofouling polymer interfaces: poly (ethylene glycol) and other promising candidates. *Polymer Chemistry, 6*(2), 198-212.

Lu, B., Iwuoha, E. I., Smyth, M. R., & O'Kennedy, R. (1997). Development of an "electrically wired" amperometric immunosensor for the determination of biotin based on a non-diffusional redox osmium polymer film containing an antibody to the enzyme label horseradish peroxidase. *Analytica Chimica Acta, 345*(1), 59-66.

Luppa, P. B., Sokoll, L. J., & Chan, D. W. (2001). Immunosensors—principles and applications to clinical chemistry. *Clinica Chimica Acta, 314*(1), 1-26.

Ma, C., Sun, Z., Chen, C., Zhang, L., & Zhu, S. (2014). Simultaneous separation and determination of fructose, sorbitol, glucose and sucrose in fruits by HPLC–ELSD. *Food Chemistry, 145*, 784-788.

Maebashi, M., Makino, Y., Furukawa, Y., Ohinata, K., Kimura, S., & Sato, T. (1993). Therapeutic evaluation of the effect of biotin on hyperglycemia in patients with non-insulin dependent diabetes mellitus. *Journal of Clinical Biochemistry and Nutrition, 14*(3), 211-218.

Márquez-Sillero, I., Cárdenas, S., & Valcárcel, M. (2013). Determination of water-soluble vitamins in infant milk and dietary supplement using a liquid chromatography on-line coupled to a corona-charged aerosol detector. *Journal of Chromatography A, 1313*, 253-258.

Mock, D. M., & Malik, M. I. (1992). Distribution of biotin in human plasma: most of the biotin is not bound to protein. *The American Journal of Clinical Nutrition, 56*(2), 427-432.

Mohanty, S. P., & Kougianos, E. (2006). Biosensors: a tutorial review. *Ieee Potentials, 25*(2), 35-40.

Moina, C., & Ybarra, G. (2012). Fundamentals and applications of immunosensors. *Advances in Immunoassay Technology*, 65-80.

Ng, K. L., Lee, S. M., Khor, S. M., & Tan, G. H. (2015). Electrochemical preparation and characterization of a gold nanoparticles graphite electrode: Application to myricetin antioxidant analysis. *Analytical Sciences, 31*(10), 1075-1081.

Oldham, P. B., & Asanov, A. N. (1999). *Control of antibody-antigen binding or dissociation by electric field.* Paper presented at the BiOS'99 International Biomedical Optics Symposium.

Omanovic, S., & Roscoe, S. G. (1999). Electrochemical studies of the adsorption behavior of bovine serum albumin on stainless steel. *Langmuir, 15*(23), 8315-8321.

Polese, D., Convertino, A., Maiolo, L., Ferrone, A., Pazzini, L., Marrani, M., Fiaschi, G. (2014, Nov). *Investigation on nanostructured biosensor for Biotin detection.* Paper presented at the SENSORS, 2014 IEEE.

Prodromidis, M. I. (2007). Impedimetric biosensors and immunosensors. *Pakistan Journal of Analytical & Environmental Chemistry, 8*(2), 3.

Radi, A. E., Muñoz-Berbel, X., Cortina-Puig, M., & Marty, J.-L. (2009). An electrochemical immunosensor for ochratoxin A based on immobilization of antibodies on diazonium-functionalized gold electrode. *Electrochimica Acta, 54*(8), 2180-2184.

Rahman, M. M. (2014). Reusable and mediator-free cholesterol biosensor based on cholesterol oxidase immobilized onto TGA-SAM modified smart bio-chips. *PLoS One, 9*(6), e100327.

Reyes, F. D., Romero, J. F., & de Castro, M. L. (2001). Determination of biotin in foodstuffs and pharmaceutical preparations using a biosensing system based on the streptavidin–biotin interaction. *Analytica Chimica Acta, 436*(1), 109-117.

Ricci, F., Adornetto, G., & Palleschi, G. (2012). A review of experimental aspects of electrochemical immunosensors. *Electrochimica Acta, 84*, 74-83.

Ricci, F., Volpe, G., Micheli, L., & Palleschi, G. (2007). A review on novel developments and applications of immunosensors in food analysis. *Analytica Chimica Acta, 605*(2), 111-129.

Santiago-Lopez, A. J., Vera, J. L., & Meléndez, E. (2014). DNA electrochemical biosensor for metallic drugs at physiological conditions. *Journal of Electroanalytical Chemistry, 731*, 139-144.

Sarika, C., Rekha, K., & Murthy, B. N. (2015). Studies on enhancing operational stability of a reusable laccase-based biosensor probe for detection of ortho-substituted phenolic derivatives. *3 Biotech, 5*(6), 911-924.

Satvekar, R. K., Tiwale, B. M., & Pawar, S. H. (2014). Emerging Trends in Medical Diagnosis: A Thrust on Nanotechnology. *Medical Chemistry, 4*(3), 4-10.

Song, Y., Wang, L., Ren, C., Zhu, G., & Li, Z. (2006). A novel hydrogen peroxide sensor based on horseradish peroxidase immobilized in DNA films on a gold electrode. *Sensors and Actuators B: Chemical, 114*(2), 1001-1006.

Staggs, C. G., Sealey, W. M., McCabe, B. J., Teague, A. M., & Mock, D. M. (2004). Determination of the biotin content of select foods using accurate and sensitive HPLC/avidin binding. *Journal of Food Composition and Analysis, 17*(6), 767-776.

Thévenot, D. R., Toth, K., Durst, R. A., & Wilson, G. S. (2001). Electrochemical biosensors: recommended definitions and classification. *Biosensors and Bioelectronics, 16*(1), 121-131.

Tothill, I. E. (2001). Biosensors developments and potential applications in the agricultural diagnosis sector. *Computers and Electronics in Agriculture, 30*(1), 205-218.

U.S. Food and Drug Administration. (2017). Investigations operations manual. Retrieved from https://www.fda.gov/ICECI/inspections/IOM/default.htm

Uzuriaga-Sánchez, R. J., Khan, S., Wong, A., Picasso, G., Pividori, M. I., & Sotomayor, M. D. P. T. (2016). Magnetically separable polymer (Mag-MIP) for selective analysis of biotin in food samples. *Food Chemistry, 190*, 460-467.

Vashist, S. K., & Luong, J. H. (2015). Recent advances in electrochemical biosensing schemes using graphene and graphene-based nanocomposites. *Carbon, 84*, 519-550.

Vo-Dinh, T., & Cullum, B. (2000). Biosensors and biochips: advances in biological and medical diagnostics. *Fresenius' Journal of Analytical Chemistry, 366*(6), 540-551.

Wang, D., Dou, W., Zhao, G., & Chen, Y. (2014). Immunosensor based on electrodeposition of gold-nanoparticles and ionic liquid composite for detection of Salmonella pullorum. *Journal of Microbiological Methods, 106*, 110-118.

Wang, H. C., & Lee, A. R. (2015). Recent developments in blood glucose sensors. *Journal of Food and Drug Analysis, 23*(2), 191-200.

Wang, J. (2006). Electrochemical biosensors: towards point-of-care cancer diagnostics. *Biosensors and Bioelectronics, 21*(10), 1887-1892.

Williams, D. B. G., George, M. J., & Marjanovic, L. (2014). Rapid detection of atrazine and metolachlor in farm soils: gas chromatography–mass spectrometry-based analysis using the bubble-in-drop single drop microextraction enrichment method. *Journal of Agricultural and Food Chemistry, 62*(31), 7676-7681.

Yoon, H. C., Lee, D., & Kim, H. S. (2002). Reversible affinity interactions of antibody molecules at functionalized dendrimer monolayer: affinity-sensing surface with reusability. *Analytica Chimica Acta, 456*(2), 209-218.

Yue, Q., Shen, T., Wang, J., Wang, L., Xu, S., Li, H., & Liu, J. (2013). A reusable biosensor for detecting mercury (II) at the subpicomolar level based on "turn-on" resonance light scattering. *Chemical Communications, 49*(17), 1750-1752.

Zempleni, J., & Mock, D. (1999). Biotin biochemistry and human requirements. *The Journal of Nutritional Biochemistry, 10*(3), 128-138.

Zempleni, J., Wijeratne, S. S., & Hassan, Y. I. (2009). Biotin. *Biofactors, 35*(1), 36-46.

Zhang, H., & Chiao, M. (2015). Anti-fouling coatings of poly (dimethylsiloxane) devices for biological and biomedical applications. *Journal of Medical and Biological Engineering, 35*(2), 143-155.

Zhang, H., Lan, F., Shi, Y., Wan, Z. G., Yue, Z. F., Fan, F., Yi, C. (2014). A "three-in-one" sample preparation method for simultaneous determination of B-group water-soluble vitamins in infant formula using VitaFast® kits. *Food Chemistry, 153*, 371-377.

Zheng, J., Li, L., Chen, S., & Jiang, S. (2004). Molecular simulation study of water interactions with oligo (ethylene glycol)-terminated alkanethiol self-assembled monolayers. *Langmuir, 20*(20), 8931-8938.

SUPPLEMENTARY

LIST OF PUBLICATIONS

Khoo, M. M., Ng, K. L., Yatimah Alias, & Khor, S. M. (2017). Impedimetric biotin-immunosensor with excellent analytical performance for real sample analysis. *Journal of Electroanalytical Chemistry, 799*, 111-121.

Khoo, M. M., Zarina Rahim, Darwish, N. T., Yatimah Alias, & Khor, S. M. (2016). Non-invasive control of protein-surface interactions for repeated electrochemical immunosensor use. *Sensors and Actuators B: Chemical, 224*, 683-691.

LIST OF PAPER PRESENTED

Khoo, M. M., Yatimah Alias, & Khor, S. M. (2016, Apr). *Development of Reusable Electrochemical Immunosensor for Direct Detection of Small Organic Molecule.* Paper presented at the Annual Conference of 3rd Regional Conference on Biosensor, Biodiagnostics, Biochips and Biotechnology 2016.